IN VIVO STUDIES OF RIBOSOMAL RNA TRANSCRIPTIONAL REGULATION WITHIN A DROSOPHILA STEM CELL LINEAGE

APPROVED BY SUPERVISORY COMMITTEE

Michael Buszczak, Ph.D.

Zhijian James Chen, Ph.D.

Melanie Cobb, Ph.D.

Jin Jiang, Ph.D.

To

My Mom, My Dad, and My Fiancé

IN VIVO STUDIES OF RIBOSOMAL RNA TRANSCRIPTIONAL REGULATION WITHIN A DROSOPHILA STEM CELL LINEAGE

by

QIAO ZHANG

DISSERTATION

Presented to the Faculty of the Graduate School of Biomedical Sciences

The University of Texas Southwestern Medical Center at Dallas

In Partial Fulfillment of the Requirements

For the Degree of

DOCTOR OF PHILOSOPHY

The University of Texas Southwestern Medical Center at Dallas

Dallas, Texas

December, 2013

IN VIVO STUDIES OF RIBOSOMAL RNA TRANSCRIPTIONAL REGULATION WITHIN A DROSOPHILA STEM CELL LINEAGE

QIAO ZHANG, Ph.D.

The University of Texas Southwestern Medical Center at Dallas, 2013

Supervising Professor: MICHAEL BUSZCZAK, Ph.D.

As the first step of ribosome biogenesis, RNA polymerase I-directed ribosomal RNA gene (rRNA) transcription is critical for cell growth, proliferation and cell survival. Upregulated rRNA levels have been observed in many types of cancers. However, the extent to which rRNA transcription is differentially regulated in cells within the same lineage during differentiation *in vivo* and how changes in rRNA levels affect cell fate determination remains unclear.

Here I present the discovery and characterization of a novel *Drosophila* RNA polymerase I transcriptional regulator Under-developed (Udd). The initial udd^{1} mutation was discovered in a

sterility screen, and was further revealed to disrupt the expression of a gene *CG18316*. The *udd* null phenotype was recessive embryonic lethal, and both *udd* mutant phenotypes were rescued by a transgene carrying the *CG18316* ORF. As a nucleolar protein, Udd colocalized with nascent rRNAs and was enriched in the rRNA gene promoter. Disruption of Udd decreased pre-rRNA levels. Moreover, Udd interacted with another two nucleolar proteins which are potential homologs of mammalian rRNA transcription initiation factors, the knockdown of which affected nucleolar expression of Udd and exhibited similar phenotypes to *udd* mutants.

I further observed that the level of rRNA transcription was correlated with the differentiation state of germ cells in *Drosophila* ovaries. The pre-rRNA level was high in germline stem cells (GSCs), then decreased in early differentiating cysts, and again increased in the later differentiated germ cells. This difference was also demonstrated in undifferentiated ovaries (*bam* mutants) before and after introduced differentiation. More intriguingly, increasing rRNA synthesis by Tif-IA overexpression led to a mild expansion of GSCs, while downregulation of Pol I transcription in the undifferentiated ovaries filled with GSC-like cells resulted in multicellular cyst formation. Additionally, I observed another cell fate change, an eye-to-antennal transformation, when rRNA transcription was reduced in the undifferentiated eye primordia. These results suggest that rRNA transcription is closely related to differentiation and development, and the modulation of rRNA synthesis could be a part of the differentiation process.

TABLE OF CONTENTS

PRIOR PUBLICATIONS

Zhang Q., Shalaby N., Buszczak M. Different levels of rRNA Transcription Promote Germline Stem Cell Maintenance and Cyst Differentiation. – **Under 2nd round Revision for *Science***. (The 2nd round reviews were back in 06/2013)

Li Y., **Zhang Q.**, Carreira A., Maines J., McKearin D. & Buszczak M. Mei-P26 Cooperates with Bam, Bgcn and Sxl to Promote Early Germline Development in the Drosophila Ovary. ***PLoS One.*** 2013; 8(3): e58301.

LIST OF FIGURES

LIST OF ABBREVIATIONS

9-HE	9-hydroxyellipticine
AML	acute myeloid leukemia
AMPK	AMP-activated protein kinase
asRNA	antisense RNAs, transcribed from antisense strand of the pre-rRNA coding region and intergenic spacers
attB	bacterial host attachment site
attP	phage attachment site
bam	bag-of-marbles
BFLS	Börjeson-Forssman-Lehmann syndrome
BLM	Bloom's syndrome protein
BMP	bone morphogenetic protein
BrUTP	5-bromouridine 5'triphophate
CB	cystoblast
CDK	cyclin-dependent kinase
CF (yeast)	core factor complex
ChIP	chromatin immunoprecipitation
CKII	casein kinase II
Col IV	type IV collagen
CP	core promoter
CSB	Cockayne syndrome group B
CTCF	CCCTC-binding factor
CTD	C-terminal domain
da	daughterless
Dad	Daughters against dpp
DDX31	ATP-dependent DEAD box RNA helicase 31
DFC	dense fibrillar component
DHX33	ATP-dependent DEAH box RNA helicase 33
Dpp	Decapentaplegic
EC	escort cell
EGF	epidermal growth factor
Eif4	translation initiation factor 4
eNoSC	energy-dependent nucleolar silencing complex
ER	endoplasmic reticulum
ERK	extracellular signal-regulated kinase
ETS	external transcribed spacer
FC	follicle cell
FC	fibrillar center
Fib	Fibrillarin
Flag-Udd	3×Flag-tagged Udd
FSC	follicle stem cell
GC	peripheral granular component

GSC	germline stem cell
HA-Udd	3×Hemagglutinin-tagged Udd
HDAC	histone deacetylase
Hts	Hu-li tai shao, drosophila homolog of adducin
IGF-IR	insulin-like growth factor I receptor
immuno-FISH	fluorescent immunohybridization
InR	insulin receptor
IRS1/2	insulin receptor substrate 1 or 2
ITS	internal transcribed spacer
JHDM	JmjC-domain-containing histone demethylase
JNK	c-Jun N-terminal kinase
Lis1	Lissencephaly 1
Lsd1	lysine-specific histone demethylase 1
Mad	Mothers against dpp
MAPK	mitogen-activated protein kinase
MBD	methyl-CpG binding domain protein
Mod	Modulo, *Drosophila* homolog of nucleolin
MTG8, ETO	myeloid transforming gene on chromosome 8
MTOC	microtubule organizing center
mTOR	mammalian target of rapamycin
NDF	nucleolus-derived foci
NE	nuclear envelope
NM1	Nuclear actin and myosin 1
NML	Nucleomethylin
Nop52	nucleolar protein 52 kDa
Nopp140	nucleolar phosphoprotein 140 kDa
NoRC	nucleolar remodeling complex
NORs	nucleolar organizer regions
nos	nanos gene
NPM, B23	nucleophosmin
NS1	nucleostemin 1
NTS, IGS	non-transcribed spacer, or intergenic spacer
NuRD	nucleosome remodeling and deacetylation complex
ORF	open reading frame
Paf1C	RNA polymerase-associating factor 1 complex
PARP-1	Poly(ADP-Ribose) polymerase 1
PGC	primordial germ cell
PH3	Ser10-phosphorylated Histone H3
PHF8	PHD finger protein 8
PI3K	phosphatidylinositol 3-kinase
PIC	pre-initiation complex
pMad	phosphorylated Mad
PNB	prenucleolar body

Pol I	DNA-directed RNA polymerase I
Pol II	DNA-directed RNA polymerase II
Pol III	DNA-directed RNA polymerase III
PP2A	protein phosphatase 2A
PR	perichromosomal region
pre-rRNA	47S pre-ribosomal RNA precursor
pRNA	rDNA promoter-associated noncoding RNAs
PTM	posttranslational modification
PTRF	Pol I and transcript release factor
pTyr	phosphotyrosine
Rb	retinoblastoma protein
RC	ring canal
RCC	renal cell carcinoma
rDNA	ribosomal RNA genes
RPA1, RPA190	DNA directed RNA polymerase I 190kD subunit
RpI135	DNA directed RNA polymerase I 135kD subunit
RpL	large subunit ribosomal protein
RpS	small subunit ribosomal protein
rRNA	ribosomal RNA
RSK	p90 ribosomal S6 kinase
RUNX	Runt-related transcription factor
S6K1	p70 ribosomal protein S6 kinase 1
Sax	Saxophone
SGP	somatic gonadal precursors
SL1, or Tif-IB (in mouse)	selectivity factor 1
snoRNP	U3 small nucleolar ribonucleoprotein
SSC	Somatic stem cell, or somatic cyst stem cells
Taf1B	TBP-associated Pol I-specific factor B
Taf1C	TBP-associated Pol I-specific factor C
TAFs	TBP-associated factors
T-ALL	T-cell Acute Lymphoblastic Leukemia
TBP	TATA-box-binding protein
TEM	transmission electron microscope
TF	terminal filament
Tif-IA, or RRN3 (in yeast)	transcription initiation factor IA
Tkv	Thick veins
TTF-I	transcription termination factor 1
UAF (yeast)	upstream activating factor complex
UBF	upstream binding factor
UCE	upstream control element
udd	under-developed
v-rDNAs	rDNA variants
WRN	Werner syndrome protein

WSTF	Williams syndrome transcription factor
Zpg	Zero population growth

CHAPTER I

Introduction about rRNA genes and regulation of RNA polymerase I transcription

The regulation of RNA polymerase I (Pol I) -directed rRNA gene transcription has been extensively studied in mammalian cell lines and yeast in the past decades. As the initial step of ribosome biogensis, rRNA synthesis is closely linked to cell growth and proliferation and has been found upregulated in many types of cancer. Therefore, rRNA gene transcription has become a new target for cancer treatment in recent years. Here in this introduction chapter, I will discuss about the regulation of Pol I transcription and potential therapeutic strategies targeting Pol I transcription for treatment of cancer and other diseases.

Introduction about rRNA genes

In eukaryotic cells, 100 to 10,000 copies of ribosomal RNA genes (rDNA) are usually arranged in clusters of tandem repeats mostly on multiple chromosomes [1-3]. The chromosome regions where rDNA localizes and rRNA transcription takes place are called nucleolar organizer regions (NORs) [4], around which the nucleolus forms. Despite the large copy numbers of rRNA genes, only a small fraction of them is actively transcribed at any give point in time. For example, in exponentially growing yeast cells, about 50% rRNA genes are active [5]. The NORs with active rRNA genes are called active NORs, while the ones with silent rRNA genes are called inactive NORs the chromatin organization of which is highly similar to the surrounding heterochromatic regions [6, 7].

From yeast to human, the rRNA gene transcribes 28S, 5.8S and 18S rRNAs together as a single pre-rRNA transcript by RNA polymerase I (Pol I), which is then processed in to mature 28S, 5.8S and 18S rRNAs (**Figure 1.1A**). Another 5S rRNA is transcribed by RNA polymerase III (Pol III),

and in yeast it is on the same chromosome with the other rRNAs while in human it is on a different chromosome [8, 9]. The processing rRNAs and mature rRNAs gradually bind to multiple ribosomal proteins as well as non-ribosomal factors and are exported from nucleolus and nucleoplasm to cytoplasm, finally becoming mature and functional ribosomes composed of rRNAs and ribosomal proteins. 18S rRNA is a component of the small subunit of cytoplasmic ribosomes, while the other rRNAs are components of the large ribosomal subunit. rRNAs are not only the structural components of ribosomes, but more importantly they exhibit catalytic peptidyl transferase activity in protein translation [10-12].

The rRNA gene repeats from different species have different lengths, ranging form less than 10 kb in yeast to more than 40 kb in mammals. In general, the coding sequences for 28S, 5.8S and 18S rRNAs are well conserved. Nevertheless, the non-coding regions including intergenic spacers (IGS, a.k.a. non-transcribed spacers or NTS), external transcribed spacers (ETS) and internal transcribed spacers (ITS) vary a lot between different organisms. Especially the intergenic spacers, where there are core promoter, upstream control element, promoter-proximal terminators, enhancer repeats, spacer promoters and other regulatory elements interacting with multiple protein complexes, share little sequence similarity. This sequence diversity leads to discrete sequence-specific DNA-protein interactions and may further result in different protein-protein interactions, causing species-specific rDNA transcription [13-15].

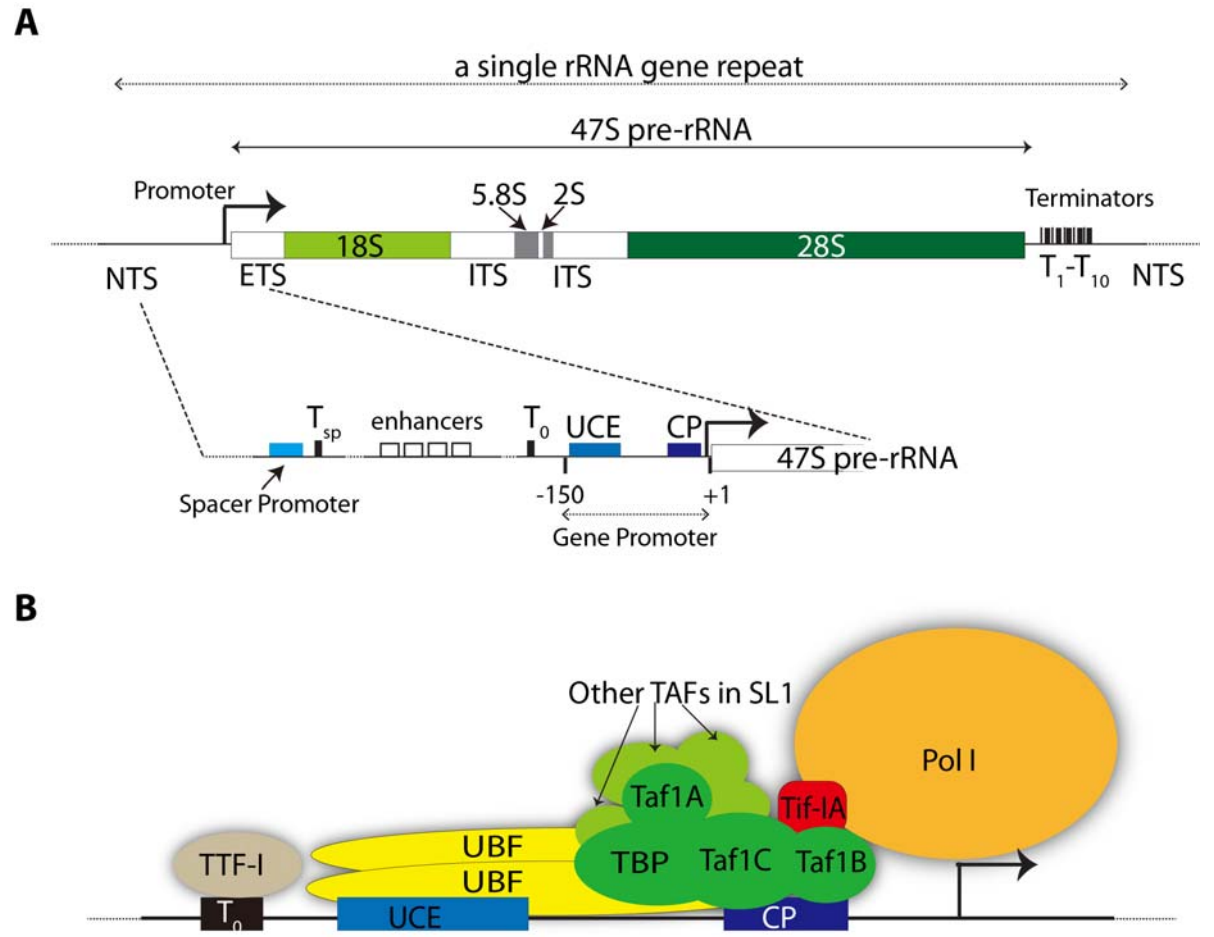

Figure 1.1. A typical eukaryotic rRNA gene repeat (A) and the mammalian basal Pol I machinery responsible for transcription initiation (B). (A) A 47S pre-rRNA is transcribed from the single rRNA gene repeat, which is then processed into the major ribosomal RNA components including18S, 28S and 5.8S rRNAs. In the non-transcribed spacer (NTS), the rDNA promoter contains the upstream control element (UCE) and the core promoter (CP), which is crucial for recruiting transcription initiation factors and PIC assembly. Upstream of the rRNA gene promoter, there are promoter-proximal terminator repeats, enhancer repeats and distal spacer promoters. NTS: a.k.a intergenic spacer (IGS); ETS: external transcribed spacer; ITS: internal transcribed spacer; T_1-T_{10}: terminator repeats at the 3' end of rRNA gene; T_0: promoter-proximal terminator repeats; T_{sp}: terminator sequence near the 3'end of the spacer promoter. (B) The dimerized mammalian UBF bind to UCE as well as other rDNA regions and interact with TBP and several TAFs in SL1. SL1 associates with the rDNA promoter mainly through Taf1B, Taf1C and TBP, and it subsequently recruits the Tif-IA bound RNA Pol I to the promoter and start PIC assembly and transcription initiation. TTF-I, when bound to promoter-proximal terminators, recruits different chromatin remodeling complex and is critical for establishing the active or silent state of rRNA genes. Note: 1. The yeast 5S rRNA gene is located upstream of and close to the 35S rRNA gene and transcribed in the opposite direction, while 5S rRNAs in other species are transcribed from a different region. 2. The NTS and ITS regions in distinct species from yeast to human exhibit different lengths and are not well conserved.

Basal RNA polymerase I transcription machinery

RNA Pol I complex consists of 12 subunits, all of which have identical or functionally related counterparts in RNA Pol II or Pol III complexes [16]. Among these subunits, the largest one RPA190 (a.k.a. RPA1) forms the polymerase active center together with the second largest subunit RPA135/RpI135 [17, 18]. It is known that there are two functionally distinct Pol I complex Pol I α and Pol I β, and only Pol I β, which is a small fraction of the total soluble Pol I pool, is initiation-competent and capable of accurate assembly at the rRNA gene promoter [19]. The major difference between these two Pol I complexes is that only Pol I β is associated with Tif-IA/RRN3, a transcription initiation factor essential for recruitment of Pol I β to the rRNA gene promoter. The promoter region of rRNA is mainly composed of two elements: core promoter and upstream control element (**Figure 1.1B**). In mammalian cells, the selectivity factor 1 (SL1) complex, which consists of TATA-box-binding protein (TBP) and several TBP-associated factors (TAFs), binds to the core promoter through direct contact of Taf1B, Taf1C and TBP with DNA sequence [3, 20-22]. In addition, an upstream binding factor (UBF) containing multiple HMG boxes dimerizes and binds to both UCE and core promoter region [23, 24]. UBF has been detected upregulated in hepatocellular carcinoma samples [25]. It is generally accepted that before rDNA transcription starts, UBF binds to TBP and a couple of TAFs recruiting SL1 complex to the core promoter, and SL1 complex recruits the Tif-IA-containing Pol I complex to the rDNA promoter through interaction of its Taf1B and Taf1C with Tif-IA, and at this time the pre-initiation complex (PIC) is assembled and ready for transcription initiation [3]. However, Zomerdijk lab has reported that the function of UBF is mainly to stimulate promoter escape of Pol I after transcription initiation, instead of facilitating recruitment or

stabilization of SL1 [26]. Additionally, a recent paper has claimed that yeast RRN3, the homologue of human Tif-IA, exhibited DNA binding activity itself which was essential for Pol I transcription [27].

After transcription initiation, RNA Pol I escapes from the rDNA promoter to be engaged in elongation, and Tif-IA is inactivated and released from Pol I complex [28]. At this time, UBF and SL1 remain bound to the promoter region, which is poised for the next round of initiation [29]. During elongation, Pol I associates with many other protein complexes. For example: in yeast, the RNA polymerase-associating factor 1 complex (Paf1C) has been reported to directly increase transcription elongation rate of Pol I [30]; in human, it is known that TFIIH, the multi-subunit DNA-excision repair protein and general transcription factor for RNA Pol II, is also essential for transcription elongation of Pol I [31, 32].

Once Pol I transcribes in to the terminator elements at the 3' end of the rRNA gene, it is paused by a DNA-binding protein called transcription termination factor 1 (TTF-I, a.k.a. Reb1 in yeast), and subsequently released from the template together with the terminated transcript by Pol I and transcript release factor (PTRF) [33-35]. Besides the function in promoting transcription termination, TTF-I has also been found to bind to promoter-proximal terminator elements and recruit different chromatin remodeling complex to the promoter region, which is critical for establishing the active or silent state of rRNA genes [36-42].

Consistent with the conservation of rRNA coding regions, the RNA Pol I complex shares a similarity from yeast to human. In addition, Tif-IA, TBP and multiple subunits of TFIIH are also well conserved. However, the protein complexes binding to the rDNA promoter or other regulatory elements in the NTS region are found to be poorly conserved and only show similarity among closely

related species, which is critical for species-specific regulation of Pol I transcription. For example, the SL1 complex in human is replaced by core factor complex (CF) in yeast, the members of which may be functionally similar but not in terms of primary sequence [21]. Also, mammalian UBF has no known homologs in *Drosophila*, *C. elegans* or yeast, and it is replaced by upstream activating factor complex (UAF) in yeast [43]. Even between mammals, there is evidence for molecular coevolution [14]. For example, the C-termini of human TTF-I and mouse TTF-I were found to be critical for species-specific DNA binding to the rDNA terminator sequence [44].

Epigenetic regulation of rRNA gene transcription

The active and silent NORs can be easily distinguished by combined immunostaining of Pol I-specific factors and fluorescent immunohybridization (immuno-FISH) of rDNA loci, and the co-localization of which can be visualized only in the active NORs [6]. Chromatin within inactive NORs is packaged quite similar to the surrounding heterochromatin. The active rRNA repeats are more open while the inactive repeats are more densely packed with nucleosomes. This difference forms the basis of assays that use psoralen crosslinking followed by restriction enzyme digestion to examine the ratio of active and inactive rRNA gene repeats in a cell line [7, 45]. The state of rRNA genes can be regulated epigenetically and multiple epigenetic marks associate with active and inactive rRNA genes. The active rRNA genes are usually hypomethylated and with the surrounding histones H3 and H4 hyperacetylated, while the silent rRNA genes are often hypermethylated at CpG and associated with hypoacetylated histones [6, 46]. The histone methylation marks are a little complicated, and usually H3K4me3 and H3K9me3 are linked to active and silent rRNA genes

repectively [47]. It has been reported that when di- and tri-methylated H3K9 marks are associated with the promoter region the rRNA gene may be repressed, however, H3K9me2&3 surrounding the rRNA transcribed region is an indicator for active transcriptional elongation [42, 48, 49].

A key factor for epigenetic regulation of Pol I transcription is TTF-I, which may also promote topological changes of rRNA genes by bringing the rRNA gene promoter in close proximity to its 3'end through oligomerization and binding terminator sequences at both ends [50-52]. When TTF-I is bound to the promoter-proximal terminator, it recruits many different chromatin remodeling complexes to rDNA and establishes the activated or repressed state in different contexts [6]. One of the earliest TTF-I interacting remodeling complexes found is the TIP5-SNF2h containing nucleolar remodeling complex (NoRC) [53]. The large subunit of NoRC, TIP5, binds to acH4K16-containing nucleosomes, recruits histone deacetylase HDAC1 and DNA methyltransferase Dnmt1 and Dnmt3b to induce H4 deacetylation and DNA methylation around the rDNA promoter respectively. NoRC also mediates dimethylation of H3K9, which further establishes the silencing of rRNA gene transcription [49, 54-56]. Besides proteins, transcripts from rDNA intergenic spacers (promoter-associated RNAs, pRNAs), which are also transcribed by Pol I, have been shown to associate with the rDNA promoter, NoRC and TTF-I and promote the formation of heterochromatic configuration near rDNA promoter *in trans* [57-59]. These noncoding RNAs together with NoRC have been recently reported to interact with a DNA damage repair protein Poly (ADP-Ribose) polymerase 1 (PARP-1), which mediates the inheritance of silent rDNA chromatin during cell division [59]. Consistently, the activation of PARP-1 in DNA damage-stimulated S phase-arrested cells has been found to inhibit rRNA synthesis [60], although *Drosophila* PARP-1 was reported to positively regulating rRNA processing and other

post-transcriptional steps [61]. A PARP-1 interacting protein and substrate CCCTC-binding factor (CTCF) has been shown to work as a chromatin insulator after poly(ADP-ribosyl)ation and involved in repressing nucleolar transcription [62-65]. Moreover, poly(ADP-ribosyl)ated CTCF is observed decreased in breast tumors [62].

Another TTF-I binding remodeling protein is Cockayne syndrome group B (CSB) protein, a DNA-dependent ATPase and DNA repair protein often found in a complex with RNA Pol I and TFIIH [42, 66]. CSB loss-of-function mutations are often found in patients with Cockayne syndrome marked by mental/physical retardation, neurological and retinal degeneration, tissue atrophy and premature ageing. Recently one paper has reported that CSB is found overexpressed in many cancer cell lines promoting tumor growth [67]. CSB has been reported to associate with TTF-I and recruit histone methyltransferase G9a which acts on mono- and di-methylated H3K9 at the transcribed rDNA region, positively regulating transcription elongation [42]. Moreover, a paper in 2013 has shown that CSB also plays a role in promoting transcription initiation by recruiting PCAF to the rDNA promoter and inducing H3/H4 acetylation [68]. In addition, the nucleosome remodeling and deacetylation (NuRD) complex, which contains Class I histone deacetylases (HDACs), the ATPases/helicases CHD3 and CHD4 and methyl-CpG binding domain proteins MBDs, binds to TTF-I and CSB and helps to establish the poised state of rRNA genes marked by hypomethylated rDNA promoter, bivalent histone modifications and altered nucleosome positions near the promoter [41]. The poised rRNA gene promoters are marked by upregulated H4K20me3 and promoter-bound nucleosomes, and the trimethylation of H4K20 is correlated with upregulation of antisense RNAs (asRNAs) transcribed by Pol II from antisense strand of the pre-rRNA coding region and intergenic spacers. asRNAs bind to

histone methyltransferase Suv4-20 which may be recruited to rDNA promoter and triggers H4K20me3 *in vivo* [69].

Besides the complexes mentioned above, an energy-dependent nucleolar silencing complex eNoSC, consisting of a nucleolar repressor protein Nucleomethylin (NML), NAD^+-dependent Class III HDAC SIRT1 and histone methyltransferase SUV39H1, has also been demonstrated to cause H3 deacetylation as well as H3K9 dimethylation, suppress rRNA gene transcription and protect cells from apoptosis under calorie-restricted conditions like glucose deprivation [70]. Consistently, the NAD^+ synthesis enzyme NMNAT1, which has recently been shown to bind to NML, stimulate SIRT1 deacetylase activity and repress rRNA synthesis, is frequently deleted in human cancers that usually exhibit high levels of rRNA transcription [71].

In addition, the Percipalle group and the Ostlund group have recently shown that a second SNF2h-containing chromatin remodeling complex B-WICH, composed of Nuclear actin and myosin 1 (NM1), WSTF (Williams syndrome transcription factor) and SNF2h, is required to activate rRNA genes, probably through recruitment of histone acetyltransferase PCAF to the rDNA promoter [72-74].

Several other histone modification enzymes activate or suppress rRNA gene transcription. For example, PHD finger protein 8 (PHF8) binds to RNA Pol I, UBF and H3K4me3, demethylates H3K9me1&2 and activates rRNA transcription [48]. Another two JmjC-domain-containing histone demethylases JHDM1A and JHDM1B have been demonstrated to associate with rRNA gene promoter and transcribed regions respectively, both of which repress transcription of rRNA genes. JHDM1A induces demethylation of H3K36me1&2 stimulated by starvation, while JHDM1B mediates

demethylation of H3K4me3 [47, 75]. Dysregulation of these enzymes are often linked to different diseases: PHF8 mutations are associated with x-linked mental retardation, while PHF8 overexpression is found in prostate cancer cells [76]; low expression of JHDM1B is found in brain tumors but its upregulation has also been observed in many other tumors including leukemias [47, 77].

In general, besides regulating rRNA genes, the chromatin modifiers mentioned above mostly have multiple targets that are regulated spatially and temporally, therefore the distinct disease phenotypes are often a combined dysregulation of different target genes. In consideration of this, therapeutic methods targeting these proteins should have a strict tissue- if not cell- specificity.

Regulation of RNA Pol I transcription by factors involved in DNA damage response, DNA repair and cell cycle progression

In addition to CSB, TFIIH and PARP-1, many other proteins involved in DNA damage response and cell cycle regulation have been related to rRNA gene transcription. ATP-dependent DNA helicases Bloom's syndrome protein (BLM) and Werner syndrome protein (WRN) associate with RNA Pol I and facilitate rRNA transcription probably through modulation of rDNA structure [78, 79]. The loss of these DNA repair proteins BLM, WRN, CSB and the TFIIH components XPB&XPD causes similar phenotypes in human including premature ageing, growth arrest and/or mental retardation and tissue atrophy.

Type I and II DNA topoisomerases produce topological changes to DNA sequences and have been shown to positively regulate RNA Pol I transcription. Topoisomerase I was reported to promote rRNA transcriptional elongation more than two decades ago, while topoisomerase IIα has

just been discovered to directly bind to TIF-IA/RRN3 and facilitate PIC formation this year [80, 81]. In consideration of their function in promoting rRNA synthesis and DNA damage response, it is not surprising to see upregulation of these factors, especially topoisomerase IIα, in many cancer cells [82]. Topoisomerases have been reported to interact with helicases mentioned above, like BLM [83, 84], and these enzymes are often anti-cancer targets [82, 85].

Other factors that play a role in DNA damage response and cell cycle regulation also influence rRNA transcription. For example, DNA-binding protein PHF6, despite the lack of catalytic domains, associates with UBF and the rRNA gene promoter suppressing RNA Pol I transcription initiation [86]. The mutations of PHF6 were initially found associated with an X-linked mental retardation disorder Börjeson-Forssman-Lehmann syndrome (BFLS) and are often present in T-cell Acute Lymphoblastic Leukemia (T-ALL) samples. It is reported that knocking down PHF6 results in increased rRNA transcription, impaired cell proliferation, cell cycle arrest at G2/M phase and increased DNA damage at the rDNA locus.

Another example is the actin-binding cytoskeleton protein Filamin A. Filamin A interacts with DNA damage response proteins BRCA1&2 and promote DNA double strand break repair, which has been considered as a biomarker and a target for DNA damage based cancer therapy. A portion of human Filamin A has been observed to localize in the nucleolus, associate with RNA Pol I, RRN3 and UBF, and suppress the recruitment of Pol I to the rDNA promoter through its actin-binding domain. Mouse Filamin A also directly interacts with Taf1B in yeast two hybrid and GST-pull down assays [87-90].

In general, most tumor cells exhibit genomic instability and increased Pol I transcription

level, and presumably the drugs designed to target DNA repair proteins related to both features could be potent killers of cancer cells.

Regulation of rRNA gene transcription by other factors

Besides DNA helicases mentioned above, some RNA helicases are also found to have novel nucleolar functions in regulating rRNA transcription. DHX33, an ATP-dependent DEAH box RNA helicase, interacts with UBF and associates with the rDNA promoter and transcribed region. This interaction is essential for pre-rRNA synthesis not rRNA processing [91]. Another ATP-dependent DEAD box RNA helicase, DDX31, exhibits increased expression in most of the renal cell carcinoma (RCC) samples. The protein colocalizes and interacts with nucleophosmin (NPM) in RCCs and is required for the nucleolar localization of NPM and for high levels of pre-rRNA biogenesis [92]. In addition, the downregulation of both helicases results in p53 stabilization and impaired cell proliferation.

Control of the activity of basal RNA polymerase I machinery by posttranslational modifications

The active rRNA gene numbers and the protein expression levels of components associated with the basal RNA polymerase I machinery demonstrate a correlation with the level of rRNA synthesis under different conditions as mentioned above. Moreover, the activity of rRNA transcription is also modulated through posttranslational modifications (PTMs) of basal components of RNA Pol I machinery including phosphorylation and acetylation events, which are cell cycle-, mitogenic factor- or nutrient- dependent.

1. UBF

The most extensively studied Pol I factor subject to PTMs is mammalian UBF. First, the C-terminal domain (CTD) of UBF has been shown to carry multiple phosphorylation sites, which promote its direct association with TBP and other members of SL1 complex and help recruiting SL1 to the rDNA promoter [24, 93]. Some phosphorylation events of UBF have been found to be cell-cycle dependent and correlated with the fluctuations of rRNA gene transcription levels during different phases. The activation of UBF starts in G1 phase from Ser484 phosphorylation by G1-dependent cyclin-dependent kinases (CDKs)-cyclin complexes [94]. UBF activity is then enhanced further during S phase and G2 phase by CDK2/cyclin E- and CDK2/cyclinA- mediated Ser388 phosphorylation which promotes UBF interaction with RNA Pol I and increases upon high glucose stimulation in kidney glomerular epithelial cells [95, 96]. The interphase CDKs or cyclins are often found overexpressed in various malignant tumors [97], and their activation of UBF and upregulation of rRNA synthesis could partially contribute to the tumor phenotype. UBF inactivation during mitosis probably also depends on phosphorylation [98], although the exact phosphorylation sites for this phase have not been discovered. In addition to PTM changes related to cell cycle progression, there are other kinases reported to mediate UBF phosphorylation in response to cell growth or other stimuli [99]. For example, casein kinase II (CKII), a kinase involved in different cellular processes including cell growth/proliferation/survival and the expression level and activity of which are upregulated in many human cancers, has been reported to co-purify with RNA Pol I/Tif-IA complex, associate with the rRNA gene promoter and phosphorylate multiple amino acids at the CTD

of UBF stabilizing the association of UBF with SL1 [99-102]. Moreover, the nutrient- and growth factor- dependent mammalian target of rapamycin (mTOR) signaling also promotes rRNA transcription through activation of Pol I-associated factors including phosphorylation of the CTD of UBF as shown in mouse fibroblasts and postmitotic cardiac muscle cells. This activation appears sensitive to rapamycin treatment and requires active ribosomal protein S6 kinase 1 (S6K1) [103]. Additionally, UBF can be directly phosphorylated by the phosphatidylinositol 3-kinase (PI3K) subunit still mostly at the CTD upon stimulation by the insulin-like growth factor I receptor/insulin receptor substrate 1 (IGF-IR/IRS1) axis [104, 105]. Distinguished from the IGF-IR/IRS1 axis, the InR/IRS2 axis promotes cell cycle progression and proliferation, although it also helps to stabilize UBF and maintain rRNA trasncription, as tested in IRS1&2-deficient 32D myeloid cells [106-108].

Second, the HMG boxes of UBF can be phosphorylated at Thr117 and Thr201, which is mediated by MAP kinase ERK1/2 upon epidermal growth factor (EGF) induction. This signaling pathway regulates rRNA gene chromatin remodeling and promotes transcription elongation instead of initiation, and the loss of HMG box phosphorylation represses elongation [109, 110].

Third, the acetylation of UBF, which mostly exists in S and G2 phase as examined in mouse fibroblasts, also promotes rRNA gene transcription [111]. HDAC1, besides its function in epigenetic regulation of rRNA gene transcription, is recruited by the osteogenic transcription factor Runx2 or the retinoblastoma protein (Rb) in different cell lines, and mediates deacetylation of UBF both *in vitro* and *in vivo*, thus preventing its association with Pol I [111-113]. Histone acetyltransferases CBP and p300 but not PCAF acetylates UBF *in vivo* and *in vitro*, especially the CREB binding protein CBP which exhibits nucleolar localization [114]. It is reported that CBP and Rb compete for the same

region of UBF to activate or repress rRNA synthesis [112]. CBP acetylates UBF at least on Lys352 [115].

2. Tif-IA

The PTMs of Tif-IA are mainly phosphorylation events occurring at multiple serine residues in response to changes in nutrients, growth factors or energy status. Many kinases have been reported to regulate the phosphorylation and activation of both UBF and Tif-IA. First, the mitogen-activated protein kinase signaling cascades target Tif-IA to induce rRNA synthesis and promote cell growth. MAP kinases ERK and RSK phosphorylate Tif-IA at Ser633 and Ser649 [116], and Ser649-phophorylated Tif-IA is required for Pol I association with NM1, a member of the B-WICH complex mentioned above which plays a positive role in growth-dependent regulation of Pol I transcription [117]. Second, mTOR signaling also regulates the activity and nucleolar localization of Tif-IA [118]. The mTOR inhibitor rapamycin inactivates Tif-IA, and leads to hypophosphorylation of Ser44 and hyperphosphorylation of Ser199. The G1-specific CDK2/cyclin E and protein phosphatase 2A (PP2A) phosphorylate and dephosphorylate Tif-IA Ser 44 respectively, in an mTOR-dependent manor. The inhibitory Ser199 phosphorylation of Tif-IA impairs its interaction with Pol I. The exact phosphatases and kinases that regulate this PTM remain unknown. Third, CKII directly phosphorylates Ser170/172 and promotes Tif-IA release from Pol I after initiation [119]. Counteracting CKII on the same residues, phosphatase FCP1 associates with the rDNA promoter and Pol I/Tif-IA complex and promotes a new round of transcription initiation. Lastly, Hoppe et al. reported that AMP-activated protein kinase (AMPK) mediates Ser635 phosphorylation of Tif-IA,

impairs Tif-IA interaction with SL1 complex and causes downregulation of rRNA synthesis under glucose restriction [120].

In addition to serine residue phosphorylation, a threonine residue Thr200 of Tif-IA is phosphorylated by c-Jun N-terminal kinase (JNK) upon cellular stress such as ribotoxic and oxidative stresses, which results in inactivation and translocation of Tif-IA from the nucleolus to the nucleoplasm and blocks PIC formation as a protection against stress [121].

3. SL1 complex

The components of SL1 complex Taf1C and Taf1B are phosphorylated in both mitotic cells and asynchronous cells [122]. The functional significance of these phosphorylation events during interphase is not known, however SL1 phosphorylation in mitotic cells has been linked to silencing of rRNA transcription. In contrast to Taf1B and Taf1C, TBP is specifically phosphorylated during mitosis. *In vitro* studies show that the mitosis-specific cdc2/cyclin B kinase mediates mitotic phosphorylation of TBP and Taf1C. Taf1C phosphorylation during mitosis may be more critical for SL1 inactivation and Pol I transcription repression by reducing SL1 interaction with UBF [122, 123].

In addition to phosphorylation events, the Taf1B subunit can be acetylated based on *in vivo* and *in vitro* studies [124]. The acetylation of Taf1B, mediated by TTF-I associated histone acetyltransferase PCAF, enhances Taf1B binding to the rRNA gene promoter and activates Pol I transcription. In addition, the NAD^+-dependent histone deacetylase Sir2 in mouse deacetylates Taf1B *in vitro* and represses rRNA synthesis.

4. Other factors in the Pol I transcription machinery

Similar to SL1, the phosphorylated form of TTF-I, the factor involved in regulation of both rRNA transcription termination and initiation, is also present in G2/M phase dependent on cdc2/cyclin B kinase and associated with inactive Pol I transcription machinery [125].

Besides the Pol I associated factors, RNA Pol I complex itself is a phosphoprotein complex with multiple site-specific phosphorylations. Phosphorylation of yeast Pol is required for stable association with RRN3/Tif-IA and efficient transcription initiation [126]. However, another paper has shown that the individual phosphorylation events of Pol I are probably not essential according to single mutation studies in yeast [127].

One thing to note is that the enzymes regulating PTMs of Pol I associated factors mostly have many targets involved in different signaling pathways and are often recognized as both tumor suppressors and oncogenes. This makes it hard to target those enzymes for downregulation of Pol I transcription and treatment of cancers. Small molecules may be designed to attenuate or enhance the PTMs of Pol I associated factors but not those of other proteins mediated by the same enzyme.

Regulation of rRNA synthesis by oncogenes, tumor suppressors, and oncogenic signaling pathways

Many oncogenes and tumor suppressors have been demonstrated to regulate Pol I transcription through both direct and indirect mechanisms: Some factors directly bind to components of basic Pol I transcription machinery; some affect the posttranslational modifications of Pol I components and change their activities; some recruit chromatin remodeling complexes and modify the

epigenetic state of rRNA genes; some others also play a role in transcriptional regulation of genes involved in ribosome biogenesis and affect the expression levels of those genes. Here I discuss a few examples that have been extensively studied.

1. c-Myc

The Myc proteins are observed upregulated in many types of cancers [128, 129]. As a beta helix-loop-helix transcription factor, Myc forms a heterodimer with its partner Max and regulates transcription of various genes to promote cell growth and proliferation. In human, c-Myc has been shown to directly bind to SL1 complex and associate with the rDNA promoter enhancing rRNA synthesis [130, 131]. Moreover, Myc also promotes transcription of genes regulating multiple steps of ribosome biogenesis including those encoding the basic Pol I components, and they are often upregulated in c-Myc-driven tumors (reviewed in [132]). In *Drosophila*, dMyc does not bind to rDNA directly and it promotes Pol I transcription only through the second mechanism [133].

2. p53

Tumor suppressor p53 regulates cell growth, cell cycle and apoptosis, and mutations of p53 are often present in many cancers [134, 135]. The protein level of p53 is regulated by an E3 ubiquitin ligase MDM2 which targets p53 for proteasome-mediated degradation, and MDM2 is phosphorylated and inhibited by another tumor suppressor protein ARF [136]. Multiple studies using different cell lines have shown that p53 deletion or mutations are correlated with upregulation of rRNA synthesis [137, 138]. The Comai group showed that p53 inhibited rRNA transcription *in vitro* and *in vivo*, and it

directly bound to SL1 and blocked SL1 interaction with UBF interfering with efficient PIC assembly [138]. Consistent with this, several studies further demonstrated that part of p53 was translocated to fibrillar center, a sub-nucleolar compartment where Pol I transcription takes place, after treatment with proteasome inhibitor MG132 [139, 140]. However, a later paper reported that nucleolar localization of p53 after MG132 treatment was not where rRNAs are synthesized, raising the possibility that the repression of Pol I transcription by p53 is through an indirect mechanism [141].

3. Rb

Tumor suppressor Retinoblastoma protein (Rb) regulates cell cycle progression/ cell proliferation and promotes genomic stability (reviewed in [142]). Rb has been observed to repress Pol I transcription by directly associating with and inactivate UBF, either blocking UBF interaction with SL1 or its binding to rRNA gene promoter [143-145]. As mentioned above, here the inactivation of UBF is caused by deacetylation mediated by HDAC1, which is recruited by Rb and opposes the activity of the acetyltransferase CBP [112].

4. Nucleophosmin

Nucleophosmin (NPM, a.k.a. B23), a ubiquitous phosphoprotein and chaperone mostly enriched in nucleoli, has various cellular functions through its interaction with different partners, and impacts many steps of ribosome biogensis (reviewed in [146, 147]). Overexpression of NPM is present in many solid tumors, while its mutations are often found in acute myeloid leukemias (AMLs). As to its role in rRNA transcription, the histone chaperone activity of NPM is important for promoting

rRNA synthesis [148]. Recently the Hann group has demonstrated that NPM directly binds to c-Myc, promotes the nucleolar localization of c-Myc independent of proteasome degradation pathway, and induces c-Myc mediated rRNA synthesis [149], which is consistent with upregulation of both genes in solid tumors. Interestingly, another group has reported that NPM recruits an F-box protein Fbw7γ, a component of the E3 ligase complex, to the nucleolus to promote the ubiquitination and proteasome degradation of c-Myc. This may explain why in AMLs there is upregulation of c-Myc together with mutations of NPM [150]. In addition to c-Myc, p53, which prevents rRNA synthesis, is also regulated differentially by NPM depending on its targeting of either MDM2 or ARF [151, 152]. These studies further reveal the complicated roles that NPM plays in a cell as both an oncogene and a tumor suppressor.

5. Oncogenic signaling pathways

Many oncogenic signaling pathways that are hyperactive in cancers promote Pol I transcription as well as other steps of ribosome biogenesis through PTMs (mainly phosphorylation events) of key factors involved in those steps. The PTEN/PI3K/AKT/mTOR/S6K pathway and the RAS/RAF/MEK/ERK/RSK pathway are two major pathways, and they are often interconnected ([153, 154], reviewed in [155]). Many kinase components, such as PI3K, S6K, ERK and RSK have been reported to regulate activities of UBF and Tif-IA and enhance either the transcription initiation or elongation step, as mentioned in the “PTM-regulation of Basic Pol I Machinery” part. Moreover, PTEN, a phosphatase and a negative regulator of PI3K signaling, was shown to repress rRNA transcription [153]. In addition, GSK-3, a kinase inhibited by AKT, negatively regulates Myc activity

through Thr58 phosphorylation, which counteracts the prior ERK phosphorylation of Myc at Ser62 and promotes Myc degradation [156, 157].

Cell-specificity and tissue-specificity of rRNA synthesis requires in-depth studies

Despite the facts that cancer cells usually exhibit upregulated rRNA transcription level and that a large number of factors have been discovered to directly or indirectly regulate Pol I transcription in different cell lines, how rRNA transcription is differentially regulated in different tissues, different lineages, or cells within the same lineage during differentiation or development is not well understood. Answering these questions will be very important for designing a Pol I transcription-specific inhibitor targeted for treatment of a specific cancer. There are several possibilities for Pol I transcriptional regulation, which may lead to various cell-specific drug design strategies: 1. pre-rRNA levels are probably varied in different cells/tissues; 2. even if two neighboring cells/tissues have quite similar pre-rRNA levels, their Pol I transcriptional activities may be different, since one might carry more active rRNA gene copies than the other; 3. even if their Pol I transcriptional activities are the same, the factors regulating rRNA transcription might exhibit diverse expression levels or PTMs, resulting in a combination of miscellaneous positive and negative effects on Pol I activities, and more importantly it may lead to translational suppression or enhancement of specific transcripts crucial for differentiation and development.

First, in terms of tissue and lineage specificity, Runt-related transcription factor 2 (Runx2) which is a lineage-specific factor important for osteoblast differentiation, not only regulates gene transcription from RNA Pol II but also represses rRNA gene transcription by recruiting HDAC1 and

causing deacetylation of UBF and histone H3/H4 [158]. However, it is not known if there are any changes of Pol I transcription levels and how Pol I transcription is related to cell fate changes in Runx2-expressing tissues. Moreover, Runx2 regulates multiple target genes and works as both an oncogene and a tumor suppressor (reviewed in [159, 160]). Besides Runx2, another Runt-related factor essential for hematopoiesis Runx1 is also related to Pol I transcription. In acute myeloid leukemia (AML), chromosome translocations often target Runx1 and produce a fusion protein between Runx1 and another protein Myeloid transforming gene on chromosome 8 (MTG8/ETO). While knocking down Runx1 led to a moderate upregulation of pre-rRNA levels in myeloid cell lines, knockdown of the fusion protein mildly reduced Pol I transcription activity [161]. This at least partially explains why AML cells are hyper-proliferative. Similar to Runx2, Runx1 and the fusion protein also have a large number of gene targets.

Next, there are some preliminary studies focusing on differentially expressed rDNA variants (v-rDNAs) in mouse [162, 163]. Based on restriction fragment length polymorphisms, it was found that some v-rDNAs were constitutive active and others were silent or selectively expressed in specific tissues. However, comparing mouse oocytes and 8-cell preimplantation embryos, there were no obvious qualitative variant subtype changes during preimplantation development. Further studies are required to determine if v-rDNA changes are critical for development of other tissues in different stages.

Although some specific Pol I regulators have been discovered to get activated or repressed upon changes of nutrients or energy status which modulates rRNA synthesis, the pre-rRNA levels are not well examined or compared during development. Several groups have shown, from either primary

or immortalized cell lines, that before and after induced *in vitro* differentiation there are changes (mostly a reduction) in rRNA transcription levels [164-166]. These differences were related to changes of UBF or SL1 quantity or activity. As to *in vivo* studies, there is not much information published. However, our group has recently demonstrated that in *Drosophila* ovaries, the level of rRNA transcription is correlated with the differentiation status of female germ cells (see **Chapter III-V** in this thesis). Female germline stem cells (GSCs) displayed higher levels of rRNA transcription than early differentiating cysts. Subsequently, pre-rRNA levels increase again in the later more differentiated germ cells (manuscript under revision). This difference was shown both in wild type ovaries and also in undifferentiated ovaries before and after introduced differentiation. In addition, increase rRNA transcription leads to a mild expansion of GSCs. Moreover, I also discovered a novel Pol I regulator Under-developed (Udd) in *Drosophila* which was shown to work together with Taf1B regulating Pol I transcription initiation, and downregulation of these factors in ovaries filled with undifferentiated GSC-like cells resulted in multicellular cyst formation. Besides germline tissue, it was also observed that knocking down Pol I associated factors specifically in the eye resulted in not only smaller eyes but also additional antennal segments in that region (See **Chapter V Discussion Figure**). Previously the DiMario group reported a similar eye-to-antenna phenotype with knockdown of *Drosophila* nucleostemin 1 (NS1), a factor affecting rRNA processing and the large ribosomal subunit biogenesis [167]. Both studies suggest that different rRNA levels are required during development of eye and antenna, which might affect the expression levels of specific genes needed for either antenna or eye development. These intriguing findings from Drosophila tissues are all indicating that RNA Pol I transcription, as the first step of ribosome biogenesis, is not only important

for cell growth and proliferation but also necessarily correlated with cell differentiation and tissue development.

Small molecules targeting RNA Pol I transcription are being investigated for cancer treatment

Several approved anti-cancer medicines have been reported to play a role in inhibiting Pol I transcription, such as cisplatin and Actinomycin D (reviewed in [168]). Moreover, developing anti-cancer drugs that target Pol I specifically has become a trending research topic in recent years. The first small molecule inhibitor is CX-3543 (Quarfloxin), which inhibits Pol I transcription, induces apoptosis in cancer cells and is currently tested in Phase II clinical trials [169]. The next generation of CX-3543, CX-5461, has been shown to specifically inhibit rRNA transcription by competing SL1 from the rRNA gene promoter and is also at the clinical stage [170, 171]. This molecule exhibits anti-proliferative activity in many cancer cell lines, but it is much less effective in normal nontransformed cells. Intriguingly, treatment of solid tumor cells by CX-5461 induces autophagy and not apoptosis, while its treatment of leukemia and lymphoma cells activates the p53-dependent apoptotic signaling pathway. Recently, some molecules from the anti-cancer ellipticine family have been observed to specifically inhibit transcription from RNA Pol I but not Pol II or Pol III [172]. These ellipticine molecules, including 9-hydroxyellipticine (9HE), affect SL1 interaction with rRNA gene promoter and influence PIC assembly and stability. In addition, structure alignment of 9HE and CX-5461 demonstrates that they have similar aromatic cores and can be docked similarly on the DNA strand, which suggests that this structure basis might be utilized to design new potent Pol I-specific inhibitors for cancer therapy.

Since most of the upstream regulators of Pol I have multiple downstream target genes, looking for drugs that are specific for basic Pol I transcriptional regulation and even for a particular cell context, is very critical for getting high efficacy and low toxicity. Besides the absolute specificity of drugs, it is necessary to study rRNA transcription levels in various tissue/lineage/developmental periods. In addition, it is also important to study the expression levels and PTMs of key Pol I transcriptional regulators in different contexts. More knowledge about those questions may help decreasing drug resistance and improving cell-sensitivity of cancer cells. Therefore, the differentially regulated Pol I factors may be targeted to repress Pol I activity cell-specifically for treatment of a specific cancer.

CHAPTER II

Materials and Methods

Fly stocks

Fly stocks were maintained on standard cornmeal molasses agar at 22-25°C unless otherwise noted. The following stocks were used in this study:

1. Fly stocks from Bloomington *Drosophila* Stock Center: (stock number given in parentheses)

   PBac{WH}f00130 (#18295),

   w^{1118} (#6326),

   CyO, P{FRT(w^{+})Hsp70-PBac\T}2/wg^{Sp-1} (#8284),

   P{ry[+t7.2]=neoFRT}42D P{w[+mC]=piM}45F (#2120),

   P{XP}d07339 (#19269),

   P{w[+mC]=His2Av-mRFP1}III.1 (#23650),

   P{otu-GAL4::VP16.R}1,w; P{GAL4-nos.NGT}40; P{GAL4::VP16-nos.UTR}CG6325*^{MVD1}

   Materal Triple Driver (MTD)-Gal4 (#31777),

   w**; Kr*$^{If-1}$*/CyO; D*^{1}*/TM3, Ser*^{1} (#7198),

   P{y[+t7.7] v[+t1.8]=TRiP.HMS00029}attP2 (#33631),

   P{y[+t7.7] v[+t1.8]=TRiP.GL00641}attP40 (#38202),

   P{y[+t7.7] v[+t1.8]=TRiP.GL00340}attP2 (#35418),

   P{y[+t7.7] v[+t1.8]=TRiP.GL00556}attP2/TM3 (#36596),

   P{y[+t7.7] v[+t1.8]=TRiP.HMS00564}attP2 (#33694),

   P{y[+t7.7] v[+t1.8]=TRiP.GL00332}attP2 (#35410),

   P{y[+t7.7] v[+t1.8]=TRiP.GL00339}attP2 (#35417),

   P{y[+t7.7] v[+t1.8]=TRiP.HMS00969}attP2 (#34096),

Deficiency kit on the 2R chromosome;

2. Fly stocks from Exelixis collection at the Harvard Medical School:

PBac{WH}f00102,

PBac{RB}e00152,

P{XP}d08197,

Some other lines that are also available from Bloomington Stock were ordered there.

3. Fly stocks form other resources:

bam$^{\Delta 86}$/TM3,

bampGFP^{702}, bam$^{\Delta 86}$/TM3

y w hsFLP; [FRT]42D UbiGFP/CyO,

P[daughterlessP-Gal4] (*da-gal4*, 3rd chromosome),

P[nanosP-Gal4] (*nos-gal4*) (two lines, on the 2nd and 3rd chromosome respectively),

P[eyelessP-Gal4] (*ey-gal4*, 2nd chromosome)

w*; wg[Sp-1]/CyO; Dr[1]/TM3, Sb[1],

hs-bam (the above lines are all gifts from D. Mckearin);

RpS2 protein trap line CB02294 (gift from A. Spradling);

18316R-2 (UASt-RNAi for CG18316, line #1, NIG-Fly in Japan).

P{GD9557}v25312 and *P{GD9557}v25313* (UASt-RNAi for CG18316, line #3 and #2, Vienna Drosophila RNAi Center (VDRC)),

P{GD6995}v16061 and *P{KK106197}VIE-260B* (UASt-RNAi for CG10496, VDRC),

P{KK104706}VIE-260B (UASt-RNAi for CG6241, VDRC),

P{GD4201}v12688 (UASt-RNAi for CG10122, VDRC),

P{GD4178}v37581 (UASt-RNAi for CG4033, VDRC),

(Note: all these UASt-RNAi lines mentioned above are used to examine knocking-down phenotype in somatic cells, and they usually do not express RNAi well in the germline.)

Generation of new mutant alleles and transgenic lines

The udd^{1} allele was isolated as a background mutation from the Exelixis stock *PBac{WH}f00130* (Bloomington stock 18295). Remobilization of the inserted piggyBac element were done by crossing those flies to a line carrying *T.ni* piggyBac Transposase under the control of *hsp70* promoter (BL8284), heat-shocking and outcrossing the progeny [173]. Excision of the piggyBac transposon did not reverse the recessive sterile phenotype. Meiotic recombination and deficiency lines were used to map the mutation causing the sterile phenotype (see Chapter III for more details, **Figure 3.5A**).

The udd^{null} allele was generated by FLP/FRT mediated recombination using two Exelixis lines in *trans; P{XP}d08197* and *PBac{WH}f00102* [174]. These lines carry FRT sites in their insertions, and recombination of FRT sites were achieved using exogenous flippase recombinase from yeast which resulted in a precise deletion of a region in between those insertions. Three other deficiency lines *Exel(e00152-d8197)*, *Exel(d07339-f00102)* and *Exel(d07339-e00152)* were made similarly by FLP/FRT mediated recombination for mapping the gene by non-complementation of the sterile phenotype (see Chapter III for more details, **Figure 3.5B**).

Our lab combined the phiC31 integrase transgenesis system [175] with the *Drosophila*

Gateway™ expression system (http://emb.carnegiescience.edu/labs/murphy/Gateway%20vectors.html) to generate pPHW vector with attB site for targeted insertion in flies. The phiC31 integrase is a sequence-specific serine recombinase from bacteriophage phiC31, mediating recombination between the phage attachment site (attP) and the bacterial host attachment site (attB). In flies and other organisms, phiC31 integrase is used to integrate the attB-containing donor plasmid unidirectionally into a genome through recombination at sites similar to attP site. Moreover, when phiC31 integrase is under a germline-specific promoter such as *vasaP* or *nanosP* in *Drosophila*, the integration takes place only in the germline and transgenic flies will come out in the next generation of the injection flies. The transgenic lines made with this pPHW vector include *UASp-HA-Udd ORF* (96E landing site), *UASp-HA-Tif-IA ORF* (51D landing site), *UASp-HA-Taf1B ORF* (51D landing site), *UASp-HA-RpI135 ORF* (51D landing site), *UASp-HA-CG10496 ORF* (86Fb landing site), *UASp-HA-Cul4 ORF* (96E landing site), *UASp-HA-CG8712 ORF* (96E landing site), *UASp-HA-CG11210 ORF* (96E landing site). The last three lines were used only for mapping the udd^{1} mutation by sterility rescue assay.

Transgenic lines made with the *P[acman] Bac* vectors *CH322 -148I23, -138I13 and -11K08* [176] were also generated using phiC31 integrase with 96E as the landing site and used for rescue experiments. *Udd-GFP* transgenic line was generated by engineering a GFP tag into the *P[acman]* vector *CH322-148I23* replacing the *udd* stop codon with GFP. This *Udd-GFP* construct was used to transform flies carrying the 65B landing site.

The VALIUM 22 and VALIUM 20 vector (gift from N. Perrimon) were used to make UAS-RNAi lines for *Taf1B*, *RpI135* and *CG10496*. The 21nt sequences

CAGGACGATCCGACAGAAGAA (for *Taf1B*), CGGAGTTTAAGCAGATACCTA (for *RpI135*) and CAAATTCAATTTGTTAACTAA (for *CG10496*) were chosen using DSIR online tool (http://biodev.extra.cea.fr/DSIR/DSIR.html). The corresponding oligos were designed, annealed, and ligated into VALIUM 22 vector and VALIUM 20 vector (*CG10496* only) following instructions from TRiP website (http://www.flyrnai.org/supplement/2ndGenProtocol.pdf). All these vectors carry attB sites, and after sequencing, the constructs were injected into embryos with attp40 as the landing site on the 2nd chromosome. Note: all the microinjection work in this project was performed by Rainbow Transgenic Flies, Inc.

To express transgenes with the *UASp* and *UASt* promoters including all the *UAS* lines created using pPHW and VALIUM20/22 vectors [177, 178], the *nos-gal4* and *da-gal4* lines mentioned above, which express yeast Gal4 proteins germline-specifically or ubiquitously, were used through the Gal4/UAS transactivation mechanism.

Generation of germline clones and follicle clones marked by negative GFP through FLPase/FRT mediated mitotic recombination

Yeast FLPase/FRT mediated mitotic recombination has been utilized in Drosophila and other organisms to study homozygous mutant cells, the mutation of which is often recessive and cause embryonic or larval lethality, in a wild-type background. This method helps to limit mutant cells spatially and temporally [179, 180]. Usually exogenous yeast FLPase is under the control of the *hsp70* promoter and is expressed upon heat shock, which then mediate recombination between two FRT insertions in identical positions on homologous arms. When it takes place in a heterozygous cell for a

specific mutation, after mitosis one of the two daughter cells can be homozygous for the mutation.

Here in the project, *udd*^{null} and *udd*^{1} were recombined onto a *FRT42D* chromosome by meiotic recombination. Heterozygous adult females *hs-FLP;FRT42D,ubiquitin-GFP*/*FRT42D,udd* were heat-shocked at 37°C for 1 hour twice a day for 3 days. *hs-FLP;FRT42D,ubiquitin-GFP*/*FRT42D* flies were used as controls. Ovaries were dissected on days 4, 7, 14, 21 and 28 after clonal induction by heat shock.

Immunofluorescent staining in ovaries and testes

Ovaries and testes were dissected in Grace's Medium. Tissue was fixed for 10 minutes with gentle rocking in 4% formaldehyde (EM grade) in PBS. After fixation, ovaries and testes were washed four times in PBT (PBS + 0.5% BSA + 0.3% Triton-X 100) at RT for 10 minutes and were incubated with primary antibodies overnight at 4°C. The samples were washed four times with PBT for 10 minutes, and incubated for five hours with secondary antibodies. Tissue was washed and mounted in VectaShield Mounting medium with DAPI (Vector Laboratories). The images were taken with Zeiss LSM 510 confocal microscope.

The following antibodies were used (dilutions noted in parentheses): rabbit anti-GFP (1:1000) (Molecular Probes), mouse anti-Hts (1B1) (1:20), rat anti-VASA (1:20), mouse anti-BamC A7 (1:10), mouse anti-Sxl (1:20) (Developmental Studies Hybridoma Bank, Iowa), goat anti-VASA (1:200) (Santa Cruz Biotechnology), rat anti-HA 3F10 (Roche), mouse anti-Fibrillarin 38F3 (1:800), rat anti-Brdu (1:50) (Abcam), mouse anti-Modulo monoclonal LA9 (1:200) [181] (gift from J. Pradel), rabbit anti-cleaved Caspase-3 (1:250) (Cell Signaling Technology), rabbit anti-Phosphotyrosine (pTyr)

(1:1000)(BD transduction laboratories), rabbit anti-phospho-Histone H3 (Ser 10) (1:250) (Upstate), guinea pig anti-Udd (1:800), guinea pig anti-A2BP1 (1:5000) and guinea pig anti-Nanos (1:1000); Cy3, Cy5, FITC (Jackson Laboratories) or Alexa 488 (Molecular Probes) fluorescence-conjugated secondary antibodies were used at a 1:200 dilution.

TOPO® Cloning and Gateway™ Cloning

Most of the cDNA constructs used for expression in flies, S2 cells and bacteria were created by TOPO® Cloning followed by Gateway™ cloning. The blunt-end PCR products with CACC at the 5' end were amplified using PfuUltra II HotStart DNA Polymerases (Agilent Technologies, Cat.No. 600850), gel-purified and directionally cloned into pENTR/D-TOPO vector (Invitrogen), which were then fully sequenced and cloned into Drosophila Gateway™ destination vectors pPHW, pTHW, pAFW, pAHW, pHGW, pHWG,, pAFHW and Invitrogen Gateway™ destination vector pDEST17 using LR reactions to generate expression vectors with UASp/ UASt/ hsp70/ actin5C/ T7 promoters and HA/ Flag/ GFP/ His tags at the N- or C- terminus. The LR reactions were catalyzed by Gateway® LR Clonase® II Enzyme mix (Invitrogen Cat. No. 11791-020), which takes advantage of the site-specific recombination properties of bacteriophage lamda.

Bacteria used for TOPO® Cloning transformation were One Shot® TOP10 Chemically Competent *E.coli* (Invitrogen Cat. No. C4040), and bacteria used for Gateway™ cloning transformation were DH5α or One Shot® OmniMAX™ 2 T1^{R} *E.coli* (Invitrogen Cat. No. C8540).

DNA Isolation and Purification

1. In order to get genomic DNA purified from whole flies for PCR and sequence verification, the protocol and buffer recipes listed on the website of Berkeley Drosophila Genome Project (http://www.fruitfly.org/about/methods/inverse.pcr.html) was followed.

2. For regular cloning, sequencing, transfecting S2 cells and transforming bacteria, the cDNA constructs, VALIUM constructs and any Gateway™ related constructs were purfied using QIAprep Spin Miniprep Kit (Qiagen Cat. No. 28106), following instructions in their handbook about "Plasmid DNA Purification using the QIAprep Spin Miniprep Kit and a Microcentrifuge".

3. For DNA constructs to be used in embryo injection to make transgenic flies, Invitrogen PureLink® HiPure Plasmid Filter Maxiprep Kit was used following their instructions (http://tools.invitrogen.com/content/sfs/manuals/purelink_hipure_plasmid_filter_purification_man.pdf, Cat. No. K2100-17). However, after the elution step, there were some revisions: first, 12 ml ice-cold isopropanol was added to the 10 ml E4 buffer eluate, mixed gently and quickly aliquoted into 16 1.5 ml microtubes (for quick ethanol evaporation from the pellet and better DNA dissolving in water); second, the mixture in the tubes was incubated at -80℃ for 30 minutes for DNA precipitation, followed by centrifugation at maximum speed for 30 minutes at 4℃; third, after decanting the supernatant carefully, the pellets were gently washed twice by ice-cold 70% ethanol followed by centrifugation at maximum speed for 2 minutes at 4℃; fourth, after removing the ethanol completely and drying the pellets to a transparent state, around 10 µl nuclease-free water was added to each tube to dissolve DNA pellet; finally, the DNA solution were combined and the concentration was measured before being sent out for injection. Maxipreps were also used to purify DNA for large-scale S2 cell transfections and *P[acman] Bac* vector sequencing reactions.

4. For DNA fragments amplified from PCR reactions or digested by restriction enzymes, either QIAquick PCR Purification Kit (Qiagen Cat. No. 28106) or Zymoclean™ Gel DNA Recovery Kit (Zymo Research Cat. No. D4002) were used for their purification.

Generation of anti-Udd antibody

Full-length udd ORF was cloned into Gateway® pDEST™17 Vector (Invitrogen, Cat. No. 11803-012) with a T7 promoter to produce a 6×His-tagged Udd protein. The protein was expressed in BL21-AI™ *E. coli* strain (Invitrogen) after induction by 0.2% L-arabinose following their instructions (http://tools.invitrogen.com/content/sfs/manuals/ecoli_gateway_man.pdf). The BL21-AI™ *E. coli* strain is different from other BL21 strains which require IPTG to trigger transcription form *lac* promoter and induce T7 RNA polymerase expression, and it contains a chromosomal insertion of the T7 RNA polymerase-encoding gene into the *araB* locus of the *araBAD* operon, therefore the expression of T7 RNA polymerase and subsequently any genes with T7 promoters can be induced by L-arabinose.

After the bacteria pellets were collected from two 500 ml LB culture at a time point for optimized protein expression, the protein was then purified with Ni-NTA agarose (Invitrogen) under denaturing conditions. The pellets were first resuspended in 20 ml 1x binding buffer (5mM imidazole, 500mM NaCl 20mM Tris pH 7.9) with 6M Guanidine HCl and incubated at RT for 20 min, while 2 ml Ni-NTA agarose beads were equilibrated in 5 ml 1× binding buffer with 6M Guanidine HCl. After spinning at 7000 rpm for 10 min to separate form the debris, the supernatant was mixed with 7 ml equilibrated Ni-NTA agarose beads and incubated at RT for 2.5 hours. Then the beads were spun

down at 1000 rpm for 1.5 minutes, washed 3× with 8ml 1× washing (30mM imidazole, 500mM NaCl, 20 mM Tris pH 7.9) + 6M Guanidine HCl followed by 3× with 8ml 1× washing + 6M Urea before being transferred to a 1.5 ml microtube. Finally, the protein was eluted at 4℃in 1× elution buffer (300mM imidazole, 500mM NaCl, 20mM Tris pH 7.9) + 6M Urea for three times (1 ml buffer for 5 minutes-incubation for each elution), and the eluates were combined and analyzed on a SDS-PAGE gel comparing to the standard protein BSA.

Polyclonal antisera were generated in two guinea pigs TX928 and TX927 (Covance), and in this project all the experiments were performed with antiserum from TX928.

S2 cell culture, transient transfection and co-immunoprecipitation assays

Schneider 2 (S2) cells, the suspension or semi-adherent cells which were derived from a primary culture of late stage (20–24 hours old) Drosophila melanogaster embryos, were cultured at 25℃ according to instructions from Invitrogen Drosophila Schneider 2 Cells Handbook (Cat. No. R690-07, http://tools.invitrogen.com/content/sfs/manuals/schneidercells_man.pdf) using Gibco® Schneider's Drosophila Medium added with Thermo Scientific HyClone fetal bovine serum (Cat. No. 30070, 10×, heat-inactivated) and Gibco® Penicillin-Streptomycin (Cat. No. 15140, 100×).

The full-length ORFs of *Udd* (*CG18316*), *Taf1B* (*CG6241*), *RpI135* (*CG4033*) and *CG10496* were generated by PCR from DGC cDNA clones GH26082, RE68448, SD02110 and LD41005 respectively. Note: RE68448 carried a point mutation that resulted in an amino acid change relative the annotated sequence. This mutation was corrected by site-directed mutagenesis. Using the cDNA cloning methods mentioned above, they were cloned in to pAHW and pAFW Gateway™

vectors which both have an *actin5C* promoter and can express 3×HA- or 3×Flag- tagged proteins in S2 cells for co-immunoprecipitation (Co-IP) tests.

Transient transfections of S2 cells were performed using Qiagen Effectene Transfection Reagent (Cat. No. 301425) following the manufacturer's instructions. Transfected cells were collected at 24-48 hours after transfection and lysed on ice in lysis buffer (50mM Tris pH8.0, 137mM NaCl, 1mM EDTA, 1% Triton X-100, 10% glycerol,10mM NaF and protease inhibitors cocktail). Mouse anti-Flag M2 Agarose (Sigma) and rat anti-HA Affinity Matrix (Roche) were incubated with lysates overnight at 4°C. The beads were then quickly washed 4 to 5 times with lysis buffer and boiled in Laemmlli sample buffer with DTT.

Tandem affinity purification in S2 cells followed by Mass Spectrometry

The full-length ORF of *Udd* was cloned into Gateway™ vector pAFHW to generate 3×FLAG-3×HA-Udd (FH-Udd). S2 cells were transiently transfected with pAFHW (negative control) and pAFHW-Udd using two 100mm plates each and lysed using the same lysis buffer as mentioned above. After centrifugation, the supernatants were incubated with mouse anti-Flag M2 Agarose (Sigma) for 6 hours at 4°C, washed with lysis buffer, and eluted with 0.5mg/ml 3×FLAG peptide overnight at 4°C. Then the eluates were incubated with rat anti-HA Affinity Matrix (Roche) for 10 hours at 4°C, washed with lysis buffer, and eluted with 1mg/ml HA peptide overnight at 4°C. The eluates were mixed with Laemmli sample buffer and boiled for western blot and silver staining. Silver staining was performed following the instructions in Invitrogen SilverQuest™ Staining Kit (Cat. No. LC6070). The protein bands from both control eluate and FH-Udd eluate were excised and sent to the

UT Southwestern protein chemistry core for mass spectrometry analysis.

Immunofluorescent staining in S2 cells

The full-length *Taf1B (CG6241)* ORF and *CG10496* ORF were cloned into Gateway™ vectors pHGW and pHWG vectors which have an *hsp70* promoter and a GFP tag at the N- or C-terminus respectively. Transient transfections of S2 cells were performed using the same method described above. Transfected S2 cells were resuspended and placed on Gold Seal® micro slides (Cat. No.3032) and allowed to settle for 30min. Fresh fix buffer (4% formaldehyde in PBS) was used to flood the slide for 15 min, followed by one 5 min wash in 1XPBS and two 5 min wash with 1XPBS + 0.1% Triton-X 100. After the 3rd wash, the cells were pre-incubated with PBTA (1XPBS + 0.1% Triton-X 100 + 0.5%BSA) for 30min. Primary antibodies were diluted in PBTA and the cells were incubated for 4 hours at room temperature. After two washes in PBS and one wash with PBS + 0.1% Triton-X 100, secondary antibodies were added to the cells and incubated for 1 hour at room temperature before final washes and mounting in VectaShield Mounting medium with DAPI (Vector Laboratories). The images were taken with Zeiss LSM 510 confocal microscope. The same antibody dilutions were used as mentioned in "Immunofluorescent staining in ovaries and testes".

Western blots

To detect endogenous proteins, ovaries from newly eclosed flies were dissected in Grace's medium, physically disrupted and extracted with Laemmlli sample buffer (Bio-Rad) with DTT using pestle followed by boiling at 95 degree for 10 minutes. Bio-Rad protein electrophoresis and wet

transfer systems were used. After running the SDS-PAGE gel, Amersham Hybond ECL nitrocellulose membrane (GE Healthcare, RPN2020D) was used for protein transfer.

For blotting, the following primary antibodies were used in fresh PBST buffer (1XPBS with 0.1%Tween20 and 5% Biorad non-fat milk): guinea pig anti-Udd TX928 (1:5000), mouse anti-Actin (1:100) (Developmental Studies Hybridoma Bank, Iowa), goat anti-VASA (1:1000) (Santa Cruz Biotechnology), rat anti-HA 3F10, (1:5000) (Roche). After overnight incubation at 4 degree, the membranes were washed for three times in PBST buffer without milk before incubating with secondary antibodies for 1 hour at room temperature. HRP-conjugated anti-guinea pig, anti-mouse, anti-goat and anti-rat secondary antibodies (Jackson Laboratories) were used at a 1:2000 dilution. Finally after incubation and three more washes, the membranes were incubated with ECL Western Blotting Detection Reagents (GE Healthcare, RPN2106) and then exposed to Kodak X-ray film in dark room followed by film developing.

In order to detect S2 cell co-immunoprecipitation results, the following antibodies were used in western blots: HRP-conjugated mouse anti-Flag M2 (1:10,000) (Sigma), rat anti-HA 3F10 (1:5000) (Roche), mouse anti-Fibrillarin (1:5000) (Abcam) and guinea pig anti-Udd (1:8000).

RNA isolation by TRIzol reagent

About 50 ovaries (or testes) for each sample were dissected in Grace's medium and homogenized in 1ml TRIzol reagent at room temperature for 5 minutes. Then 0.2ml chloroform per 1 ml TRIzol (Invitrogen) reagent was added to each sample. After vigorous shaking by hand for 15 seconds and incubation at room temperature for 2-3 minutes, the samples were centrifuged at no more

than 12,000g for 15 minutes at 4 degree. Then the upper aqueous phase (about 60% of the volume of TRIzol reagent) was transferred carefully without disturbing the interphase into fresh tubes, and mixed with 0.5ml isopropyl alcohol and 1μl glycogen (10mg/ml) per 1ml TRIzol reagent used for the initial homogenization. After incubation at room temperature for 10min., the samples were centrifuged at no more than 12,000g for 10 minutes at 4 degree and the supernatants were removed completely. After washing the RNA pellets twice with 75% ethanol, the alcohol was removed completely and pellets were air-dried for 10 minutes before being dissolved in DEPC-treated water. The RNA concentration was measured using Nanodrop 2000c Spectrometer, and isolated RNAs were used for RT-PCR and Northern Blot experiments.

RT-PCR Analysis

Two-step RT-PCR was performed for all the experiments. The reverse transcription step was done with Invitrogen SuperScript® III First-Strand Synthesis SuperMix (Cat. No. 18080-400) using a primer mixture of both oligo$(dT)_{20}$ and random hexamers.

The 2nd step for regular PCR (Chapter III), Roche Taq polymerase was used with the following primer sequences for udd and RpL32 mRNA detection:

udd-F: 5'-ATGAAAACAAAAGATGAGAAGCCATCG-3'

udd-R: 5'-CTAGGATAGAATAGCATTTAATGAATCGTC-3'

RpL32-F: 5'-CACCAGTCGGATCGATATGC-3'

RpL32-R: 5'-CACCAGGAACTTCTTGAATCC-3'

The 2nd step for real-time PCR (qPCR, see Chapter IV and V), Power SYBR® Green PCR

Master Mix from Applied Biosystems (Part No. 4367659) was used and reactions were executed on Bio-Rad CFX96 Real-Time PCR Detection System. Standard curves were created for each primer set using cDNA template. The qPCR results for all genes were normalized to the reference gene αTublin84B. RNA samples without RT reaction (No-RT) were also included for each RT sample. The following primer sets were used for detection of each gene:

udd-F	5'-CTCCTCCGGCCAGTAACGAG-3'
udd-R	5'-ATCCCGGGCCAGTCGTAGTT-3'
Taf1B-F	5'-GCACTGCCACCTCGGCTACT-3'
Taf1B-R	5'-TGGCCTCATAGCGCGGATAC-3'
CG10496-F	5'-TGGCCAAGGGTGTGAATCCT-3'
CG10496-R	5'-ATGCGTCCAGGTGACGACAG-3'
CG4033-F	5'-TTACCAGCGTCTTCGGCACA-3'
CG4033-R	5'-GCATCCCGTTCCATCTCACC-3'
Fibrillarin-F	5'-GGTATTCGCTGCCGAGGTGA-3'
Fibrillarin-R	5'-TCTCGCTCGTAGGGCTCCAG-3'
Tif-IA-F	5'-TGCGGTGGGATACATGGCTA-3'
Tif-IA-R	5'-TGCTAAGCGGCAAAAATCGTG-3'
αTublin84B-F	5'-TGGGCCCGTCTGGACCACAA-3'
αTublin84B-R	5'-TCGCCGTCACCGGAGTCCAT-3'

Northern Blot Analysis

Northern blots were performed using Ambion NorthernMax® Kit (Cat. No. AM1940, for Formaldehyde Gel Electrophoresis/ Membrane Transfer/ Hybridization steps), Roche DIG Wash and Block Buffer Set (Cat. No. 11585762001, for protocol and buffer recipes used in Washing/ Blocking/ DIG Detection steps following Hybridization.), Roche Anti-Digoxigenin-AP antibody (Cat. No. 11093274910) and CDP-star reagent from the New England BioLabs Phototope®-Star Detection Kit (discontinued) with the following probes which were DIG-labeled with Roche DIG Oligonucleotide 3'-End Labeling Kit, 2nd generation (Cat. No. 03 353 575 910):

Pre-rRNA and rRNA processing probe [182]:

5'-CACCATTTTACTGGCATATATCAATTCCTTCAATAAATG-3'

Mature 5S rRNA probe:

5'-ACGAGAACCGATGTATTCAGCGTGGTATGGTC-3'

In situ run-on transcription assay

Ovaries were dissected in Grace's Medium, washed once with ice-cold PBS, and permeabilized with digitonin (200ng/µl; Sigma) in permeabilization (PB) buffer (22mM NaCl, 100mM CH_3COOK, 2mM $MgCl_2$, 8mM KCl, 11mM K_2HPO_4, add 1mM dithiothreitol and protease inhibitors (Roche Cat. No. 04 693 159 001) freshly before use) for 5 minutes on ice. Then the ovaries were washed once with PB buffer and incubated on ice for 10 minutes with PB buffer supplemented with α-amanitin (250ng/µl; Sigma) to inhibit activities of RNA polymerases II and III. Subsequently, transcription mix was added to give final concentrations of 2mM ATP, 0.5mM CTP, 0.5mM GTP, and 2mM 5-bromouridine 5'triphophate (BrUTP; Sigma). The run-on transcription was carried out at

25°C for 20 minutes and was terminated by rinsing the ovaries with ice-cold PBS. For control experiments, (A) actinomycin D (0.72ng/µl; Sigma) was added to the transcription reaction mixture to inhibit global transcription. The fixation and staining procedures were the same as mentioned above for the immunofluorescent staining. Rat Anti-BrdU antibody (Abcam Cat. No. ab6326) was used at 1:50 dilution.

Chromatin Immunoprecipitation and Real-Time PCR

For ChIP experiments in Fig.2E, 200 pairs of ovaries from *da-gal4>UASp-HA-Udd* flies were used per immunoprecipitation reaction, and *da-gal4* flies were used as negative control; for ChIP experiments in Fig.S8C, 400 pairs of ovaries from udd^{null}/udd^{null}*; da-gal4>UASp-HA-Udd* flies were used per immunoprecipitation reaction, and the same extracts were used in negative control without adding anti-HA antibody.

Chromatin from each 200 pairs of ovaries was cross-linked for 10 minutes at room temperature in a 1.5ml tube with 1ml 1% formaldehyde in 1×PBS; Cross-linking was stopped by adding 100µl of 1.25M Glycine solution to each tube. After three quick washes with cold 1XPBS, 400µl ChIP sonication buffer (1% Triton X-100, 0.1% Deoxycholate, 50mM Tris 8.1, 150mM NaCl, 5mM EDTA, and a protease inhibitor cocktail tablet (Roche; Cat. No. 04 693 159 001) was added to each tube. Ovaries were disrupted with a pestle and kept on ice for 10-20 minutes. The cell lysate was sonicated on wet ice for 4 minutes using 10 second pulses followed by 10 second “cooling-off” period and centrifuged at maximum speed for 10 mins at 4°C. The volume of the supernatant was brought up to 1mL with ChIP sonication buffer. After 1 hour preabsorption with 40µl Protein G Agarose

(Millipore Cat. No. 16-201) at 4°C, 30µl of the supernatant (3%) were kept as Input and the rest were incubated O/N with 3µl anti-HA antibody (Abcam rabbit polyclonal ChIP grade anti-HA ab9110) at 4°C.

The next day, 40µl Protein G Agarose were added and incubated for 5 hours at 4°C with rotation. Then the beads were washed for 5 minutes at 4°C with 1ml of the following buffers: 2 washes with ChIP Sonication Buffer; 3 washes with High Salt Wash Buffer (1% Triton X-100, 0.1% Deoxycholate, 50mM Tris-Cl 8.1, 500mM NaCl, 5mM EDTA); 2 washes with LiCl Immune Complex Wash Buffer (0.25M LiCl, 0.5% IGEPAL CA630, 0.5% deoxycholate, 1mM EDTA, 10mM Tris, pH 8.1); 1 wash with TE buffer (10mM Tris-Cl pH8.1, 1mM EDTA).

Elution Step: Each ChIP sample was incubated with 250µl Elution Buffer (1%SDS, 0.1M $NaHCO_3$) at room temperature for 20 minutes; after repeating once and the supernatants were combined. 500µl of elution buffer was added to the Input samples. 20µl 5M NaCl was added to each sample, mixed and incubated O/N at 65°C.

The next day, 10µl RNaseA was added to each sample and incubated for 30 minutes at 37°C. Then 10µl 0.5M EDTA, 20µl 1M Tris-HCl pH6.5 and 1µl Proteinase K were added to each sample and incubated at 45°C for 2 hours. With addition of 5 times volume of Qiagen PB binding buffer, the samples were passed through a Qiagen PCR Purification Kit column, washed once with Qiagen PE buffer and the DNA was eluted with 30µl nuclease-free water. Real-Time PCR was used for quantification of precipitated DNA using the Standard Curve method. Biorad iTaq™ Fast SYBR® Green supermix with ROX (172-5100) was used as the PCR reaction buffer.

Primers used to amplify rDNA sequence fragments (around 350bp each) in the 5’

non-transcribed spacer (NTS), external transcribed spacer (ETS) and the 5' end of 18S rRNA were described by Guerrero et al [62] as follows:

1-F GGTTGCCAAACAGCTCGTCATC,

1-R CGAGGTGTTTGGCTACTCTTG,

2-F GAGTAGCCAAACACCTCGTC,

2-R GAGAGGTCGGCAACCAC,

3-F GCTGTTCTACGACAGAGGGTTC,

3-R CAATATGAGAGGTCGGCAACCAC,

4-F GGTAGGCAGTGGTTGCCG,

4-R GGAGCCAAGTCCCGTGTTC,

5-F ATTACCTGCCTGTAAAGTTGG,

5-R CCGAGCGCACATGATAATTCTTCC,

6-F TTCTGGTTGATCCTGCCAGTAG,

6-R CGTGTGTACTTAGACATGCATGGC.

The primer sets 1-6 amplified rDNA regions labeled by bars from left to right in **Figure 4.19.** Primers 5S control-F AAGTTGTGGACGAGGCCAAC and 5S control-R CGGTTCTCGTCCGATCACCGA were used to amplify a fragment of the 5S rDNA which served as a negative control.

Live imaging

Ovaries from newly eclosed *udd*^{null}; *Udd-GFP, His2Av-mRFP* flies were dissected in

Scheider's Drosophila medium (Gibco®) supplemented with 10% Fetal Bovine Serum (Hyclone), 1:10,000 Penicillin-Streptomycin and 200 ug/ml human insulin (Sigma). The muscle sheath was removed and separated ovarioles were placed on a drop of medium on a microscope slide, and a coverslip was placed on top. A single germarium was imaged every 3-4 min for 12-14 hours, or a continuous scan for 15-30 min, using a Resonance Scanning Confocal Microscope Leica SP5. 4D data sets were processed using Image J (Rasband, W.S., ImageJ, U. S. National Institutes of Health, Bethesda, Maryland, USA, http://imagej.nih.gov/ij/, 1997-2012) and Adobe Photoshop, CS4. **Note:** the live imaging work was done by Dr. Nevine Shalaby, and Dr. Robin Hiesinger (Professor in Department of Physiology at UTSW) kindly provided the Leica scope in his lab for us to use.

CHAPTER III

Mapping and Characterization of the *under-developed* (*udd*) Mutation

A. Introduction

Drosophila oogenesis

Drosophila oogenesis, which is the process of egg formation starting from a germline stem cell (GSC), requires the coordinated development of somatic cells and germ cells. The Drosophila ovary provides a powerful and useful model for studying different aspects of developmental biology, genetics and cell biology. As a model organism *Drosophila melanogaster* has several good features distinguished from other higher organisms: first, the reproduction period is short (around 14 days); second, a large number of progeny are produced after each cross; third, the genetic manipulation is convenient.

The initial germ cells and somatic cells required for adult oogenesis start to appear and develop during embryonic, larval and pupal stages. Drosophila germ cells are derived from embryonic pole cells [183]. These pole cells inherit maternally deposited pole plasm and become primordial germ cells (PGCs), which then migrate from the posterior pole to the interior of the embryo. PGCs meet the somatic gonadal precursors (SGPs), form the embryonic gonads, and remain undifferentiated until the niche cells start to develop during third-instar larval stage and pupal stage. Niche development begins with terminal filament (TF) formation. Somatic TF precursor cells are separated into several clusters and rearranged to become mature functional TFs, which is followed by cap cell formation anterior to PGCs. Then a subset of PGCs adjacent to cap cells becomes GSCs, while the other germ cells away from the niche start to differentiate during pupal development.

Each adult fly has a pair of ovaries consisting of 16-20 ovarioles. The anterior tip of an ovariole is a region called germarium, which contains both GSCs and somatic stem cells called

follicle stem cells (**Figure 3.1A**). Two to three GSCs reside at the anterior region of the germarium next to cap cells in the niche and asymmetrically divide into a GSC daughter and a differentiating daughter called cystoblast (CB). The CB undergoes four mitotic divisions with incomplete cytokinesis, producing 2-cell, 4-cell, 8-cell and 16-cell cysts. The germ cells within a single cyst are interconnected by a germline-specific endoplasmic reticulum (ER)-like structure called fusome, which is branched and directs the division orientation [184]. In GSCs, fusome is also called spectrosome, which is usually round. Another cyst-specific structure is the ring canal (RC), which forms from arrested cleavage furrows at the interface between two cells in a single cyst [185, 186]. In contrast to fusomes, which disappear during egg chamber development, RCs become more obvious during later stages of oogenesis. Within 16-cell cysts, two cells have four ring canals, and one of them develops a microtubule organizing center (MTOC) that extends microtubules into all 16 cells. This MTOC containing cell becomes an oocyte and undergoes incomplete meiosis which is blocked at metaphase I and remains diploid throughout the following stages of oogenesis until the mature egg is activated. The oocyte condenses its nucleus to form a structure called the karyosome. The other 15 “nurse” cells within the same cyst become polyploid and provide enough proteins and RNAs for the oocyte. These nurse cells undergo DNA replication without further division. [187]

The anterior GSCs and cysts in the germarium regions I and IIA are surrounded by a layer of somatic cells called escort cells (ECs). Follicle cells (FCs), which are derived from follicle stem cells (FSCs) residing in between region IIA and IIB, take the place of escort cells during later cyst and egg chamber development. By the time meiosis starts, the 16-cell cyst is wrapped by a layer of FCs and starts to bud off as an egg chamber (Region III/Stage 1) with oocyte residing at the posterior

position.

Drosophila oogenesis can be divided into 14 stages based on morphological criteria. Signaling pathways including Notch/Delta and JAK/STAT pathways, which are utilized several times during oogenesis between germline and follicle cells and between different subtypes of follicle cells, are critical for the development of egg chambers. The morphological difference in the oocyte follows two major polarization events. The first one takes place at around stage 5 when its nucleus moves from near the center of the oocyte to the posterior region. The oocyte produces *gurken* mRNA and Gurken protein, an EGF-like ligand signaling to the adjacent follicle cells to set up posterior identity of the egg chamber. The 2nd polarization event starts to take place at around stage 7, when Par1 protein and Par3/Bazooka protein start to accumulate at the posterior and anterior ends respectively and the oocyte nucleus then moves to the anterior corner. By stage 10, the *bicoid* mRNAs and *oskar* mRNAs are all localized to the anterior and posterior regions of the oocytes. Besides the oocyte changes, nurse cells at stage 4 are polytene and the replicated DNAs remain associated with the parent chromosomes producing giant chromosomes. From stage 5-6, the replicated chromosomes are gradually separated as individual copies, during which they first go into a bulbous state and then become dispersed polyploidy cells. In addition to germ cells, the cell fate of follicle cells and active signaling pathways in those cells at different positions and developmental stages also exhibit relevant alterations during oogenesis.[187]

Drosophila **Spermatogenesis in adult male flies**

Each adult male fly has a pair of testes. At the tip of the testis there are stromal hub cells,

which act as a stem cell niche similar to cap cells in the germarium (**Figure3.1B**) [188]. In wild type testis, around ten GSCs are adjacent to the hub cells, which undergo asymmetric division followed by four mitotic divisions with incomplete cytokinesis generating a series of germline cysts, which then become spermatogonia. After spermatocyte growth, meiosis and spermatid differentiation, male germ cells ultimately develop into sperm. The male germ cells, starting from GSCs, are surrounded by somatic cells. These somatic cells are initially produced by somatic stem cells (SSCs, a.k.a. somatic cyst stem cells) next to GSCs, and their function is similar to escort cells and follicle cells in the ovaries.

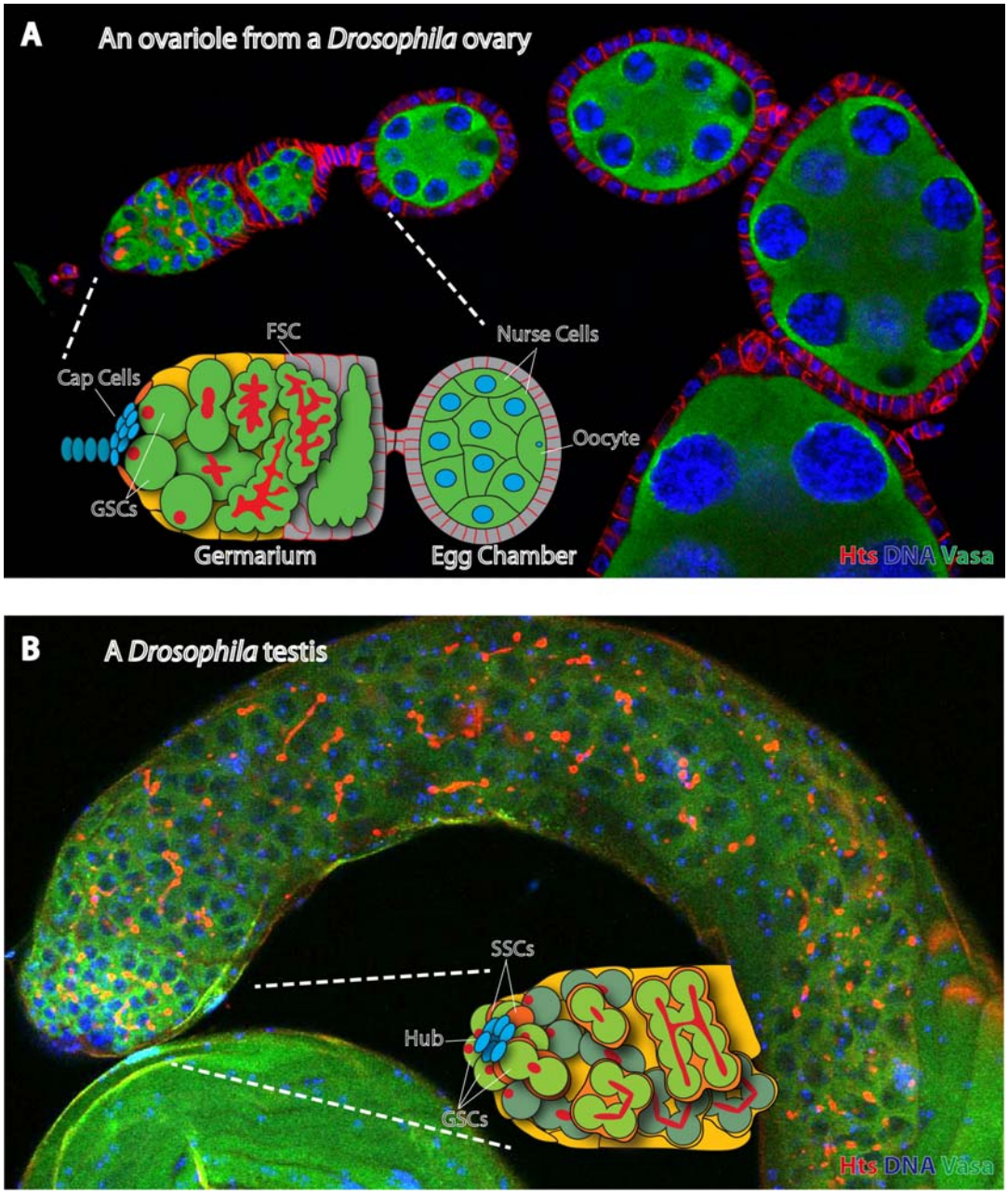

Figure 3.1 The typical *Drosophila* ovariole (A) and testis (B) after immunofluorescent staining, together with schematics of their tip regions. (A) Each germarium houses two to three germline stem cells (GSCs) that are maintained by a cluster of cap cells. These stem cells carry round fusomes (red), which become branched as they divide and form multi-cellular cysts. A layer of follicle cells surround mature 16-cell germline cysts and together these groups of cells bud off of the germarium to form egg chambers. Vasa (green) is used to label germ cells. DAPI (blue) is used to label DNA. (B) Each testis houses around ten GSCs that are adjacent to hub cells at the tip. These male GSCs also undergo divisions similar to female GSCs producing germline cysts which then become spermatogonia and ultimately develop into sperms. Surrounding male germ cells, there are somatic stem cells (SSCs) and somatic cyst cells help protecting them and promoting germ cell development.

Female germline stem cells in Drosophila

Female GSCs reside in a niche created by a small cluster of cap cells in the germarium [189, 190]. Cap cells produce ligands from the bone morphogenetic protein (BMP) family including Decapentaplegic (Dpp) and Glass bottom boat (Gbb) which then binds to the type II and type I transmembrane serine/threonine kinase receptors Punt and Thick veins (Tkv) or Saxophone (Sax) in the GSCs (Figure 3.2). The type I receptors subsequently phosphorylate and activate the downstream component Mothers against dpp (Mad) protein, a homolog of human Smad 1 which then forms a complex with the Smad 4 homolog Medea and represses the transcription of the differentiation factor *bag-of-marbles* (*bam*) [191-194]. Upon Dpp signaling activation, the transcription of the *Drosophila* Smad 6 homolog Daughters against dpp (Dad) is also upregulated, although this downstream target plays an antagonistic role. Usually phosphorylated Mad (pMad) and a lacZ enhancer trap for Dad (Dad-lacZ) are used to monitor the changes of Dpp signaling in the receptor cells. In the germarium, only GSCs that are in direct contact with cap cells are able to get Dpp signals from the niche. CBs and early cysts away from the niche have greatly reduced Dpp signaling and a gradual increase in Bam expression levels, which is both necessary and sufficient for early cyst differentiaion. Knocking down or mutating *dpp* in the cap cells causes a rapid loss of GSCs, while overexpressing *dpp* in all the somatic cells surrounding the GSCs or upregulating the level of Dpp receptors in all the germ cells greatly increase the undifferentiated GSC number [189, 195, 196]. Deletion or germline knockdown of *bam* also results in undifferentiated GSC-like cells with round fusomes, but in the *bam* mutant only two or three cells adjacent to the cap cells are positive for pMad and Dad-lacZ, which is different from *dpp* overexpression. Nevertheless, *bam* overexpression under a heat shock promoter is sufficient

to induce differentiation of GSC-like cells in both mutants [193, 197].

Active Dpp signaling is restricted within GSCs adjacent to cap cell niche through several levels of regulation (**Figure 3.2**) [198]. First, in the cap cells, Notch signaling controls the number of niche cells that express Dpp, and JAK-STAT signaling positively regulates the transcription of *dpp* [199-201]. Second, in the escort cells, some factors like lysine-specific histone demethylase 1 (Lsd1) represses Dpp signaling through an indirect mechanism [202]. It is also reported that in escort cells EGFR signaling represses the expression of Dally, a glypican protein normally expressed in the cap cells required for DPP movement and stability, and plays a significant role in preventing Dpp diffusion to outside the niche [203]. In addition, type IV collagen (Col IV) also binds to Dpp and prevents Dpp diffusion probably by anchoring the ligand to cap cells [204]. Third, E-cadherin mediates cell-cell adhesion and helps to anchor GSCs in the niche. The germline-specific gap junction protein Zero population growth (Zpg) is also required for GSC survival. Fourth, in the early differentiating daughters, several complexes including Bam/Bgcn, Smurf/fused and Brat/Pumilio further repress Dpp signaling in those cells; while in GSCs many other factors like Pelota and Lissencephaly 1 (Lis 1) are required to promote Dpp signaling [198].

Here in this chapter, I describe the initial characterization of the germ cell loss phenotype of a newly discovered female- and male-sterile mutant, *under-developed* (udd^{1}). Using multiple genetic methods I determined that *udd* disrupts a gene previously called *CG18316* (henceforth called *udd*). The mRNA and protein levels of *udd* were greatly reduced in the udd^{1} mutants. In addition, I made a null allele of *udd* (udd^{null}), homozygotes of which were embryonic lethal. The lethality of udd^{null} and the sterility of udd^{1} were rescued by the same cDNA transgene for *CG18316*. Immunofluorescent

staining of both endogenous Udd using anti-Udd antiserum and exogenous HA-Udd using anti-HA antibody exhibited an enrichment in nucleoli.

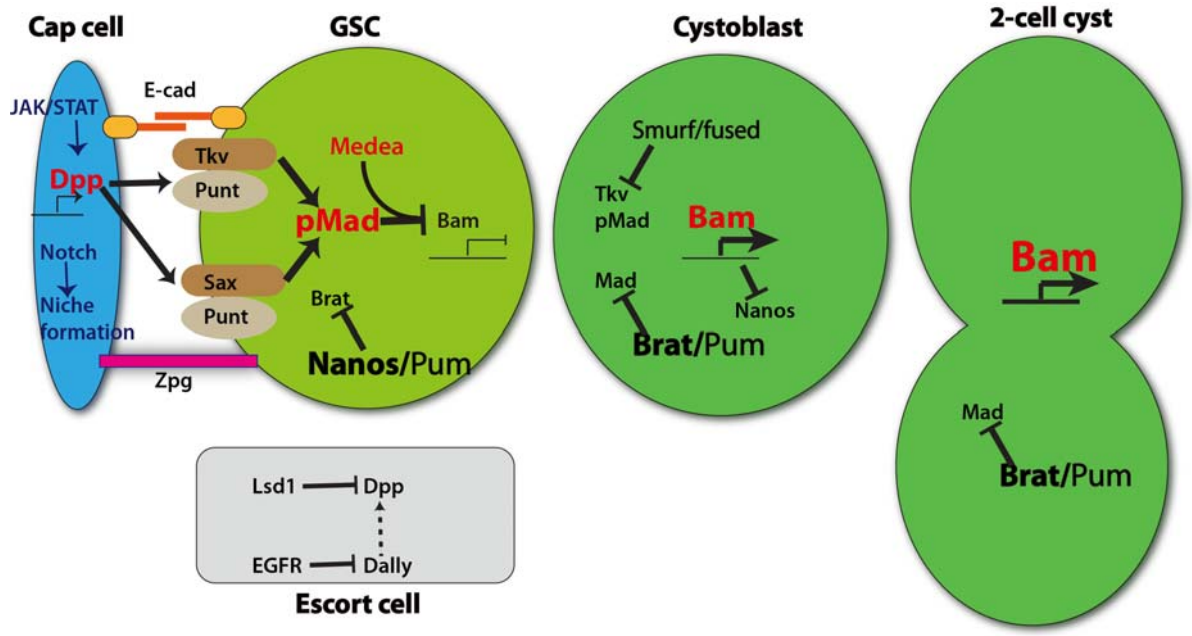

Figure 3.2 Major intrinsic and extrinsic regulatory mechanisms controlling germline stem cell maintenance and differentiation. The cap cells-produced Dpp molecules are received by GSCs, activating downstream components including phosphorylated Mad which together Medea represses transcription of the key differentiation factor *bam*. In the cystoblast and early differentiating cysts away from the cap cell niche, Bam expression is gradually increased, and other factors like Smurf/Fused and Brat/Pumilio could further repress Dpp signaling through promoting the degradation and repressing the translation of Dpp downstream components respectively. In the cap cells, JAK-STAT signaling promotes *dpp* transcription, while Notch signaling is critical for the formation and maintenance of niche size. In the escort cells, Lsd1 and EGFR signaling are indirectly involved in repressing Dpp expression.

B. Results

The *under-developed*^{1} (*udd*^{1}) mutants exhibit germ cell loss in males and females.

As part of a screen in the lab looking for mutations that disrupt normal *Drosophila* germ cell development among a collection of piggyBac insertion lines [173], I identified a recessive mutation in Stock BL18295 that resulted in sterility in both female and male flies. Immunofluorescent staining for the germline markers Vasa, which is an RNA helicase and Hts, which labels a germline-specific endoplasmic reticulum-like structure called the fusome, showed that homozygous mutant ovaries and testes exhibited a germ cell-loss phenotype that worsens with age (**Figure 3.3**). I named this mutation *under-developed*^{1} *(udd*^{1}*)*.

Antibodies against activated Caspase 3 revealed that *udd*^{1} homozygous egg chambers undergo programmed cell death during stage 4 or 5 (**Figure 3.4**). Caspase 3 staining was not observed in *udd* mutant germaria, even in aged flies.

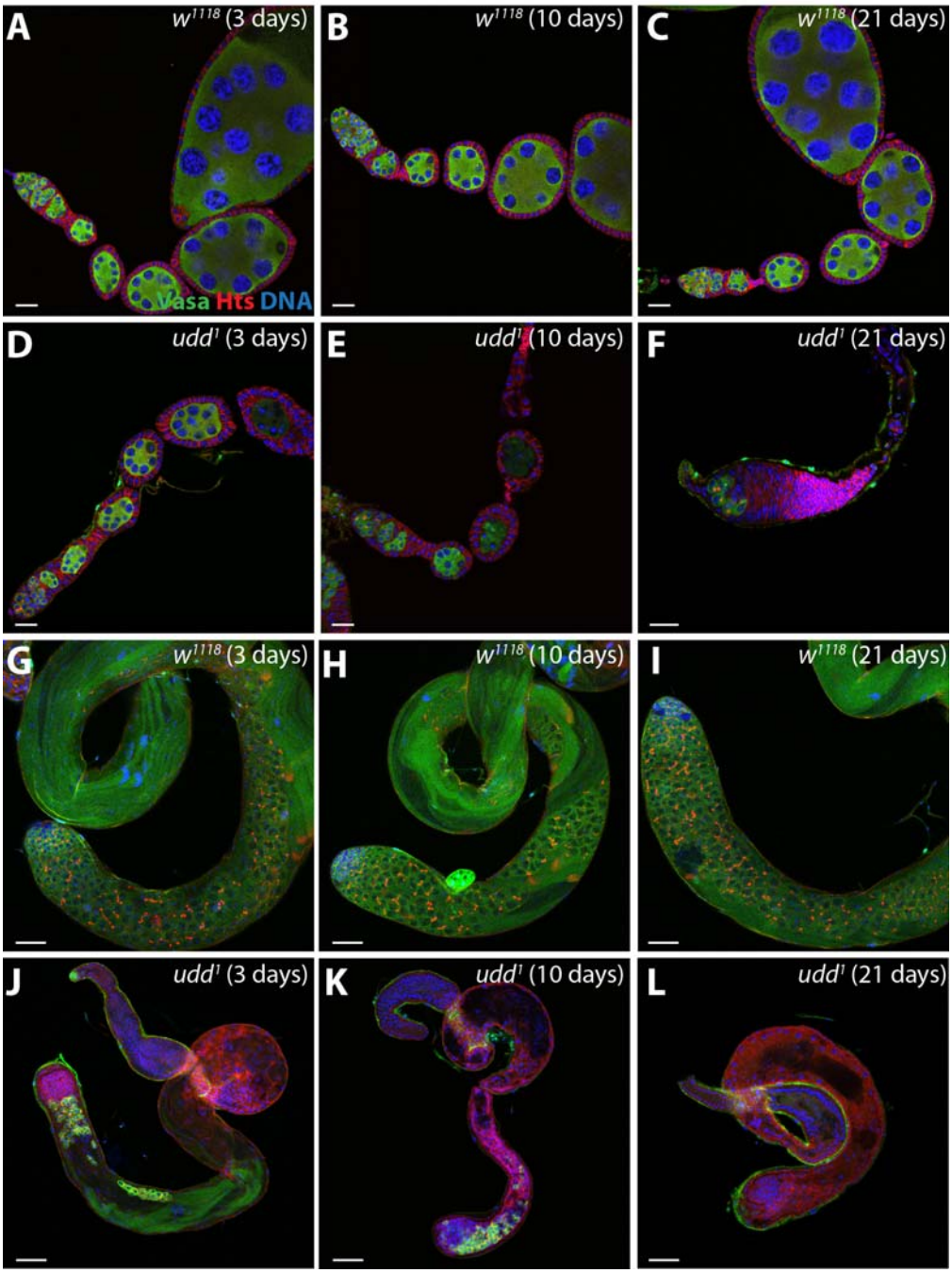

Figure 3.3 *udd*^{1} mutant ovaries and testes exhibit a germ cell loss phenotype that worsens with age. *w*^{1118} control ovarioles (A-C) and testes (G-I), and *udd*^{1} mutant homozygous ovarioles (D-F) and testes (J-L) dissected (A,D,G,J) 3 days, (B,E,H,K) 10 days or (C,F,I,L) 21 days after eclosion stained for Vasa (green), Hts (red) and DNA (blue). Scale bars represent 20 μm (A-F) and 50 μm (G-L).

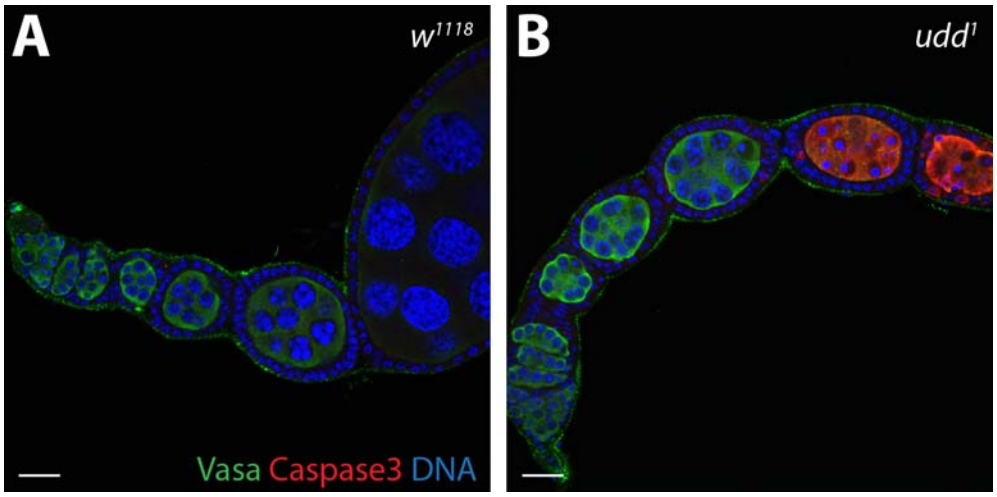

Figure 3.4 *udd*^{1} mutant egg chambers undergo programmed cell death during stages 4 or 5. (A) w^{1118} control and (B) *udd*^{1} homozygous ovarioles stained for Vasa (green), Cleaved (Activated) Caspase 3 (red) and DNA (blue). Scale bars represent 20 μm

The *udd*^{1} mutation is unrelated to the original piggyBac insertion.

Using genetic tests I found that the mutation responsible for the sterile phenotype did not map to the piggyBac insertion site. **First**, in Stock BL18295, the element PBac{WH}CG8232^{f00130} was inserted to chromosomal location 2R(44F9). I crossed multiple deficiency lines that uncovered this region to flies from Stock BL18295 and found that the trans-heterozygous progeny were fertile and healthy, so these lines all complemented the original sterile phenotype. **Second**, to remove the inserted piggyBac element precisely, I crossed the *udd*^{1} heterozygous flies to a transgenic line carrying *T.ni* piggyBac Transposase under the control of *hsp70* promoter (BL8284). By precisely excising the original element, I found that the 2nd chromosome-homozygous flies in these stocks were still sterile and exhibited the same germ cell-loss phenotype, which further confirming that the *udd*^{1} mutation is unrelated to the piggyBac insertion. Hereafter, one of the newly-isolated *udd*^{1} stocks without the original piggyBac element was used for all subsequent experiments.

The *udd*^{1} mutation disrupts the expression of a gene *CG18316*, which was confirmed by non-complementation tests, sterility-rescue assays and RT-PCR.

To identify the gene disrupted by the *udd*^{1} mutation on the 2nd chromosome, I performed non-complementation tests by crossing *udd*^{1} heterozygous flies to more than 100 2nd-chromosome deficiency lines, each of which carries a specific deletion (**Figure 3.5A**). Transheterozygous progeny of *udd*^{1} and 5 deficiency chromosomes still gave rise to the same sterile phenotype. These 5 lines have an overlapping deletion of a 42kb region (2R: 3970399-4012164) containing 10 genes.

Next, I performed genomic rescue experiments using three transgenic lines carrying single 21kb P[acman] BAC insertions mapping to different parts of the 42kb region, CH322 -138I13, -148I23 and -11K08 [176, 205]. One, CH322-148I23, rescued the *udd*^{1} sterile phenotype while the other two did not (**Figure 3.6**), which further narrowed down the region to less than 20kb.

In addition, I made four molecularly defined high-resolution deletion lines within the 42kb region using FLP/FRT recombination: Df(2R)Exel$^{d07339\text{-}e00152}$, Df(2R)Exel$^{e00152\text{-}f00102}$, Df(2R)Exel$^{e00152\text{-}d08197}$, and Df(2R)Exel$^{d08197\text{-}f00102}$ (the superscripts indicate two FRT-bearing insertion lines used for each deletion)(**Figure 3.5**; material and methods) [174]. Non-complementation tests using these deficiency lines showed that two of them, Df(2R)Exel$^{e00152\text{-}f00102}$ and Df(2R)Exel$^{d08197\text{-}f00102}$, did not compliment the *udd*^{1} sterile phenotype. Together with previous genomic rescue assay, *udd*^{1} was mapped to an 8 kb region (2R: 3993891-4001996) that contains one predicted and previously uncharacterized open reading frame (ORF), *CG18316*, and two naturally occurring transposons *297,* and *Tc1*, both having more than 20 copies in the *Drosophila melanogaster* genome (**Figure 3.5**).

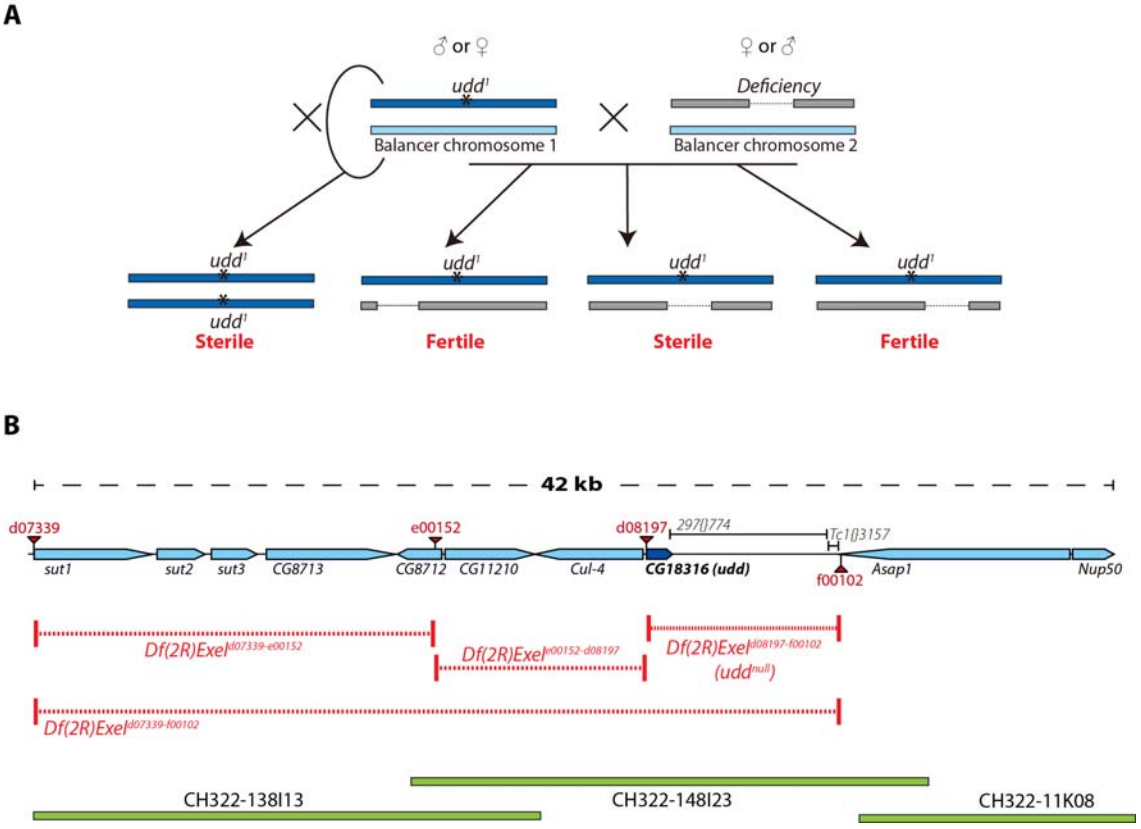

Figure 3.5 Non-complementation tests and sterility-rescue assays reveal that *udd*^{1} disrupts a gene *CG18316*. (A) The principle of non-complementation test with deficiency lines. If the F1 progeny *udd*^{1}*/Deficiency* demonstrates similar sterile phenotype to *udd*^{1} homozygotes, it means this deficiency line does not complement the *udd*^{1} mutation and probably the same gene is disrupted in *udd*^{1} allele and in the deficiency line. (B) Schematic of the region where *udd* maps. This 42 kb interval contains ten ORFs. The CH322-148I23 genomic clone rescued the *udd*^{1} phenotype, while the other two, CH322 -138I13 and -11K08, did not. Four molecularly defined deletions were made using FRT/FLP-mediated recombination: *Df(2R)Exel*$^{d07339\text{-}f00102}$, *Df(2R)Exel*$^{d07339\text{-}e00152}$, *Df(2R)Exel*$^{e00152\text{-}d08197}$ and *Df(2R)Exel*$^{d08197\text{-}f00102}$, which was confirmed to be *udd*^{null} later. The *udd*^{1} allele complemented *Df(2R)Exel*$^{d07339\text{-}e00152}$ and *Df(2R)Exel*$^{e00152\text{-}d08197}$ but did not complement *Df(2R)Exel*$^{d07339\text{-}f00102}$ and *Df(2R)Exel*$^{d08197\text{-}f00102}$. 297{}774 and Tcl{}3157 are natural transposons that lie immediately downstream of the *udd* gene, previously known as *CG18316*.

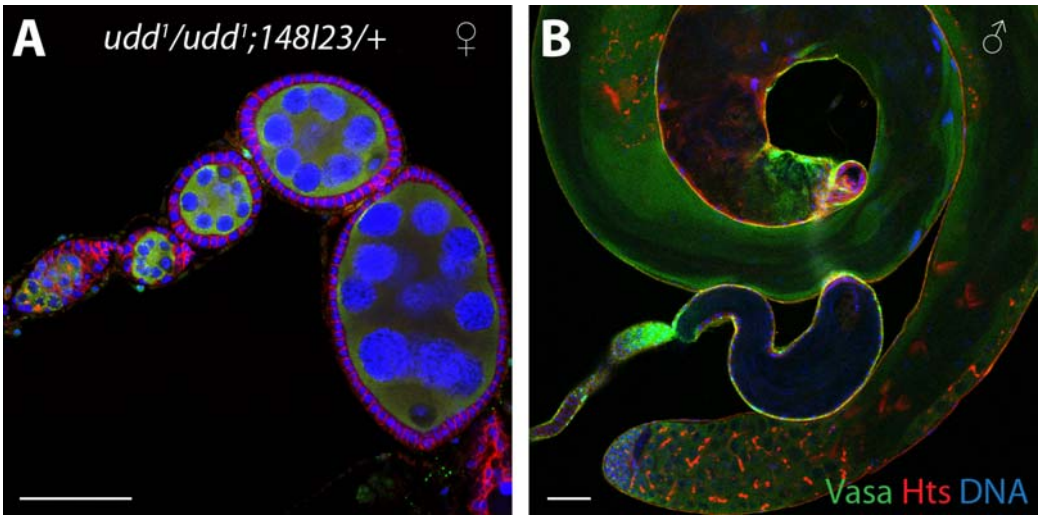

Figure 3.6 The CH322-148I23 genomic clone rescues the *udd*^{1} homozygotes' sterility. (A-B) The morphologies of ovaries and testes are restored, compared to *udd*^{1} homozygotes in **Figure 3.3**. Vasa (green), Hts (red) and DNA (blue). Scale bars represent 50 μm.

Sequencing genomic DNA from *udd*^{1} homozygotes did not reveal any mutations within the 5'UTR and coding region of *CG18316*. It is hard to sequence the 3'UTR of *CG18316* since it overlaps with the natural transposon *297* which has a lot of copies in the genome. However RT-PCR analysis demonstrated that the mRNA levels of *CG18316* were greatly reduced in *udd*^{1} mutant gonads (**Figure 3.7A**). The female and male sterility of *udd*^{1} homozygotes was fully rescued by the expression of *CG18316* ORF driven by the ubiquitous *da-gal4* driver. Immunofluorescent staining using anti-Vasa and anti-Hts antibodies showed that the normal morphology of ovaries and testes was restored upon expression of the *CG18316* transgene (**Figure 3.7 B-C**), suggesting that the *udd*^{1} allele contains a regulatory mutation that disrupts the expression of *CG18316*. I will therefore refer to *CG18316* as *udd* hereafter.

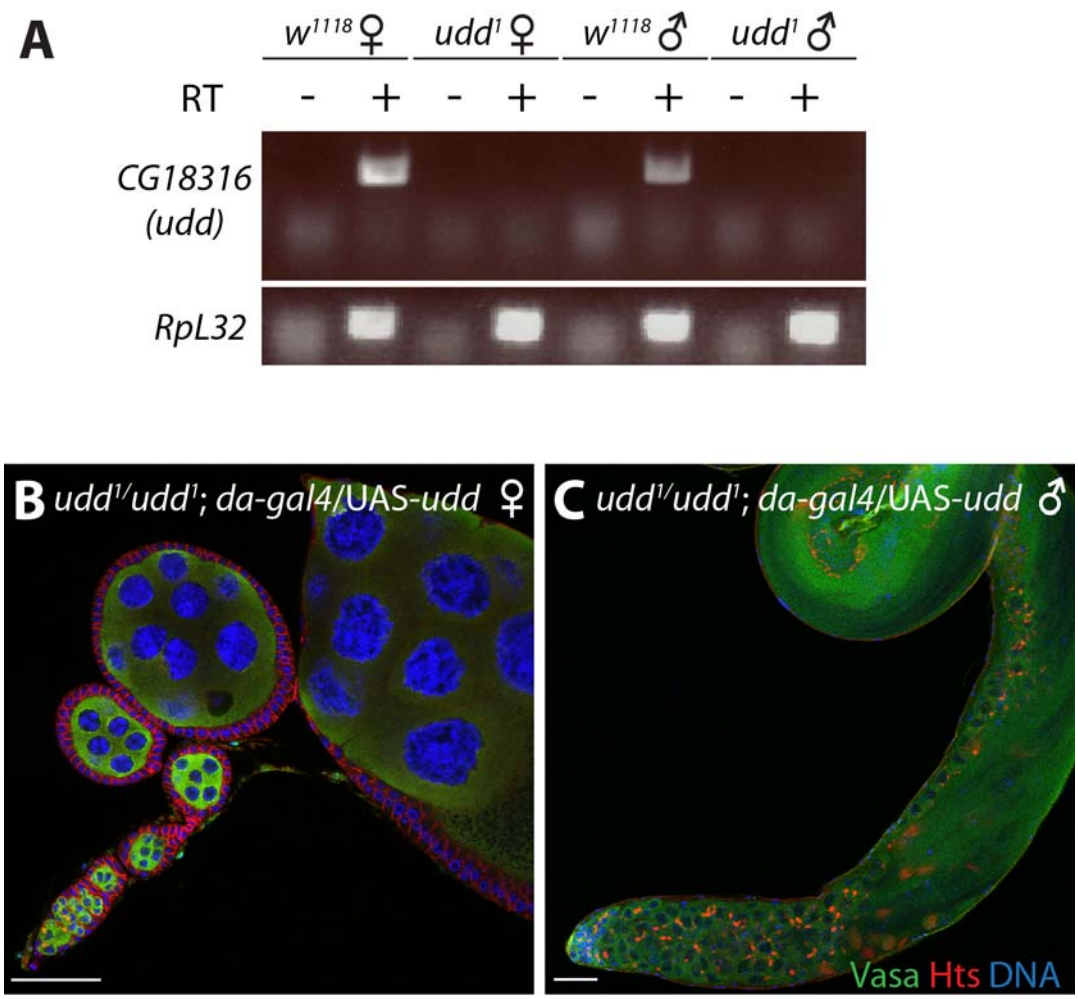

Figure 3.7 RT-PCR and cDNA rescue assay further confirm that *udd*^{1} disrupts a gene *CG18316*. (A) The *udd*^{1} mutation results in reduced levels of *CG18316 (udd)* mRNA. EtBr stained agarose gel showing the products from RT-PCR using primers specific for *CG18316* or *RpL32*, which serves as a loading control. (-): No-RT control samples. (B-C) Ubiquitous expression of HA-tagged *CG18316* rescues the *udd*^{1} homozygotes' sterility. The morphologies of ovaries and testes are restored, compared to *udd*^{1} homozygotes in Figure 3.1. Vasa (green), Hts (red) and DNA (blue). Scale bars represent 50 μm.

The null phenotype of *udd* is embryonic lethal.

To determine the null phenotype of *udd*, I analyzed the smallest deletion line I made, Df(2R)Exel$^{d08197\text{-}f00102}$, which completely deletes the *udd* gene and two downstream natural transposons *297* and *Tc1* (**Figure 3.5B**). By crossing Df(2R)Exel$^{d08197\text{-}f00102}$ heterozyotes to a balancer chromosome with *actin*-GFP reporter and looking for GFP-negative embryos/larvae/pupae, I found

that the GFP-negative Df(2R)Exel$^{d08197\text{-}f00102}$ homozygotes were embryonic lethal.

The lethality of Df(2R)Exel$^{d08197\text{-}f00102}$ homozygotes was rescued by ubiquitously expressing the *udd* ORF under control of *da-gal4* (**Figure 3.8A**), and the rescued flies were healthy and fertile. Therefore, Df(2R)Exel$^{d08197\text{-}f00102}$ will be referred to as *udd*^{null} hereafter, and the null phenotype of *udd* suggests that *udd* has essential functions outside of the gonad.

In addition, I examined *udd*^{1}/*udd*^{null} hemizygotes and found that these flies were viable but sterile. They exhibited a similar but more severe germ-cell loss phenotype than *udd*^{1} homozygotes in both egg chambers and germaria (**Figure 3.8**).

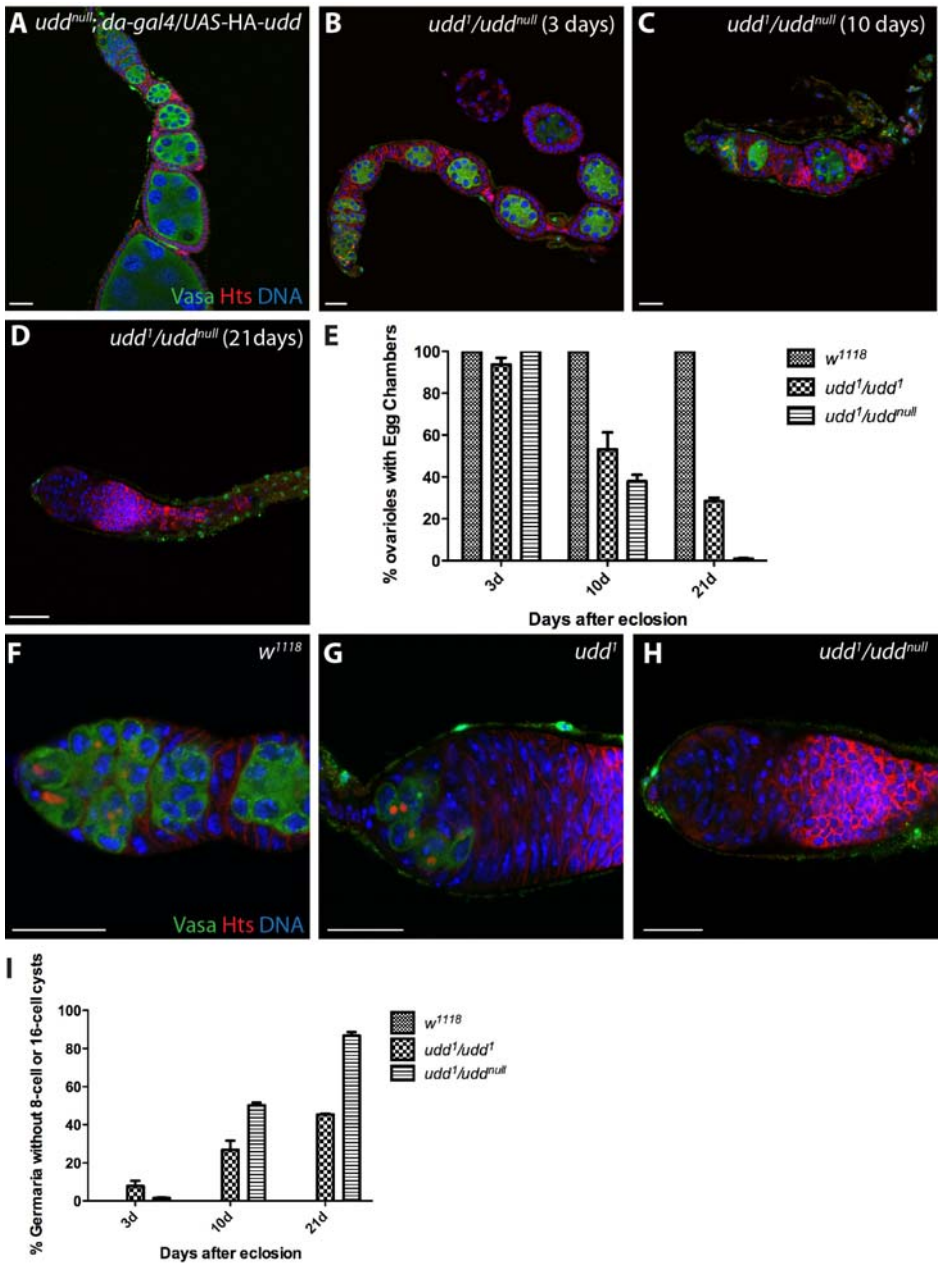

Figure 3.8 The null phenotype of *udd* is embryonic lethal and udd^{1}/udd^{null} mutant ovaries exhibit a similar but more severe germ-cell loss phenotype than udd^{1} homozygotes in both egg chambers and germaria. (A) A udd^{null} /udd^{null}*; da-gal4/UAS-HA-udd* ovariole stained for Vasa (green), Hts (red) and DNA (blue). Ubiquitous expression of HA-tagged *CG18316* rescues the udd^{null} homozygotes' lethality and the flies are fertile. (B-D) udd^{1}/udd^{null} mutant ovarioles dissected (B) 3 days, (C) 10 days or (D) 21 days after eclosion stained for Vasa (green), Hts (red) and DNA (blue). (E) Graph showing changes in the percentage of ovarioles that contain egg chambers over time. (F) w^{1118} control, (G) udd^{1}/udd^{1}, (H) udd^{1}/udd^{null} germaria stained for Vasa (green), Hts (red) and DNA (blue). Twenty-one days after eclosion udd^{1} homozygous germaria carry a small number of largely inactive single germ cells while udd^{1}/udd^{null}, the hemizygous udd^{1} germaria exhibit a complete germ cell loss phenotype. (I) Graph showing changes in the percentage of germaria that do not contain 8-cell and 16-cell cysts over time. (A-D, F-H) Scale bars represent 20 μm.

***udd* functions cell-autonomously in the ovary, and *udd* mutants exhibit GSC quiescence and loss.**

To determine whether *udd* functions cell-autonomously in the ovary, I performed mosaic analysis using FLP/FRT mediated mitotic recombination with both udd^{1} and udd^{null} alleles.Negatively marked udd^{1} and udd^{null} homozygous germline clones had egg chamber degeneration similar to the phenotype of udd^{1}/udd^{1} and udd^{1}/udd^{null} ovarioles (**Figure 3.9 A-C**), which demonstrates that *udd* functions autonomously in the germline. Moreover, I also examined *udd* mutant follicle cell clones, to see if they affect normal germ cell development. I found that egg chambers with wild type germ cells but surrounded by only udd^{1} homozygous follicle cells differentiated and developed normally without degeneration (**Figure 3.9 D-F**), although their development was a bit more delayed compared to that of egg chambers with both wild type germ cells and wild type follicle cells in the same ovariole (**Figure 3.9F**). No complete udd^{null} homozygous follicle clones were observed in egg chambers, demonstrating that these clones were much less competitive compared to heterozygous clones and indicating that *udd* is also critical for normal somatic cell development in the ovary, and demonstrate that the udd^{1} allele affects follicle cell development less severely compared to the udd^{null} allele. The cell-autonomous function of *udd* in germ cells was further confirmed by rescuing the udd^{1} sterile phenotype with a germline specific *nanos* (*nos*)-*gal4* driver (**Figure 3.9 G-H**).

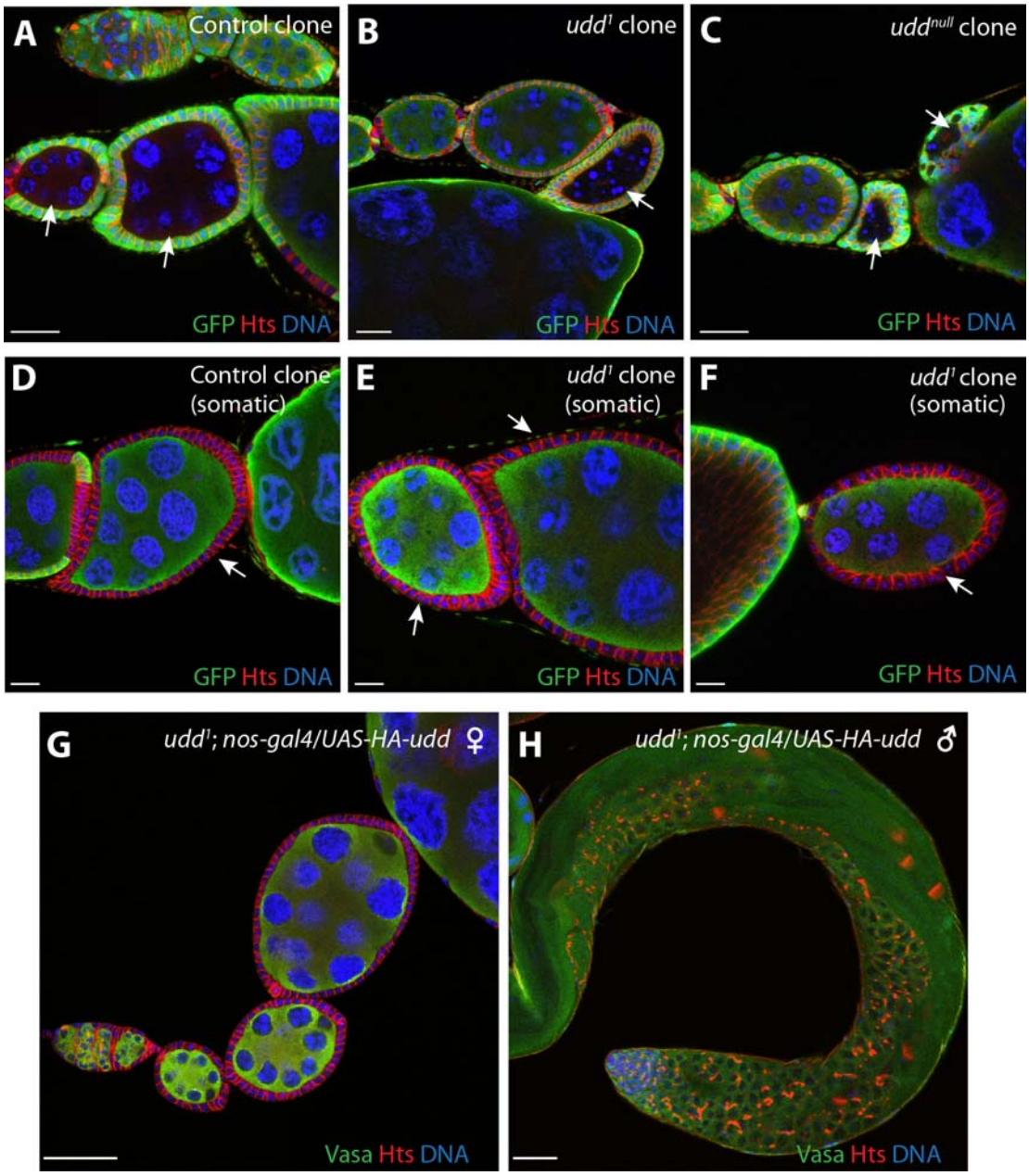

Figure 3.9 *udd* functions cell-autonomously in the germline. (A-C) Ovarioles carrying wild type control (A), udd^{1} (B) and udd^{null} (C) germline clones dissected 14 days after heat shock-induced clone induction stained for GFP (green), Hts (red) and DNA (blue). The control germline clones forms late stage egg chambers (arrows in A) while the udd^{1} and udd^{null} clones exhibit egg chamber degeneration (arrows in B,C). (D-F) Ovarioles carrying wild type control (D) and udd^{1} (E-F) follicle clones dissected 21 days after heat shock stained for GFP (green), Hts (red) and DNA (blue). Ovarioles with both control and udd^{1} follicle clones (D-F) form late stage egg chambers, although in the same ovariole the egg chamber with udd^{1} follicle clones develops slower compared to the one with control follicle clones (F). (G-H) An Ovariole (G) and a testis (H) from udd^{1}/udd^{1}; *nos-gal4(III)/UASp-HA-udd ORF* stained for Vasa (green), Hts (red) and DNA (blue). Germline specific expression of Udd rescues the sterility of udd^{1} phenotype. Scale bars represent 20 μm (A-F) and 50 μm (G-H).

Using the same mosaic analysis, I observed that over time, *udd*^{1} and *udd*^{null} homozygous GSCs became quiescent, producing fewer differentiating clones, and were eventually lost from the cap cell niche (**Figure 3.10 A-E**), indicating that Udd promotes normal GSC activity and maintenance. In addition, I also found that there was a mild reduction of *udd* mutant follicle stem cell (FSC) clones over time (**Figure 3.10 F**).

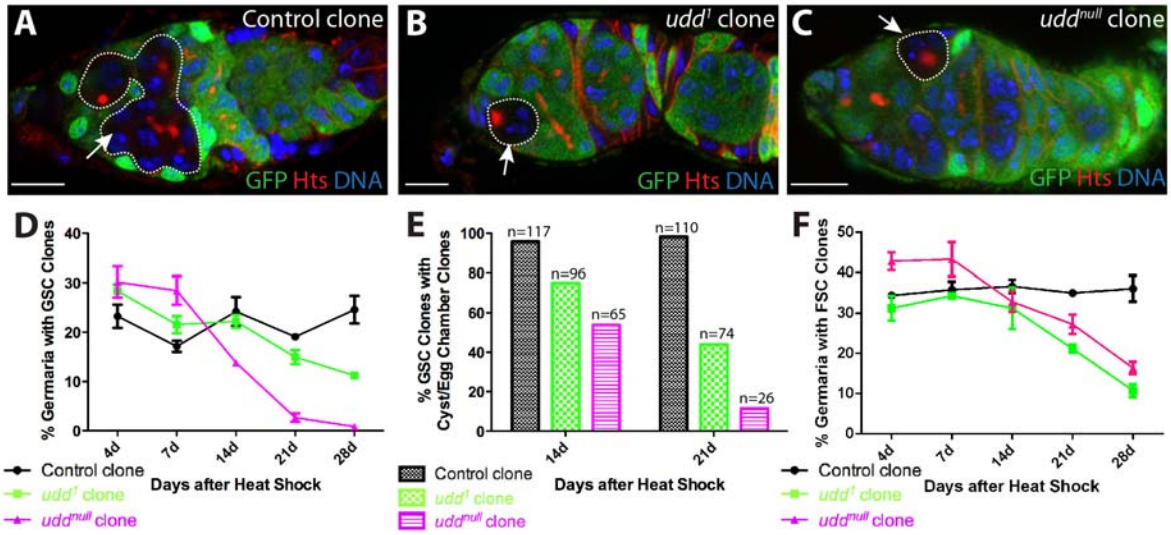

Figure 3.10 Disruption of *udd* results in germline stem cell quiescence and loss. Negatively marked (A) control, (B) *udd*^{1} and (C) *udd*^{null} clones (white dotted lines) dissected 21 days after clone induction stained for GFP (green), Hts (red) and DNA (blue). (D) Graph showing the percentage of germaria that retain control (black line), *udd*^{1} (green line) and *udd*^{null} (magenta line) GSCs clones over time. (E) Graph showing the percentage of ovarioles with a GSC clone and also a downstream differentiating clone over two time points. Scale bars represent 10 μm.

***udd* encodes an 18 kDa rapidly-evolving nucleolar protein.**

Sequence annotation of *udd* (http://flybase.org/reports/FBgn0033261.html) predicted the gene encodes a previously uncharacterized 18 kDa protein consisting of 159 amino acids with no recognizable functional domains. Blasting the primary sequence of Udd protein revealed no mammalian or yeast homologs but only a moderate conservation across multiple *Drosophila* species

(**Figure 3.11**).

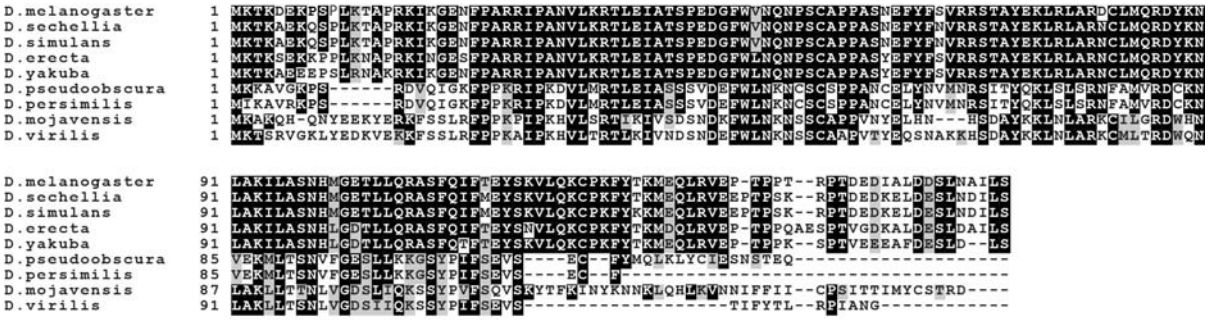

Figure 3.11 Sequence alignment of Udd orthologs from different *Drosophila* species.

To further characterize the molecular function of Udd, I purified 6×His-tagged full length Udd protein in *E.coli* BL21-AI^{TM} and sent it to Covance Inc. for production of polyclonal antiserum against Udd. I examined the anti-Udd antiserum by western blot using ovarian extracts and S2 cell lysates (**Figure 3.12**), and observed that it specifically recognized an 18 kDa protein as predicted. Moreover, the corresponding protein band was greatly reduced in *udd* mutant ovarian extracts, which further confirmed that the band recognized by anti-Udd antiserum was endogenous Udd protein (**Figure 3.12**). In addition, in the western blot using ovarian extracts from the lethality- and sterility-rescued udd^{null} and udd^{1} flies which carried exogenous 3×Hemagglutinin-tagged Udd (HA-Udd), I found there was a strong 25 kDa protein band recognized by anti-Udd antibody and it was the predicted size for HA-Udd protein (**Figure 3.12**).

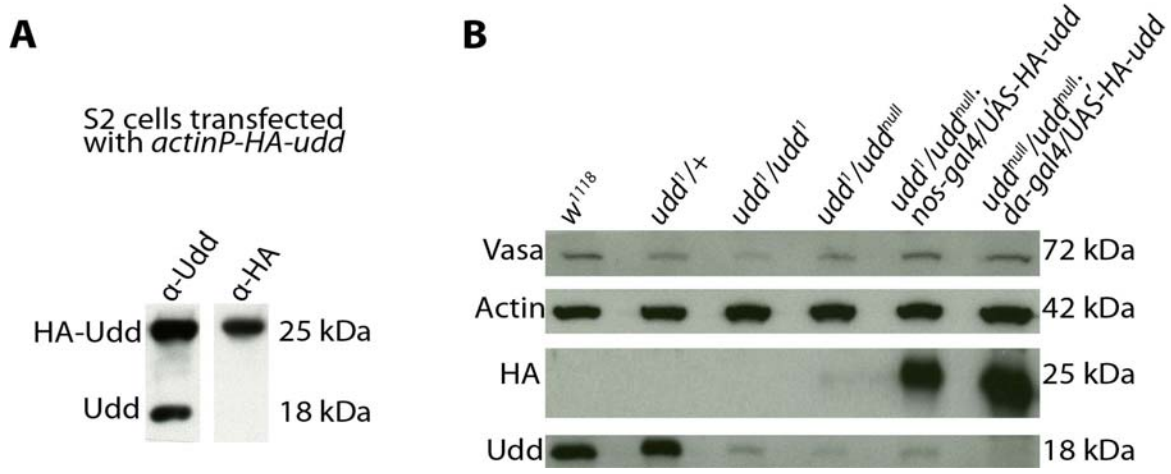

Figure 3.12 The polyclonal anti-Udd antiserum specifically recognizes the 18 kDa Udd protein in both S2 cell lysates (A) and ovarian lysates (B). (A) Western blot analysis using S2 cells transfected with 3×HA-tagged Udd showing that the anti-Udd antibody recognizes both endogenous Udd and HA-tagged Udd. (B) Western blot analysis showing that Udd protein level is greatly reduced in udd^1/udd^1 and udd^1/udd^{null} mutant ovaries compared to w^{1118} and $udd^1/+$ heterozygous ovaries. Vasa (germline only) and Actin are loading controls, and the anti-HA blot shows the expression of HA-Udd in the rescued flies.

To determine the expression pattern and sub-cellular localization of Udd, wild-type ovaries were stained using the anti-Udd antiserum. The immunofluorescence analysis showed that Udd was broadly expressed in both germline and somatic cells and appeared tightly localized to a sub-domain within the nucleus that resembled the nucleolus (**Figure 3.13 A-D**). The rescuing HA-Udd protein showed similar sub-nuclear localization (**Figure 3.13 E-F**). Interestingly, staining mutant ovaries with anti-Udd antibody suggested that the udd^1 mutation disrupted Udd expression strongly in the germline and less severely in somatic cells, like follicle cells (**Figure 3.13G**). This difference likely explains the germline specific defects observed in udd^1 mutants.

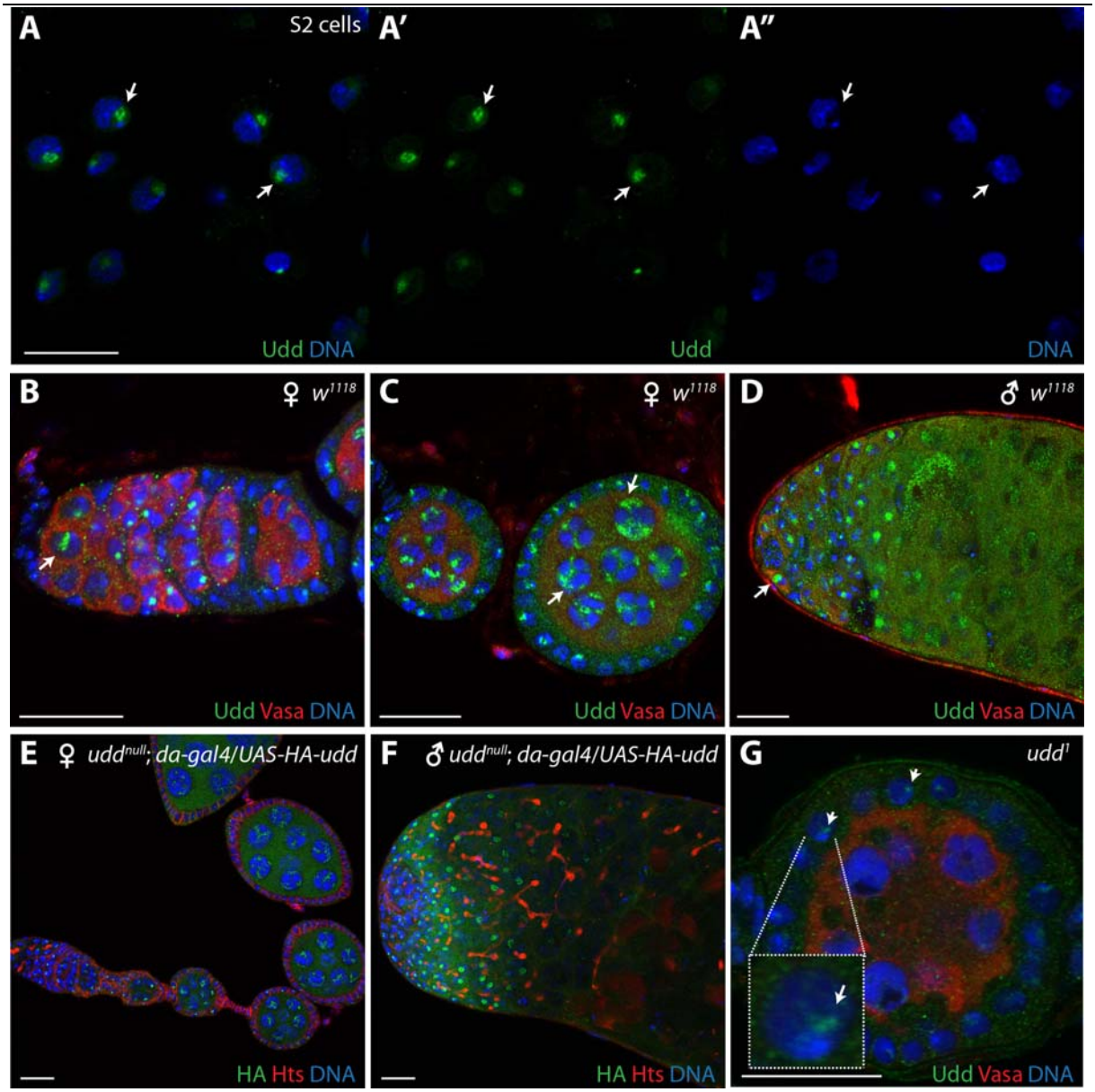

Figure 3.13 Udd is a nucleolar protein in S2 cells, ovaries and testes. (A-A'') S2 cells stained for Udd (green) and DNA (blue). (B-D) Wild type germarium (B), egg chambers (C) and testis (D) stained for Vasa (red), Udd (green) and DNA (blue). (E-F) Ovariole (E) and testis (F) from udd^{null}/udd^{null}; *da-gal4(III)/UASp-HA-udd* flies stained for HA-Udd (green), Hts (red), DNA (blue). HA-tagged Udd is also nucleolar. (G) udd^{1} egg chamber stained for Vasa (red), Udd (green) and DNA (blue). The udd^{1} mutant follicle cells still have visible Udd expression. Scale bars represent 20 μm.

C. Discussion

1. Comparison and evaluation of methods used to identify a gene responsible for a phenotype

Here I discuss about the methods mainly used to determine a gene of which the mutation is recessive and exhibits a phenotype in homozyogous flies. The most popular and essential method in *Drosophila* is non-complementation test by crossing the lines carrying the mutation to large deficiency lines on different chromosomes and looking for the lines giving rise to a phenotype in the transheterozygotes similar to that in the homozygotes (lethal, sterile, or other phenotypes), as shown in **Figure 3.3 and 3.8**. The weakness of this method is that the result from the available deficiency lines usually gives a large number of candidate genes within a chromosome region ranging from less than 100 kb to hundreds of kilobases. To improve the result and reduce the candidate genes, I made several much smaller deficiency lines using FLP-FRT mediated recombination. However, it does not fit for every gene, since the available transgenic lines with FRT site insertions only exist in limited chromosome regions.

The second method that compensates for the non-complementation test is to rescue the mutant phenotype with available duplication lines each of which carries an additional copy of a certain chromosome regions. Similar to the first method, the result from the duplication lines also gives many candidate genes. A better way to do this, which is also what I did, is to create transgenic lines with P[acman] BAC insertions for phenotype rescue. These P[acman] BAC insertions are duplications of a much smaller chromosome region around 20 kb each. However, making transgenic lines are time- and money- consuming, so it should be used only to rule out candidate genes in a certain region achieved from the non-complementation test.

After the rescue assay with the small duplication lines and/or non-complementation test with the small deficiency lines, there should be only a few candidate genes left. At this time, if the flies are homozygous viable, RT-PCR can be performed to examine the expression changes of these genes. In addition, the protein levels can be examined if the antibodies are available. If the homozygotes are lethal, since the potential genes are already known in a small range on a specific chromosome, then FLP-FRT mediated clonal analysis with an FRT site recombined on the same chromosome arm can be used. Clonal analysis enables a comparison of expression levels of those genes in wild-type and homozygous-mutant cells in multiple tissues by in situ hybridization and/or immunofluorescent staining. However, these methods are of no use if the mutation only causes a functional change but not an alteration of expression level in a specific gene.

The most important experiment is to make cDNA transgenic lines for each candidate gene and perform rescue assay with these lines. Although this method is still time- and money- consuming, it definitely gives you the final result convincingly.

Besides the methods mentioned above to determine the gene, genomic DNA sequencing can be used to map the exact mutation inducing the phenotype. In my case, it turned out very hard to figure out the exact mutation. I first sequenced the *udd* ORF and its 5'end sequence up until the ORF of a gene immediately upstream, comparing *udd* homogotes to a control line, which is initially from the same screen but does not exhibit the same phenotype. No mutations were found in that region. Nevertheless, the 3'end of *udd* overlaps a lot with a natural transposon that have hundreds of copies in the whole genome, and I was not able to pick out a good primer to PCR amplify that region and sequence it. Therefore, in the udd^{1} homozygotes, although the Udd protein and RNA levels are greatly

reduced and I believe some regulatory element(s) is mutated upstream or downstream of the gene, the exact location of the *udd*^{1} mutation is still unknown.

CHAPTER IV

Udd protein functions as a novel *Drosophila* RNA polymerase I regulator.

A. Introduction

The nucleolus and ribosome biogenesis

The nucleolus is a subnuclear region formed around nucleolar organizer regions (NORs) composed of clusters of tandemly arrayed rRNA genes. Nucleoli are typically organized into three regions: The fibrillar center (FC), the dense fibrillar component (DFC), and the peripheral granular component (GC) (**Figure 4.1**) [206]. Although nucleoli are mostly visible under light microscopy, these sub-compartments can be distinguished under transmission electron microscope (TEM).

The nucleolus is the site where most steps of ribosome biogenesis take place in eukaryotic cells. Ribosome biogenesis is closely related to cell growth and proliferation, and it starts from RNA Pol I- mediated rRNA gene transcription at the NORs which are the boundary between FC and DFC (see **Chapter I** for more information about RNA Pol I transcription). RNA Pol I subunits and other Pol I transcription related proteins reside in the FC. A single rRNA gene repeat in the nucleolus is first transcribed into a 47S pre-ribosomal RNA precursor (pre-rRNA) which is subsequently cleaved, modified and processed into 28S, 18S and 5.8S rRNAs by U3 small nucleolar ribonucleoprotein (snoRNP)- containing complex and other processing factors. The early rRNA processing steps mainly take place in the DFC, and Fibrillarin, an rRNA 2'-O-methyltransferase and a component of snoRNP complex, is often used to label this specific compartment. The later rRNA processing steps are in the GC, which is also the region where ribosome assembly starts. Nucleolin, B23, nucleostemin can be used to label the GC region.

In most eukaryotic organisms, 5S rRNA gene is located on a different chromosome region and is transcribed in the nucleoplasm by RNA Pol III, the transcripts of which join ribosome

biogenesis in the assembly steps. Besides rRNAs, more than 70 ribosome protein genes are transcribed by RNA Pol II in the cytoplasm, and after translation the proteins are transported into the nucleus or nucleolus to participate in distinct steps of ribosome assembly. Moreover, unlike prokaryotes, the rRNA processing and ribosome assembly steps in eukaryotic organisms require numerous non-ribosomal proteins and non-ribosomal RNAs, like methyltransferase, RNA helicase, endo-/ exo- nuclease, GTPase/AAA-ATPase, transportation factors and snoRNAs.

rRNA transcription, rRNA processing and ribosome assembly are not clearly distinguished temporally [207]. It has been observed before in some cells that rRNA processing machinery starts to assemble on nascent pre-rRNA transcripts co-transcriptionally [208]. Ribosome assembly also initiates earlier, when rRNA processing is still ongoing. A 90S ribosome precursor (90S pre-ribosome) is assembled first, composed of snoRNPs, ribosomal proteins of the small subunit, non-ribosomal proteins and rRNA precursors. The 90S pre-ribosome is subsequently cleaved into 40S and 60S pre-subunits in the GC and the nucleoplasm which require further association and dissociation of multiple factors before exiting into the cytoplasm and function as mature ribosome subunits in protein synthesis. The rRNA components of these two subunits are different: 18S rRNA is the major rRNA component in the 40S subunit; 28S, 5.8S and 5S rRNAs are in the 60S subunit. Compared to the 40S pre-subunit, the 60S pre-subunit has more complicated processing and assembly procedures, and the majority of 60S pre-subunit- associated factors including ribosomal proteins are recruited after cleavage. Most factors associated with 40S and 60S ribosome subunits have distinct and specialized functions and can not work for biogenesis of both subunits.

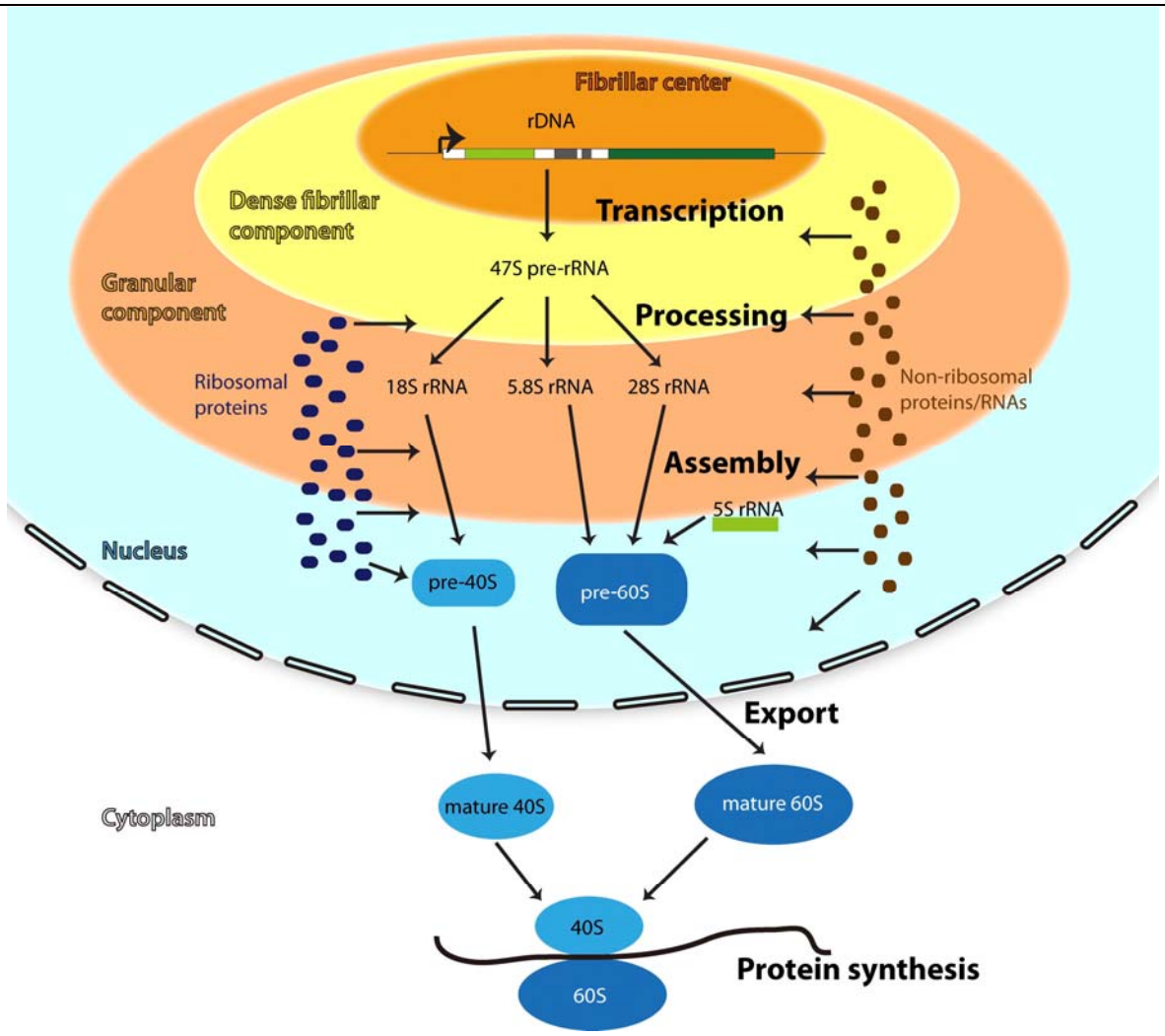

Figure 4.1 Model of ribosome biogenesis. RNA Pol I- mediated rRNA gene transcription occurs at the boundary between FC and DFC. The 47S pre-rRNA is then processed into 18S, 28S and 5.8S rRNAs by snoRNP complex and other processing factors mainly in the DFC. In the GC, ribosome assembly occurs during later steps of rRNA processing, starting with the formation of a 90S pre-ribosome precursor which is subsequently cleaved into the 60S and 40S pre-subunits. Ribosomal proteins for the small subunit associate with 18S rRNA to form 40S subunit; large subunit ribosomal proteins bind to 28S, 5.8S and 5S rRNAs to form 60S subunit. These subunits are exported into the cytoplasm to be involved in protein translation.

Here in this chapter, I mainly describe the characterization of Udd protein as a novel positive regulator of *Drosophila* RNA Pol I transcription. Mass Spectrometry analysis revealed that Udd interacts with potential *Drosophila* homologs of Taf1B and Taf1C, both of which are in mammalian SL1 complex and critical for RNA Pol I transcription initiation. Co-IP and co-localization

in S2 cells further confirmed the association of Udd with these proteins, and knocking down these factors in *Drosophila* reduced nucleolar localization of Udd. Moreover, germline-specific knockdown of *Taf1B* gave rise to the same germ-cell loss phenotype as *udd* mutants. Immunofluorescent staining together with *in situ* run-on assay revealed that Udd was enriched in a specific subnucleolar region for rRNA transcription, instead of rRNA processing or ribosome assembly. Co-IP in S2 cells and ChIP-qPCR analysis in *Drosophila* ovarian lysates demonstrated that the Udd/Taf1B complex could bind to the RNA Pol I complex and was specifically enriched in the rRNA gene promoter region. Downregulation of Udd or Taf1B reduced pre-rRNA levels as shown in northern blot and *in situ* run-on assay.

B. Results

Udd localizes to a specific region in the nucleolus.

To further characterize the localization of Udd in the nucleolus, I stained wild-type ovaries for Udd and other previously characterized nucleolar markers. Nucleoli are organized into three regions as mentioned above: FC, DFC and GC (**Figure 4.1**) [206]. Fibrillarin (Fib), an rRNA 2'-O-methyltransferase functioning in one of the first steps of pre-rRNA processing, is enriched in the DFC while Modulo (Mod), a structural homolog of vertebrate nucleolin, localizes mainly to the nucleolar periphery [209] [210]. Udd exhibited tight association with both of these nucleolar markers (**Figure 4.2**). However, close examination revealed that Udd did not perfectly co-localize with either Fib or Mod, but rather appeared enriched in a more central region of the nucleolus.

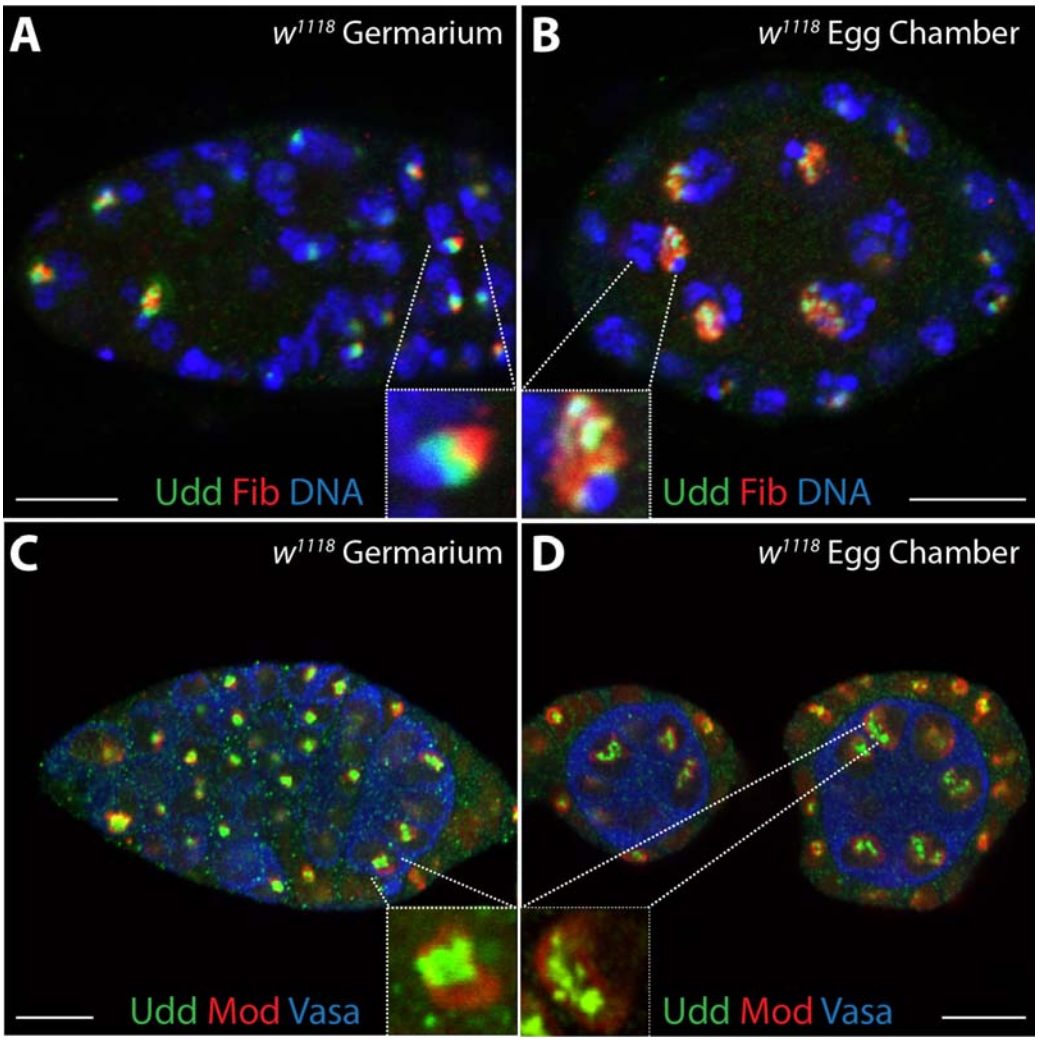

Figure 4.2 Udd localizes to a specific region in the nucleolus. (A, B) Wild type germarium (A) and egg chamber (B) stained for Fibrillarin (red), Udd (green) and DNA (blue). (C, D) Wild type germarium (C) and egg chamber (D) stained for Modulo (red), Udd (green) and Vasa (blue). Udd does not perfectly co-localize with these two nucleolar markers. Scale bars represent 20 μm.

Udd associates with *Drosophila* Taf1B encoded by *CG6241* and a structural homolog of human Taf1C encoded by *CG10496*.

To further investigate the function of Udd in the nucleolus, I performed Tandem Immunoprecipitation followed by Mass Spectrometry using 3×Flag-3×HA-Udd transfected S2 cells, since Udd is ubiquitously expressed in most tissues and also expressed in S2 cells as a nucleolar protein. The results showed that Udd associated with a previously uncharacterized 102 kDa protein

encoded by *CG6241*, and their physical association was confirmed by Co-IP test in transiently-transfected S2 cells in both directions (**Figure 4.3**). Based on its shared primary sequence and secondary structure homology with human Taf1B (TATA box-binding protein-associated factor RNA polymerase I subunit B) and yeast Rrn7, both of which are RNA Pol I transcription factors, CG6241 will be called Taf1B hereafter (**Figure 4.4**). GFP-tagged *Drosophila* Taf1B localized to the nucleolus in S2 cells (**Figure 4.5**) and ovaries. (Note: I've just made and examined the transgenic line recently, and data from the ovaries are not shown here.)

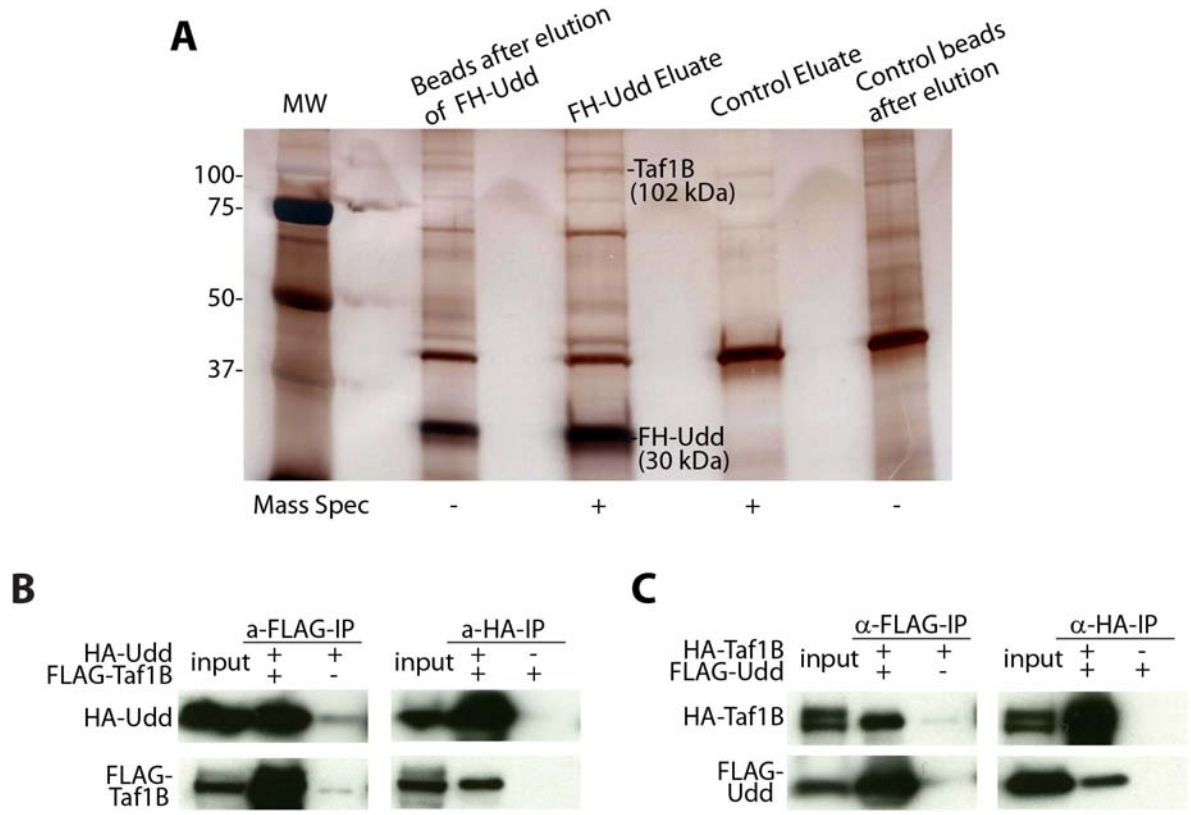

Figure 4.3 Biochemical analysis demonstrates that Udd associates with Taf1B in *Drosophila*. (A) Silver-stained SDS Polyacrylamide gel showing that tandem-affinity-purified and peptide-eluted 3×Flag-3×HA-Udd (FH-Udd) and interacting proteins from S2 cells under native conditions. The band corresponding to Taf1B, which was identified using Mass Spectrometry, is indicated (MW, protein molecular weight marker in kDa). S2 cells transfected with empty vector were used as negative control. (B) Western blots of co-immunoprecipitation (Co-IP) between FLAG-tagged Taf1B, HA-tagged Udd from transfected S2 cells. (C) Western blots of Co-IP between FLAG-tagged Udd, HA-tagged Taf1B from transfected S2 cells.

A The Taf1B/RRN7 family

```
gi_82078563     5 E. [9]. CGQ     CAAV. [1]. WGVSDEGQFFC. [1]. SCHNVIE 41  Taf1B_DANRE
gi_74726856     3 L. [9]. CTQ     CAAV. [1]. WGLTDEGKYYC. [1]. SCHNVTE 39  Taf1B_HUMAN
gi_342187029    3 V. [9]. CSQ     CAAV. [1]. WGLTDEGKYYC. [1]. SCHNVTD 39  Taf1B_MOUSE
gi_26399334     3 G. [7]. CSV. [2]. CKST     WYFKNAGQTFC     RRGHAQH 37  RRN7_SCHPO
gi_1008140      3 T. [6  CGT. [2]. CPSR     LWRIIDGRRTC     QYGHVME 36  RRN7_SACCE
gi_74956228     1 M. [7]. CNA     CGGY     RFSVNDGFKYC. [1]. RCGALFE 34  Taf1B_CAEEL
gi_74869043     5 L. [9]. CDV     CEGT     TFQEREGFYYC. [1]. ECGTQKD 40  Taf1B_DROME
```

DANRE: Danio rerio; **SCHPO**: Schizosaccharomyces pombe; **SACCE**: Saccharomyces cerevisiae;
CAEEL: Caenorhabditis elegans; **DROME**: Drosphila Melanogaster.

B Drosophila vs Human Taf1B alignment

```
1   MEEVLETMQLENMHCDVCEGTTFQ-EREGFYYCVECGTQKDQIRAVDITAEDNFDDTAAG  59 TAF1B_DROME
1   --MDLEEAEEFKERCTQCAAVSWGLTDEGKYYCTSCHNVTERYQEVTNT--DLIPNTQ--  54 TAF1B_HUMAN

60  RYTARTIRQKKDTEKEDEDDITSWEFY-----NYVLRGFLQELLNMGAKPELKLMTL-QV 113 TAF1B_DROME
55  ------IKALNRGLKKKNNTEKGWDWYVCEGFQYILYQQAEALKNLGVGPELKNDVLHNF 108 TAF1B_HUMAN

114 WAAYLDSMEVAFSKSNKTGLPKLNVRALPIDARIIYNHKTFKKGKKGKKSTLTGDPNDER 173 TAF1B_DROME
109 WKRYLQKSKQAYCKNPVY----------------------TTGR---KPTVLED----N 138 TAF1B_HUMAN

174 AKFRLWNRTKRNL---DASGYRSHGGASESEGEQSLHLQWSMRARKSLKRHMPLKHLDKH 230 TAF1B_DROME
139 LSHSDWASEPELLSDVSCPPFLESGAESQSD----IHT------R----KPFPVSKASQ- 183 TAF1B_HUMAN

231 SRDSKGSMSCHSLRPRVKQLHNFDRNIYCLNIIKLYVVLGIALNMVEDDIQLSDLLRFID 290 TAF1B_DROME
184 ----SETSVCSGSLDGVEYSQRKEKGIVKMTMPQTLAFCYLSLLWQREAITLSDLLRFVE 239 TAF1B_HUMAN

291 EEHLTKRCMLNYLPGNVAAKGKA--LLKDMELSKMKDKVTNKLLRVNIACMSRFINLSEY 348 TAF1B_DROME
240 EDHIPYINAFQHFPEQMKLYGRDRGIFGIESWPDYEDIYKKTVEVGTFLDLPRFPDITED 299 TAF1B_HUMAN

349 QKPNLHSLAERYILELALPPRLLKYVNSLLDLHPP------TFFNAMTVHPYPRYEARTM 402 TAF1B_DROME
300 CYLHPNILCMKYLMEVNLPDEMHSLTCHVVKMTGMGEVDFLTFDPIAKMAKTVKYDVQAV 359 TAF1B_HUMAN

403 AYILYAMKLLFGLDDLKERNISESAAKINEKLLEVGGDEAPLLFVFTEWMEFVEMRKVIV 462 TAF1B_DROME
360 AIIVVVLKLLFLLDDSFEWSLSNLAEKHNEKN-----KKDKPWFDFRKWYQIMKK----- 409 TAF1B_HUMAN

463 SHYNQSFARRFGVSTRTGCQVDDILAKEWKEKEQGETFGWM----------QGSAAMKRQ 512 TAF1B_DROME
410 -AFDEK-------------------KQKWEEAR--AKYLWKSEKPLYYSFVDKPVAYKKR 447 TAF1B_HUMAN

513 H--ENLTHIIETMLKDH--FGESSKESMEKEHIEFQPSLTPAHSYFNRILLQVSRSDGAK 568 TAF1B_DROME
448 EMVVNLQKQFSTLVESTATAGKKSPSSF---QFNWTEEDTDRTCFHGHSLQGVLKEKGQS 504 TAF1B_HUMAN

569 MKITIP-DHMKVDHSARNLDPFVLETTELSQYL-------SQHGLKLRVEELACQEDI-- 618 TAF1B_DROME
505 LLTKNSLYWLSTQKFCRCYCTHV-TTYEESNYSLSYQFILNLFSFLLRIKTSLLHEEVSL 563 TAF1B_HUMAN

619 QNVGIFRPL-TIIRGDGREYRANTEIKTETWISELKRKEKRPDFRFTQPTGTYGARYLKR 677 TAF1B_DROME
564 VEKKLFEKKYSVKRKKSRSKK-------------VRRH---------------------- 588 TAF1B_HUMAN
```

Figure 4.4 *Drosophila melanogaster* Taf1B, encoded by *CG6241*, is a homolog of human Taf1B, and belongs to the Taf1B/RRN7 protein family. (A) The Taf1B/RRN7 family includes multiple members from yeast to human. (B) Sequence alignment of *Drosophila melanogaster* Taf1B (1-677aa, full-length 872aa) and Human Taf1B (1-588aa, full length 588aa). Uniprot online alignment tool was used. Magenta: Zinc finger. Blue: Zinc-binding cysteine. Dark grey and ***** indicate identical amino acids in these two sequences. **:** and **.** indicate amino acids that share high and low similarity.

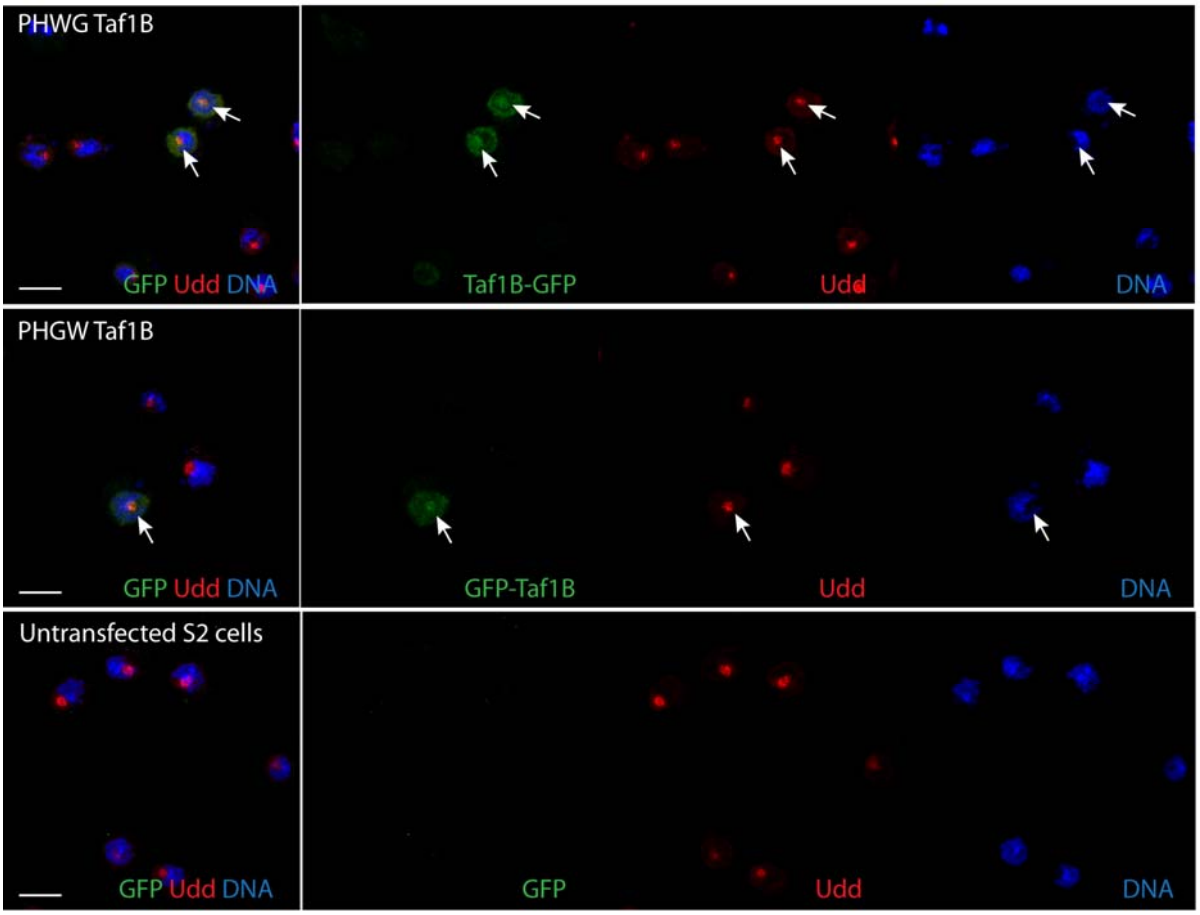

Figure 4.5 GFP-tagged Taf1B co-localizes with Udd in the nucleolus. The *Taf1B* ORF was introduced into the pHGW and pHWG gateway vectors, which both contain a weak hsp70 promoter for low levels of expression in the absence of heat-shock and a N- or C-terminal GFP tag respectively. Transfected S2 cells at room temperature were examined for Taf1B expression. Arrows point out the co-localization of tagged Taf1B and endogenous Udd in the nucleoli. Scale bars represent 10 µm. (Note: I've just made and examined the transgenic line for GFP-Taf1B recently which exhibits the same nucleolar localization as Udd in the germline, and data from the ovaries are not shown here.)

Besides Taf1B, I found another potential Udd binding partner from Mass Spectrometry results, which is a 95 kDa protein encoded by *CG10496*. I further confirmed the physical binding between CG10496 and Udd using S2 cells transfected with Flag- or HA- tagged constructs (**Figure 4.6**). CG10496 was also previously uncharacterized, and did not have any mammalian homologs according to its protein sequence. However, using HHpred server (http://toolkit.tuebingen.mpg.de/hhpred) which detects homology according to both primary sequence

and secondary structure, I found that the top hits in *Homo sapiens* proteome for CG10496 were different isoforms of human Taf1C (TATA box-binding protein-associated factor RNA polymerase I subunit C), which is in the same SL1 complex with Taf1B regulating RNA Pol I transcription initiation (**Figure 4.7**). Blasting human Taf1C did not reveal any sequence homologs from *Drosophila melanogaster*; however, searching different human Taf1C isoforms using HHpred server in *Drosophila melanogaster* proteome showed that CG10496 was almost always the No. 1 hit (**Figure 4.7**). Interestingly, Drosophila Protein Interaction Mapping Database (DPiM) (https://interfly.med.harvard.edu/index.php) [211] revealed that CG6241, the *Drosophila* Taf1B, was pulled down with CG10496 in systematic IP studies, which further confirmed the results of my biochemical studies. Consistent with all the above results, exogenous CG10496 was also shown to be enriched in the nucleoli of S2 cells, similar to Taf1B and Udd (**Figure 4.8**).

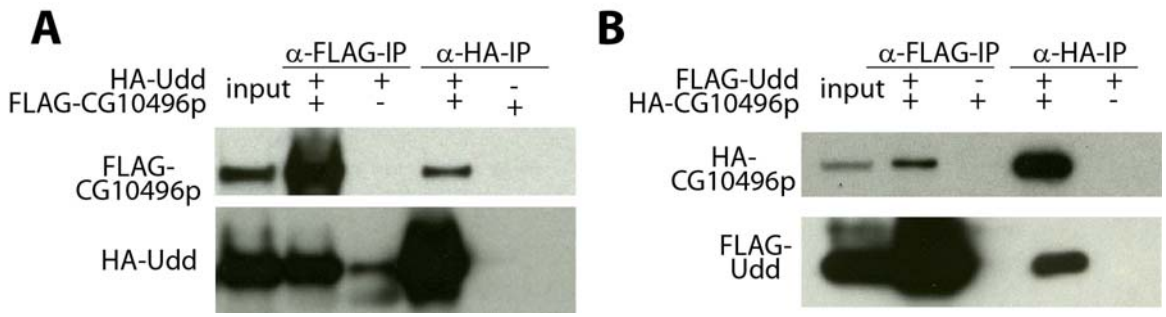

Figure 4.6 Co-IP test demonstrates that Udd associates with CG10496, which is also a candidate from Mass Spectrometry results. (A) Western blots of Co-IP between FLAG-tagged CG10496 and HA-tagged Udd from S2 cells. (B) Western blots of Co-IP between FLAG-tagged Udd and HA-tagged CG10496 from S2 cells.

A

Input Protein Sequence	Proteome searched	Hit Ranking	Hit Name	Probability (%)	E-value	P-value	Score
CG10496p	*Homo* sapiens	1	Taf1C isoform 2	98.9	7.60E-09	1.20E-13	117.3
		2	Taf1C isoform 1	98.9	1.40E-08	2.10E-13	115.9
		3	gi|56243590	98.1	3.70E-05	5.80E-10	96.4
		4	gi|8922301	97.8	0.0025	3.90E-08	74.5
		5	gi|2136115	97.7	0.0018	2.90E-08	76.2
hTaf1C isoform 1	*Drosophila* melanogaster	1	CG10496	100	5.20E-70	1.10E-74	408.6
		2	gi|24586100	98.6	4.70E-06	9.60E-11	57.9
		3	gi|20129115	98.5	1.20E-05	2.40E-10	55.8
		4	gi|19922838	98.3	5.10E-05	1.00E-09	52.3
hTaf1C isoform 2	*Drosophila* melanogaster	1	CG10496	100	7.40E-48	1.50E-52	419.1
		2	gi|17933648	99.8	3.20E-17	6.50E-22	177.5
		3	gi|28573273	99.7	6.50E-15	1.30E-19	162.9
		4	gi|20129115	99.5	7.80E-12	1.60E-16	131.5
hTaf1C isoform 6	*Drosophila* melanogaster	1	CG10496	100	4.20E-49	8.60E-54	431.2
		2	gi|17933648	99.5	3.90E-12	8.00E-17	138.4
		3	gi|28573273	99.4	1.70E-11	3.60E-16	136.1
		4	gi|20129115	99.2	1.40E-08	3.00E-13	107.1
		5	gi|45552461	99.2	4.70E-09	9.50E-14	120.8

B

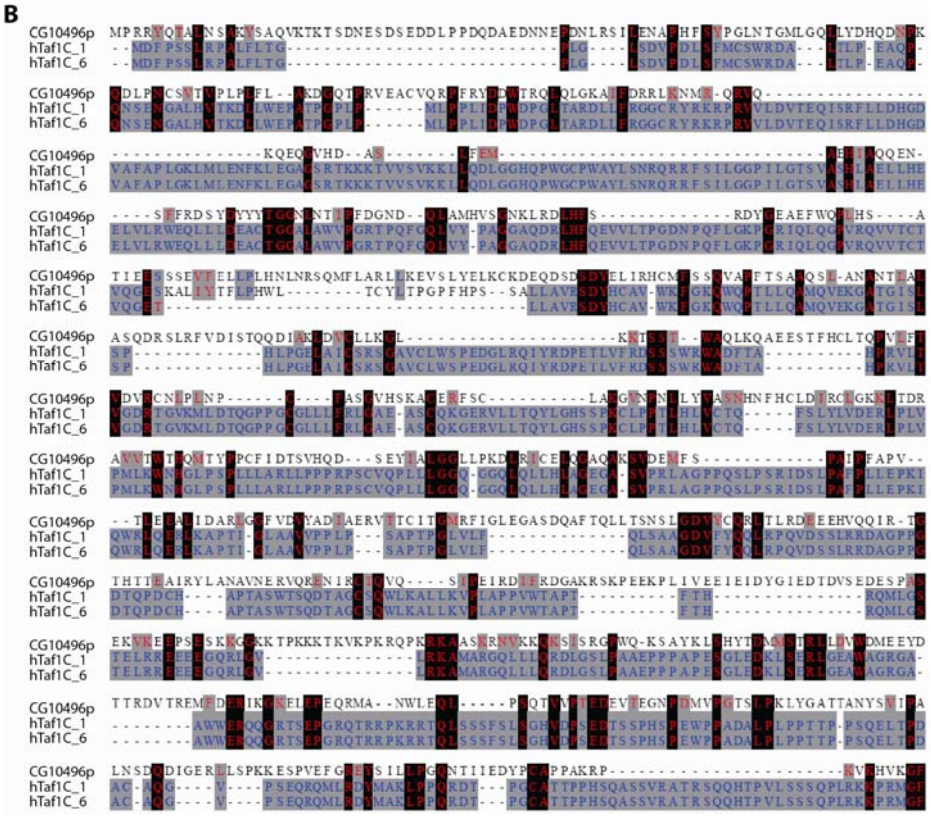

Figure 4.7 CG10496 is a potential homolog of human Taf1C according to their secondary structures and primary sequences. (A) HHpred server which detects homology according to both primary sequence and secondary structure shows that the top hits for CG10496 in *Homo sapiens* proteome are different isoforms of human Taf1C, and vice versa, the number 1 hit for different human Taf1C isoforms in *Drosophila melanogaster* proteome is CG10496. (B) Sequence alignment of *Drosophila melanogaster* CG10496 and two isoforms of human Taf1C. Taf1C isoform 1 and 6 are chosen because they both have more than 800aa, similar to CG10496. Clustal Omega alignment tool was used. Identical amino acids in all sequences are in red with black background. Identical amino acids in two of these three sequences are in blue with grey background. Similar amino acids are in red with grey background.

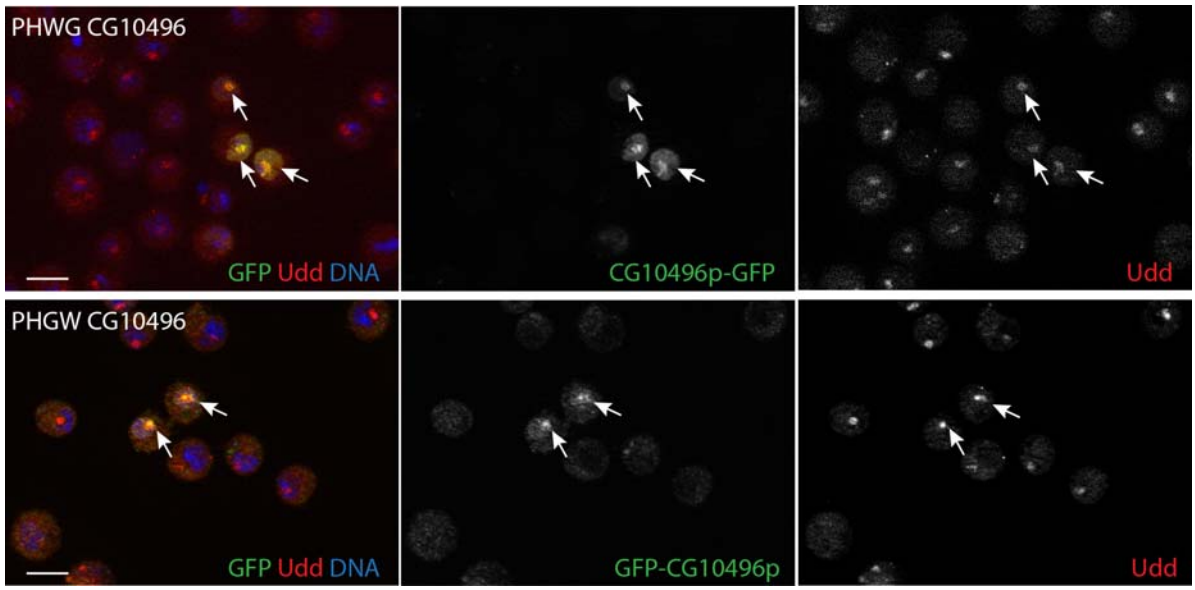

Figure 4.8 GFP-tagged CG10496 co-localizes with Udd in the nucleolus. The *CG10496* ORF was introduced into the pHGW and pHWG gateway vectors, which both contain an hsp70 promoter for leaky expression at room temperature in the absence of heat-shock and a N- or C-terminal GFP tag respectively. Transfected S2 cells were examined for GFP tagged CG10496 expression. Arrows point out the co-localization of tagged CG10496 and endogenous Udd in the nucleoli. Scale bars represent 5 μm.

Germline specific knock-down of *Taf1B* exhibits a similar phenotype to *udd* mutants.

Next, to examine if knocking down these Udd binding partners give rise to the same *udd* mutant phenotype, I made UAS-RNAi constructs with TRiP VALIUM vectors (http://www.flyrnai.org/TRiP-REA.html) for *Drosophila Taf1B* and *CG10496*, the expression of which are driven by Gal4/UAS system. It was observed that at 29℃ knocking down *Taf1B* ubiquitously using *da-gal4* induced lethality at the larval and embryonic stage, similar to udd^{null} homozygotes which are embryonic-lethal; knock-down of *Taf1B* in the germline using *nos-gal4* resulted in similar germ-cell loss to *udd* mutants exhibited in both egg chambers and germaria (**Figure 4.9**). However, the RNAi line made for *CG10496*, which was able to reduce the *CG10496* RNA level by more than 85%, failed to cause any visible phenotype no matter using ubiquitous Gal4 driver or germline

specific Gal4 driver, and no obvious germ cell loss was observed even in three to four week-old flies. In my opinion, CG10496 might play a less important role compared to Udd and Taf1B in this complex (see Discussion).

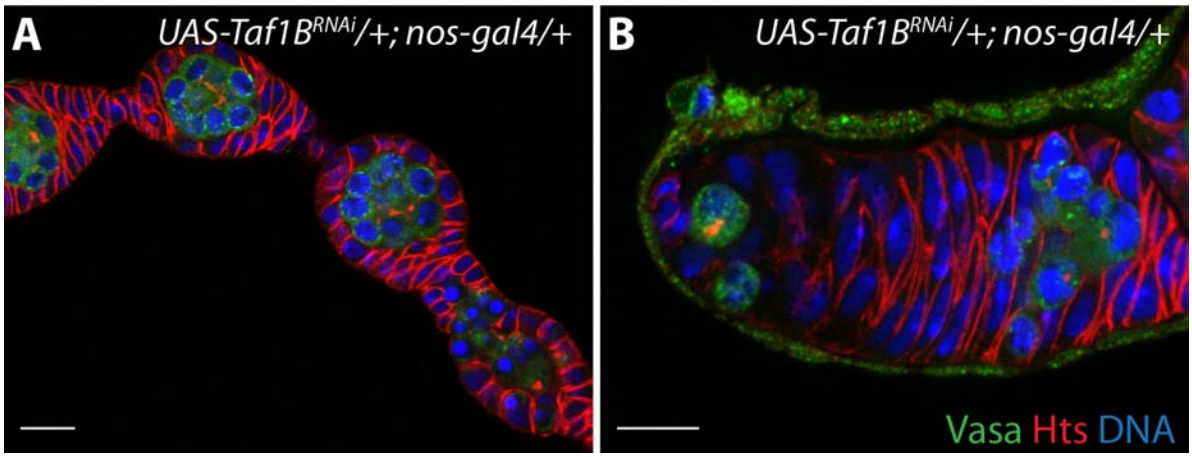

Figure 4.9 Germline-specific knock-down of *Taf1B* exhibits germ-cell loss similar to *udd* mutants. *UAS-Taf1B^{RNAi}/+;nos-gal4/+* flies kept at 29°C were examined. (A) Egg chambers and (B) a germarium stained for Vasa (green), Hts (red), DNA (blue).

Taf1B helps to stabilize Udd protein and is required for the proper localization of Udd in the nucleolus.

In addition to the *udd*-type germ-cell loss phenotype observed with the *Taf1B* germline knocked-down ovaries, immunofluorescent staining of these ovaries for Udd and another nucleolar protein Fibrillarin demonstrated that the nucleolar Udd level was greatly reduced while Fibrillarin level was not obviously affected in the germ cells (**Figure 4.10**). Moreover, ovaries with *CG10496* knocked-down in the germline were also observed with a mild reduction of nucleolar Udd (**Figure 4.11**, see discussion).

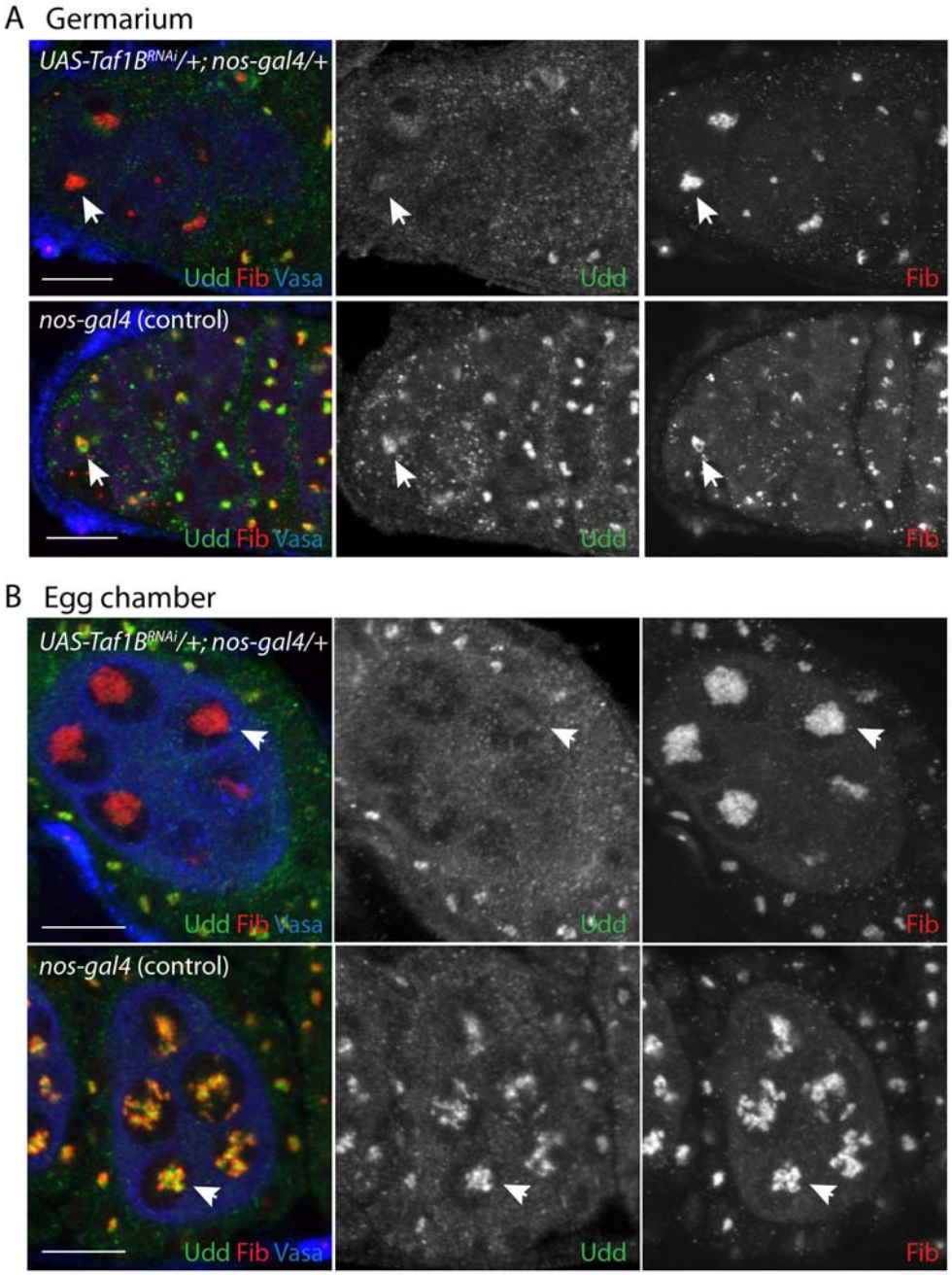

Figure 4.10 Knock-down of *Taf1B* in the germline greatly reduces the nucleolar localization of Udd. (A) Germaria and (B) egg chambers from *UAS-Taf1B*^{RNAi}*/+;nos-gal4/+* and *nos-gal4* control flies stained for Udd (green), Fibrillarin (red) and Vasa (blue). Although the morphology of nucleoli changes upon *Taf1B* knock-down, Fibrillarin level and its nucleolar localization appear largely unaffected. (A, B) Vasa marks germ cells. Arrowheads mark germ cell nucleoli in all panels. Scale bars represent 10 μm.

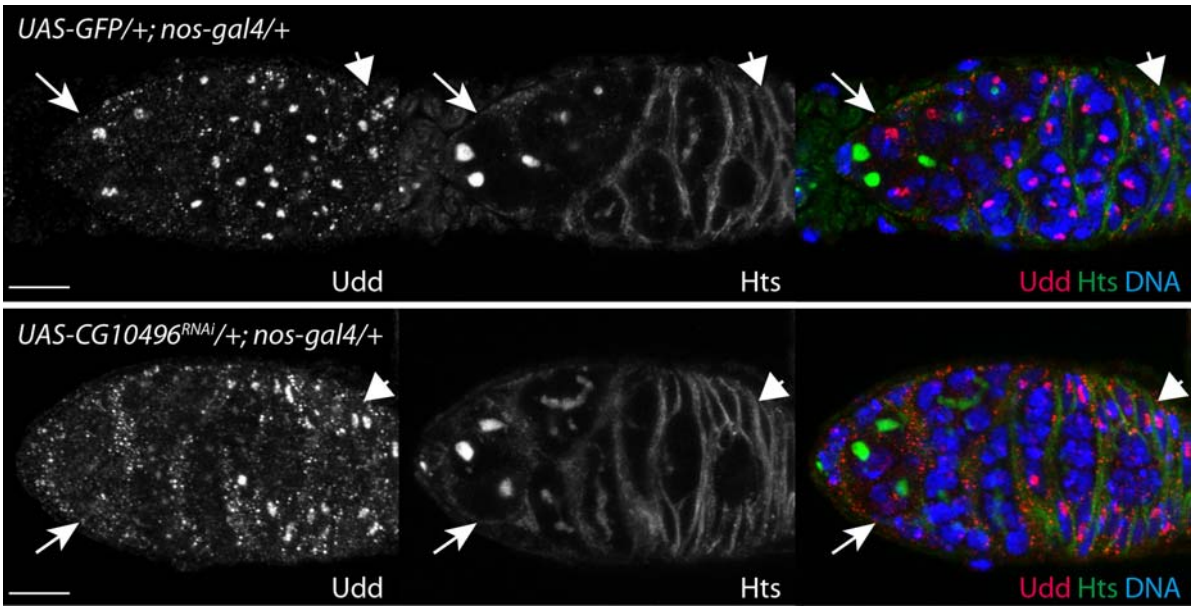

Figure 4.11 Knock-down of *CG10496* in the germline also reduces the nucleolar localization of Udd. Germaria from *UAS-CG10496^{RNAi}/+;nos-gal4/+* (bottom panel) and *UAS-GFP/+;nos-gal4/+* (top panel) control flies stained for Hts (green), Udd (red) and DNA (blue). Although the *CG10496* RNAi line does not exhibit an obvious germ-cell loss phenotype using *nos-gal4* driver, the reduction of nucleolar Udd is still observed. Arrows mark germ cell nucleoli, and arrowheads mark somatic cell nucleoli as an internal control. Scale bars represent 10 μm.

There are several possible explanations for the reduction of Udd in the nucleoli: the nucleolar localization of Udd requires the presence of Taf1B; Udd protein is stabilized in the presence of Taf1B; Udd is regulated by Taf1B at translational or posttranscriptional level; the *udd* gene is regulated by Taf1B at transcriptional level. First, to examine if there was any change of *udd* expression level in *Taf1B* knocked-down cells, I performed western blot and RT-qPCR using fly ovaries (**Figure 4.12**). For these experiments, *da-gal4* was used to ubiquitously knock down *Taf1B* in both germ cells and somatic cells, and crosses were kept at room temperature to obtain viable adult flies. The experiments showed that in *Taf1B* knocked-down ovaries there was a great reduction of Udd protein level while the *udd* transcript level only mildly decreased compared to *da-gal4* control flies, which suggests that transcriptional regulation of *udd* is not the main cause for the change observed.

One thing to note is that *CG10496* transcript level was greatly reduced when *Taf1B* is knocked down, indicating there might be a positive feedback loop between their expression levels, and when there are less Taf1B molecules interacting with CG10496, there are less *CG10496* transcripts and proteins translated (**Figure 4.12B**).

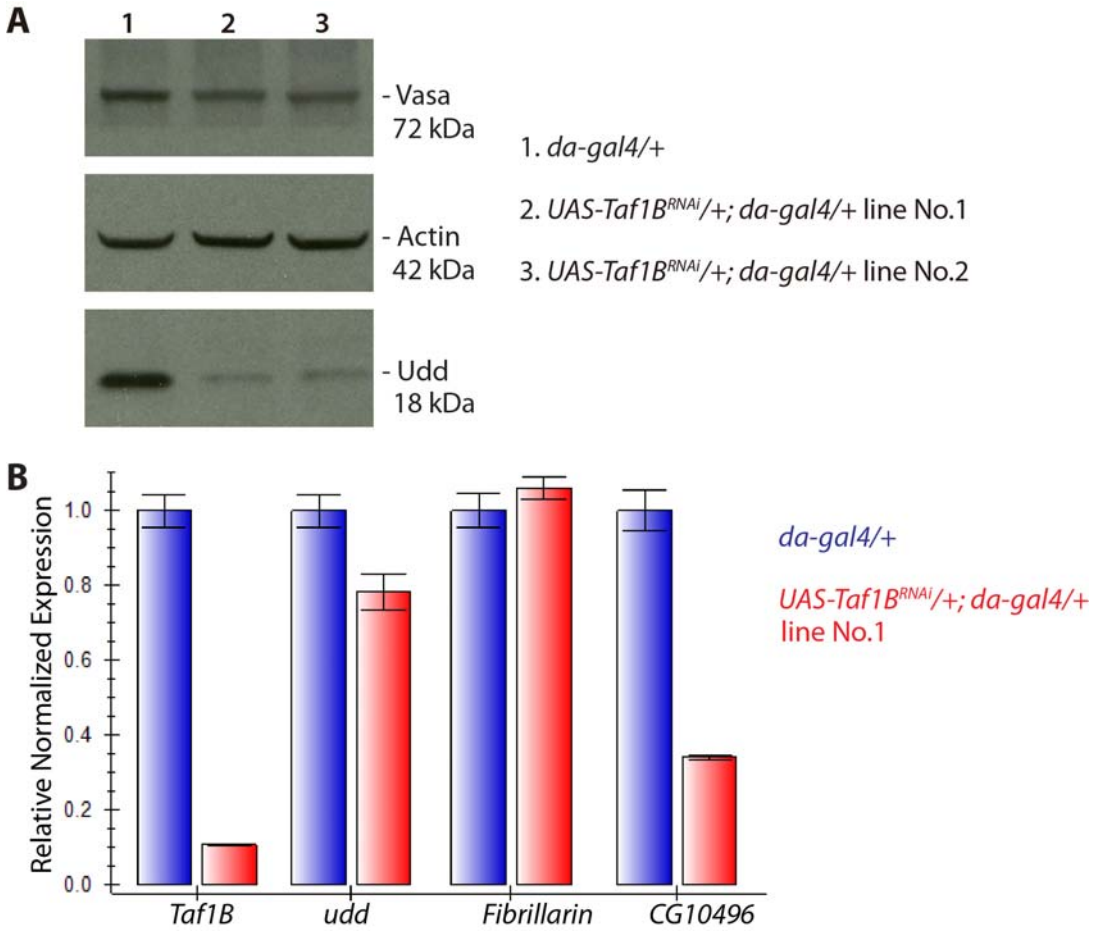

Figure 4.12 The Udd protein level is dramatically decreased in *Taf1B* knocked-down cells, while its transcript level is only mildly affected. Western blots (A) and RT-qPCR (B) are performed using ovaries from *da-gal4* and *UAS-Taf1B*^{RNAi}; *da-gal4* flies kept at room temperature. (A) Two individual RNAi transformants with the same targeted sequence are examined. Actin and Vasa are somatic cell and germ cell loading controls respectively for western blot analysis. (B) The RNA levels of all genes tested are normalized to that of reference gene *α-Tublin84B* in each sample. Besides the mild reduction of *udd* RNA level, the transcript level of *CG10496* is greatly reduced, while that of *Fibrillarin* does not change.

Next, a rescuing transgenic line with 3×HA tagged Udd ORF was utilized, which does not

contain endogenous *udd* promoter or UTR regions and the expression of which is driven by Gal4/UAS system. In this case, the expression of *udd* transgene should not be regulated in the same way as that of endogenous *udd* at transcriptional, posttranscriptional or translational levels. In wild type background, the transgenic HA-Udd protein under the control of *nos-gal4* was highly enriched in the nucleoli of germ cells; however, in *Taf1B* knocked-down cells, the HA-Udd protein level was still greatly reduced, and was not localized to the nucleoli but mostly accumulated in the cytoplasm (**Figure 4.13**, marked by arrowheads). These results strongly indicate that Taf1B helps to stabilize the Udd protein and is required for the nucleolar localization of Udd.

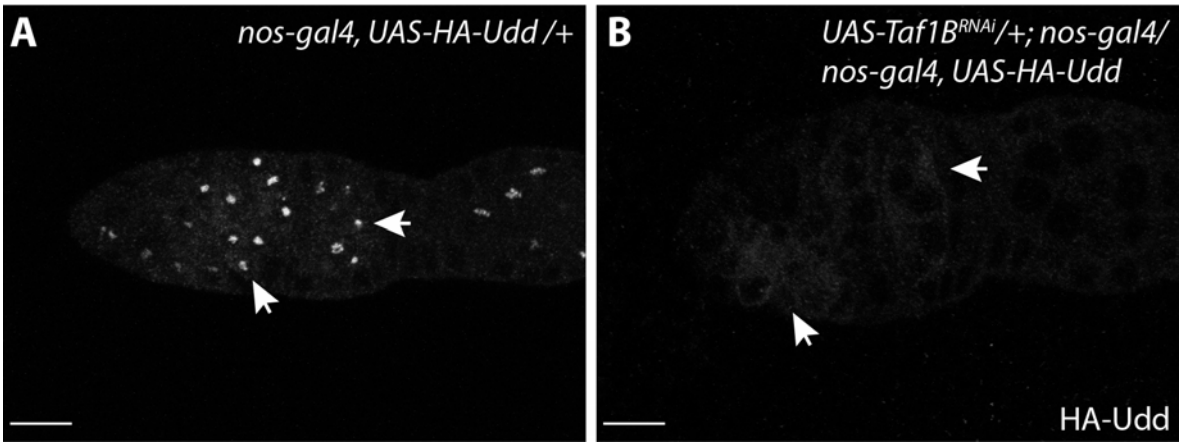

Figure 4.13 The nucleolar localization of HA-tagged Udd is replaced by cytoplasmic accumulation in *Taf1B* knocked-down cells. (A, B) Germaria from control *nos-gal4,UAS-HA-Udd/+* (A) and *UAS-Taf1B^{RNAi}/+; nos-gal4/ nos-gal4,UAS-HA-Udd* (B) flies stained for HA-Udd (white) using anti-HA antibody. Arrowheads indicate germ cells positive for Udd, which appears nucleolar in control cells and cytoplasmic in *Taf1B* knocked-down germ cells. In addition, the level of Udd also seems greatly reduced.

In consideration of the important role Taf1B plays in Udd stability and localization, I examined if Udd has a similar function for Taf1B or CG10496. There was no antibody available against Drosophila Taf1B or CG10496, however, I examined their expression levels by RT-qPCR comparing wild-type w^{1118} and udd^{1} homozygous ovarian RNAs. It showed that *Taf1B* mRNA level

was obviously decreased in *udd*^{1} mutants, while *CG10496* expression was mildly affected, comparing to control *Fibrillarin* (**Figure 4.14**). Therefore, it indicates that the Taf1B protein level is probably also decreased, nevertheless, it is hard to say if Udd also promotes the proper localization and stability of Taf1B.

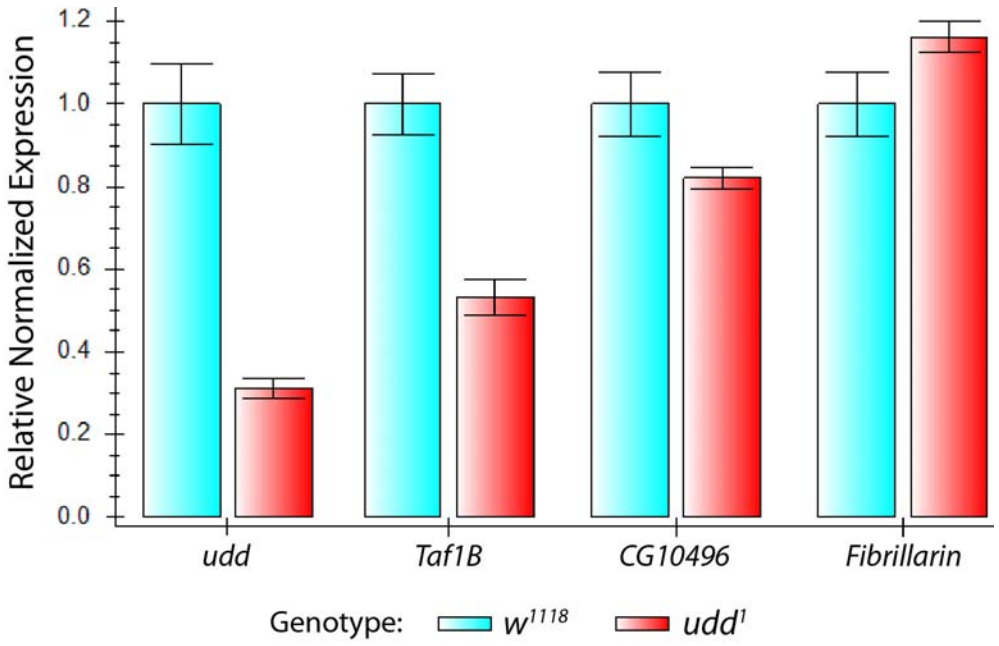

Figure 4.14 RT-qPCR analysis shows that there is a decline of *Taf1B* transcript level in *udd*^{1} mutant ovaries compared to wild-type *w*^{1118} ovaries. The RNA levels of all genes tested are normalized to that of reference gene *α-Tublin84B* in each sample. Besides the reduction of *Taf1B* level, the transcript level of *CG10496* also drops a little, while that of *Fibrillarin* has a mild increase.

The Udd/Taf1B complex associates with RNA Pol I complex in S2 cells.

The localization of Udd (**Figure 4.2**) suggests that it might participate in either rRNA production or the earliest steps of rRNA processing. Moreover, the homology of *Drosophila* Taf1B and CG10496 with human Taf1B and Taf1C suggest that the Udd/Taf1B complex might be involved in rRNA transcription. To begin to distinguish between these possibilities, I conducted Co-IP experiments to test whether Udd and Taf1B physically associated with the Pol I complex or

Fibrilliarin in S2 cells (**Figure 4.15**). It is known that the human SL1 complex including Taf1B and Taf1C promote rRNA transcription initiation by recruiting RNA Pol I complex to the rDNA promoter [15, 19, 20, 24]. Here my results demonstrated that in *Drosophila*, Udd and Taf1B associated with the highly conserved and second largest Pol I subunit RpI135 which does not exist in RNA Pol II complex [212] **(Figure 4.16**). In **Figure 4.15A**, Udd and RpI135 were tagged with 3×HA and 3×FLAG at the N-termini respectively and transfected into S2 cells. RpI135 was pulled down together with Udd. Likewise, Udd was present in RpI135 IP pellets. Their physical association was still detectable when the epitope tags were swapped between the proteins (**Figure 4.15B**). Similar results were also observed in Co-IP tests between Taf1B and RpI135 (**Figure 4.15 C-D**). In contrast, I did not detect physical interactions between Fibrillarin and RpI135 or Udd. These results indicate that the Udd/Taf1B complex specifically associates with components of the RNA Pol I transcriptional machinery.

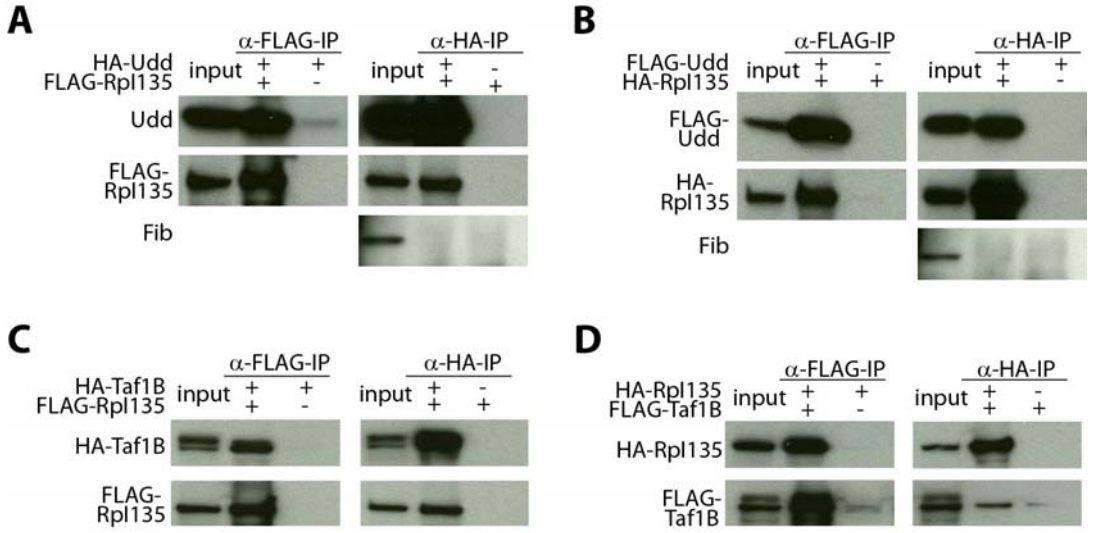

Figure 4.15 The Udd/Taf1B complex associates with RNA Pol I complex in S2 cells. (A) Western blots of co-immunoprecipitation (Co-IP) between FLAG-tagged RpI135, HA-tagged Udd and endogenous Fib (negative control) from transfected S2 cells. (B) Western blots of Co-IP between FLAG-tagged Udd, HA-tagged RpI135 and endogenous Fib from transfected S2 cells. (C) Western blots of Co-IP between FLAG-tagged RPI135 and HA-tagged Taf1B from S2 cells. (D) Western blots of Co-IP between FLAG-tagged Taf1B and HA-tagged RpI135 from S2 cells.

In addition to biochemical studies about these complexes, I also examined the phenotype of RpI135 knocked-down ovaries by immunofluorescent staining. Germline specific knock-down of *RpI135* induced a very strong germ cells loss resulting in empty germaria or germaria with only a couple of germ cells as soon as the flies elcosed, which is not surprising due to the key function of RNA Pol I complex. Moreover, the nucleolar Udd protein is still observed in the remaining *RpI135* knocked-down cells **(Figure 4.16)**, which is different from *Taf1B* knocked-down cells. This further confirmed that although Udd and Taf1B can associate with RpI135, they are probably not in the same complex with RNA Pol I.

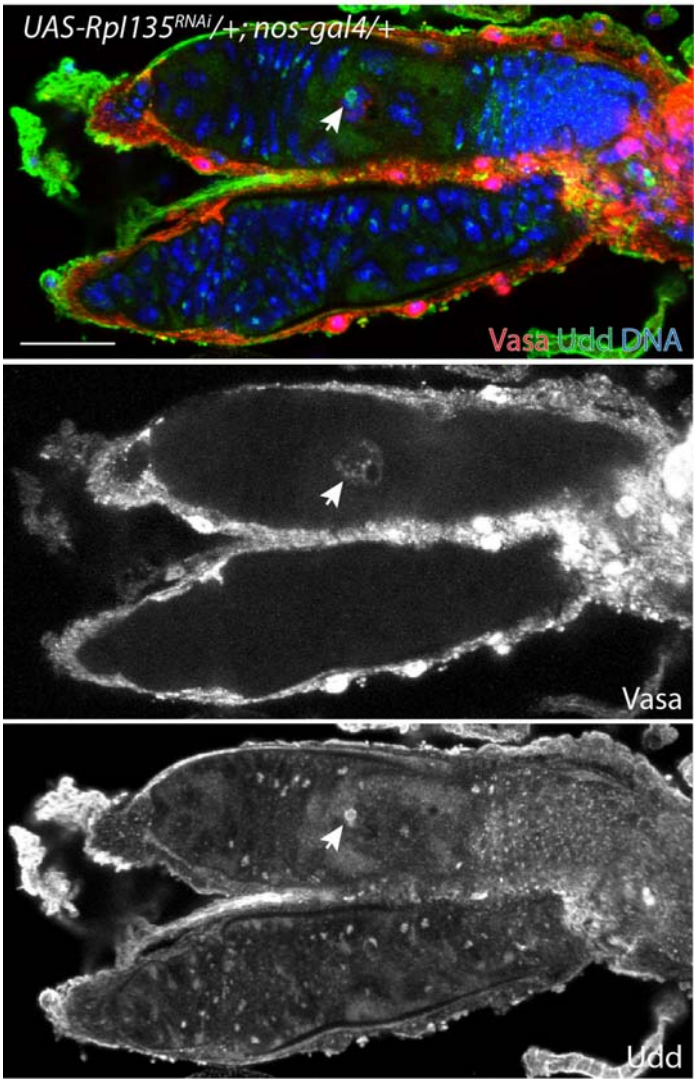

Figure 4.16 Knock-down of *Rpl135* does not affect the nucleolar localization of Udd. Ovarioles from *UAS-Rpl135^{RNAi}/+; nos-gal4/+* females labeled for Udd (green), Vasa (red) and DNA (blue) exhibit a very strong germ-cell loss. In this example, the one remaining germ cell (arrowheads) still maintains nucleolar Udd. Scale bar represents 20 µm.

***In situ* run-on assay demonstrated that Udd associates with newly synthesized rRNAs.**

Next, with the idea that the Udd/Taf1B complex is involved rRNA transcription, I considered the possibility that Udd associated with actively transcribing rDNA genes where pre-rRNAs are newly synthesized. To test this, I performed BrUTP *in situ* run-on transcription assays to label newly synthesized rRNAs in live tissue. Wild-type ovaries were dissected, permeabilized,

pulse-labeled with BrUTP in the presence of the Pol II and Pol III inhibitor α-amanitin for 20 minutes, fixed and stained for BrUTP and Udd protein. These experiments showed a very tight co-localization between newly transcribed rRNA and Udd protein in most cells examined (**Figure 4.17**). Two control experiments were performed: 1. BrUTP labeling without adding α-amanitin to visualize global transcription from all three polymerases; 2. BrUTP labeling in the presence of Actinomycin D to inhibit transcription globally. The results from all three conditions were as expected, shown in **Figure 4.18**.

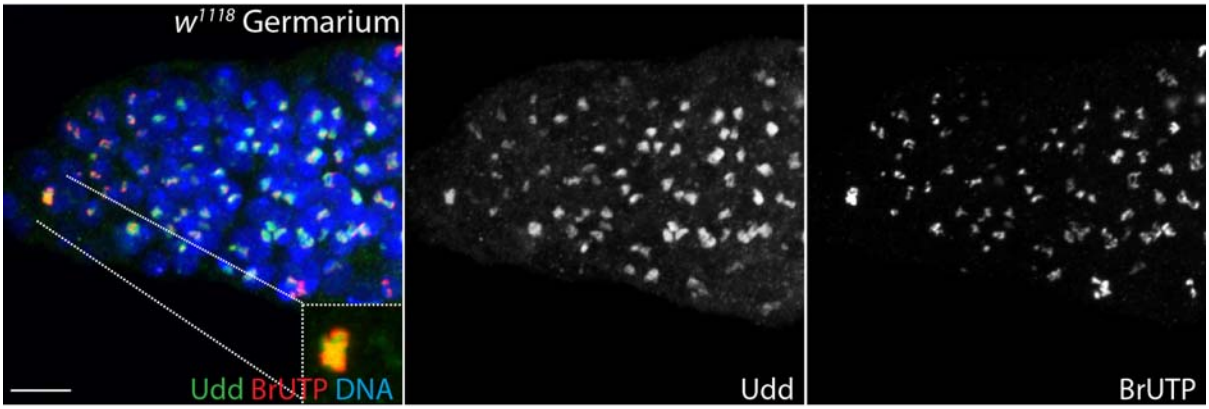

Figure 4.17 Udd associates with newly synthesized rRNAs. Wild-type w^{1118} germarium is stained for Udd (green), BrUTP (red) and DNA (blue). Scale bar represents 20 μm.

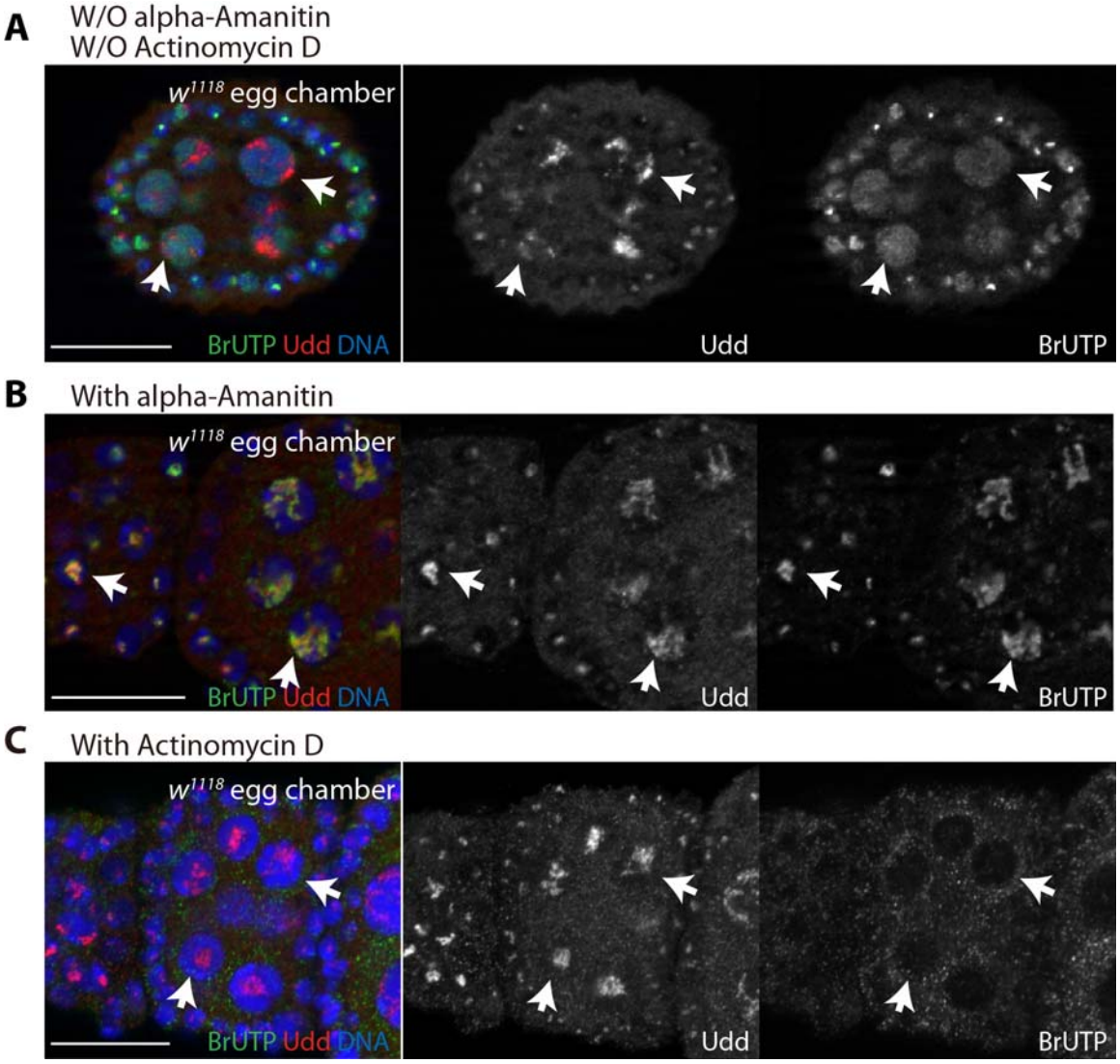

Figure 4.18 Actinomycin D inhibits global transcription, while α-Amanitin specifically inhibits transcription by RNA Pol II and Pol III in cultured w^{1118} ovaries. (A-C) Egg chambers were stained for Udd (red), BrUTP (green) and DNA (blue). (A) Ovaries cultured with BrUTPs for 20 minutes without alpha-Amanitin or Actinomycin D exhibited global nuclear BrUTP labeling, as expected since, without drug, Pol I, Pol II and Pol III RNAs all incorporate BrUTPs. (B) Ovaries treated with α-Amanitin, displayed BrUTP incorporation into pre-rRNAs within nucleoli. (C) No BrUTP incorporation was observed in the nuclei or nucleoli of egg chambers treated with Actinomycin D. Scale bars represent 20 μm.

Udd specifically associates with the rRNA gene promoter region.

Considering that human Taf1B and Taf1C are in the SL1 complex binding to the rRNA gene promoter region and promoting Pol I transcription initiation, I examined if the Udd/Taf1B complex also specifically binds to the *Drosophila* rRNA promoter using chromatin immunoprecipitation (ChIP) followed by qPCR. Although Drosophila Taf1B has a zinc finger with four conserved cysteine to bind to DNA directly, there was no antibody or any tagged transgene that could be used for this purpose. Therefore, a rescuing 3×HA-tagged *udd* transgenic line and a ChIP-grade anti-HA antibody were used, and the experiments were performed using ovarian lysates in two different conditions: 1. the transgene was ubiquitously expressed using *da-gal4* in wildtype background, and negative control used the lysate from *da-gal4* flies without *udd* transgene (**Figure 4.19A**); 2. the transgene was ubiquitously expressed in udd^{null} background where there was no endogenous Udd, and negative control was performed with the same lysate without adding anti-HA antibody for IP (**Figure 4.19B**). These experiments confirmed that Udd specifically associates with the rRNA gene promoter immediately adjacent to the ETS and to 5' end of the ETS itself (**Figure 4.19**; also see **Figure1.1**). Udd does not have a recognizable DNA binding motif and its association with rRNA gene promoter region is likely through Taf1B or other members in this complex, which needs further studies (see Discussion).

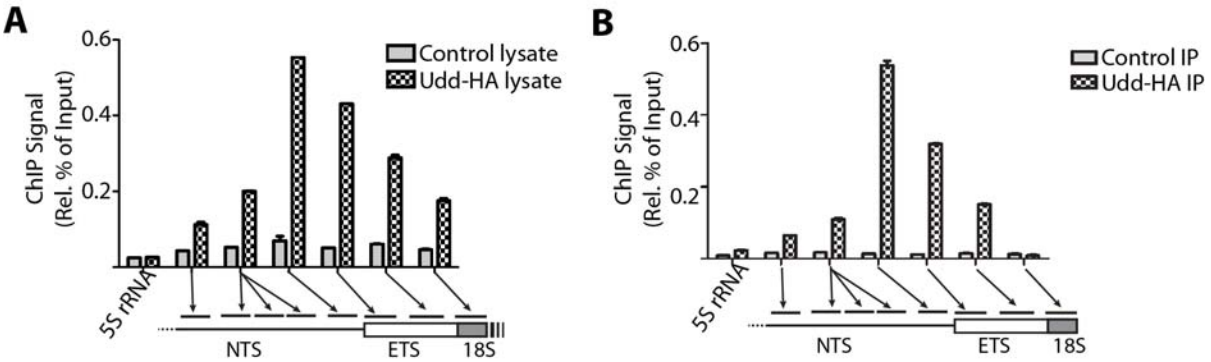

Figure 4.19 Udd associates with the rRNA gene promoter region. (A) ChIP-qPCR analysis of *da-gal4,UASp-HA-udd* ovaries and *da-gal4* control ovaries using anti-HA antibody. (B) ChIP-qPCR analysis of udd^{null}/ udd^{null}; *da-gal4*/*UAS-HA-udd* ovaries. The same extracts were subjected to the ChIP protocol without antibody as a negative control. *da-gal4* was used to drive ubiquitous expression of HA-Udd. Both results reveal that a rescuing HA-tagged Udd associates with specific sites within the rRNA promoter and external transcribed spacer (ETS), as indicated by the 5th and 6th arrows and bars.

The Udd/Taf1B complex promotes pre-rRNA transcription as RNA Pol I transcriptional regulators.

After confirming the association of Udd/Taf1B complex with rRNA promoter and newly synthesized rRNAs, I tested whether or not they are important for rRNA transcription. RNA Pol I initially transcribes 47S pre-rRNA, which is then cleaved and processed to yield mature 18S, 5.8S and 28S rRNAs (**Figure 4.20**) [213]. First, total RNAs were isolated from wild-type control and *udd* mutant ovaries and subjected to northern blot analysis using a probe against the Internal Transcribed Spacer (ITS) which exists in only pre-rRNA and early processing intermediates [214] (**Figure 4.20**). 5S rRNA, transcribed by RNA Pol III from an independent locus in the nucleoplasm, served as a loading control. The experiment showed that *udd* mutants displayed a great reduction of both pre-rRNA and processed rRNA intermediates, suggesting that Pol I transcription was greatly disrupted

in *udd* mutants (**Figure 4.20**). Next, I also performed BrUTP labeling on *udd*^{null} mutant clones to examine the levels of newly synthesized rRNAs. Control heterozygous nurse cells (**Figure 4.21 A**) exhibited high levels of BrUTP labeling, reflecting normal rRNA transcription, while *udd*^{null} homozygous cells (dotted line) displayed only a little BrUTP incorporation indicating low level of rRNA transcription. The same BrUTP labeling experiment was also performed with *Taf1B* knocked-down ovaries (**Figure 4.21 B**). In the egg chamber where *Taf1B* was knocked down specifically in the germline, there was a dramatic reduction of nascent rRNAs (top panel in **Figure 4.21B**) compared to that in the control egg chamber with normal endogenous Taf1B (bottom panel in **Figure 4.21B**). Together these data indicate that the Udd/Taf1B complex directly fosters RNA Pol I activity, although without them the basal level of rRNA transcription still takes place (see **Discussion 3**).

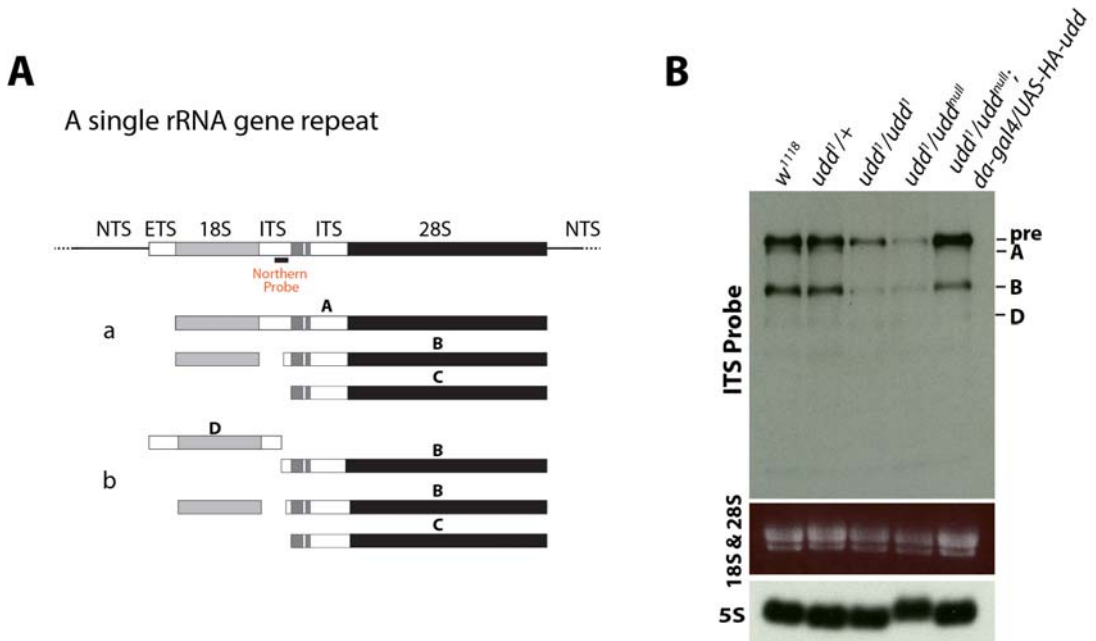

Figure 4.20 Northern blot analysis demonstrates that *udd* mutants display a great reduction of both pre-rRNAs and processed rRNA intermediates (A) Schematic of a single *Drosophila* rRNA gene showing the two different rRNA processing pathways, referred to as a and b, and the location of the probe used in northern blot which is in the ITS region. (B) Northern blot of total RNA isolated from ovaries of the indicated samples. Ethidium Bromide staining of an agarose gel shows the mature 28S

and 18S rRNAs. A probe specific for the 5S rRNA was used as a loading control.

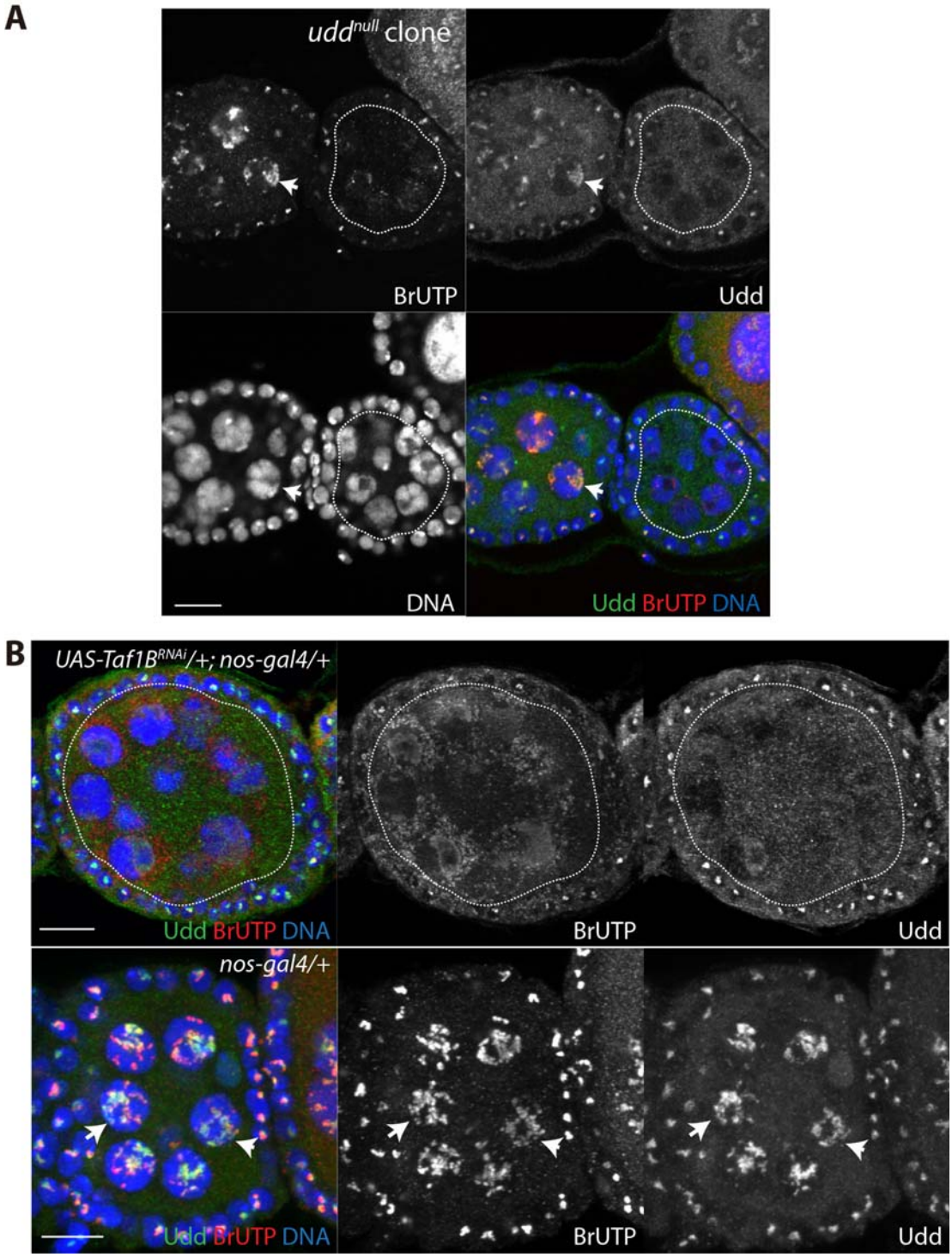

Figure 4.21 Disruption of Udd or Taf1B induces a dramatic reduction of newly synthesized rRNAs. (A) *udd*^{null} mutant clone stained for Udd (green), BrUTP (red) and DNA (blue). Heterozygous nurse cells in the adjacent egg chamber (arrowhead) exhibit Udd expression and BrUTP incorporation, while the *udd* mutant clone (white dotted line) shows very little BrUTP labeling. (A,B,F) DNA is labeled in blue. Scale bars represent 20 μm. (B) Nascent rRNA labeled by BrUTP incorporation (red)

and Udd (green) in egg chambers from *Taf1B*-knocked down flies (top, white dotted line) and control *nos-gal4* flies (bottom, arrowheads). Scale bars represent 10 µm.

Moreover, loss of Udd appears to impede ribosome production based on the accumulation of ribosomal protein reporter RpS2-GFP within nuclei of udd^{1}/udd^{null} mutant germ cells (**Figure 4.22**). In control samples, a RpS2-GFP protein trap was largely absent from nuclei (**Figure 4.22**). In contrast, germ cells within udd^{1} homozygous mutant egg chambers displayed clearly detectable nuclear and nucleolar accumulation of the RpS2 reporter, which suggested that ribosome assembly in the mutant cells was delayed due to the reduction of newly transcribed rRNAs.

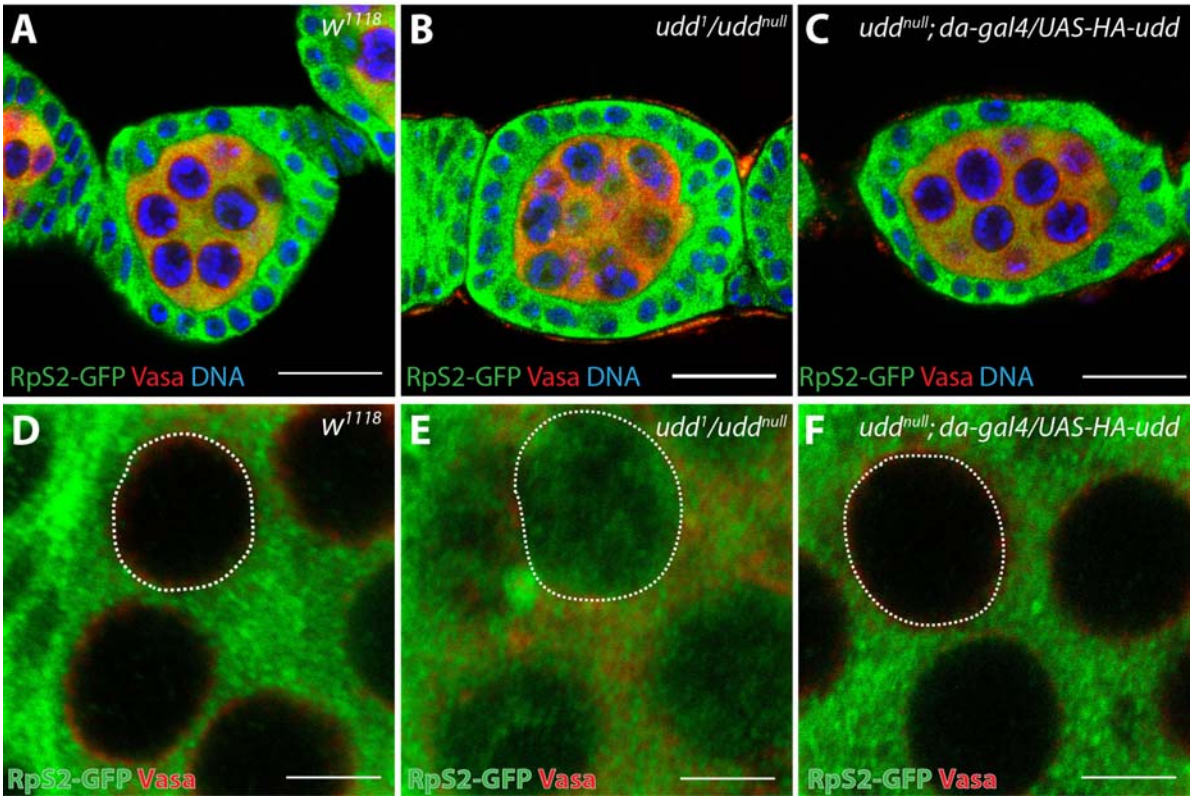

Figure 4.22 *udd* mutant cells exhibit nuclear accumulation of a ribosomal protein reporter. (A) w^{1118}, (B) udd^{1}/udd^{null} and (C) udd^{null}/udd^{null}; *da-gal4*/*UAS-HA-udd* egg chambers which carry the RpS2-GFP protein trap (*CB02294*) stained for GFP (green), Vasa (red) and DNA (blue). (D) w^{1118}, (E) udd^{1}/udd^{null} and (F) udd^{null}/udd^{null}; *da-gal4*/*UAS-HA-udd* nurse cells stained for RpS2-GFP (green) and Vasa (red). The dotted lines outline nurse cell nuclei. (A-C) Scale bars represent 20 µm. (D-F) Scale bars represent 5 µm.

With all these results, it is convincing to claim that Udd is a novel *Drosophila* RNA Pol I transcriptional regulator and works together with Taf1B and other factors such as CG10496 to promote pre-rRNA transcription.

C. Discussion

1. Conservation of Pol I transcription machinery between *Drosophila* and other organisms.

Consistent with the conservation of rRNA coding regions, the RNA Pol I complex shares a fair degree of similarity from yeast to human. In addition, the transcription initiation factor Tif-IA, SL1 complex member TBP and multiple subunits of the elongation factor TFIIH are also well conserved. However, the protein complexes binding to the rDNA promoter or other regulatory elements in the NTS region are poorly conserved and only show similarity among closely related species, which is critical for species-specific regulation of Pol I transcription.

First, the SL1 complex in human is composed of TBP and TBP-associated TAFs, some of which are shared with Pol II or III machinery while others are Pol I-specific including Taf1A, Taf1B, Taf1C, etc. Among these components, Taf1B and Taf1C directly bind to the rDNA core promoter and they also interact with other factors including Tif-IA and UBF, and Taf1A mainly promotes the selective binding of TBP to SL1 complex instead of TFIID complex for Pol II transcription. However, this mammalian SL1 complex is replaced by core factor complex in yeast composed of RRN6, RRN7 and RRN11, the members of which may carry out similar functions but do not share similar primary sequence. The yeast RRN7 and human Taf1B have been discovered to have similar secondary structures and both function as TFIIB-like factors [21]. *Drosophila* Taf1B as I mentioned in this chapter is a homolog of human Taf1B according to primary sequence alignment, and it also has similar structure to yeast RRN7. I also talked about *Drosophila* CG10496, and in spite of the lack of primary sequence homologs in human proteome, its secondary structure is highly similar to Taf1C. In addition, human Taf1C has no sequence homologs in *Drosophila*, and its secondary structure has no

other *Drosophila* homologs better than CG10496 (see Results part). As to human Taf1A, no obvious sequence or structural homologs were found in *Drosophila*. Besides, yeast factors in the CF were also examined and still no obvious homologs were observed in *Drosophila melanogaster*.

Second, *Drosophila melanogaster* has no obvious homologs of the mammalian UBF which plays a role in recruiting SL1 complex to the rDNA promoter, helps with transition of Pol I from initiation to the elongation process, and is also considered as an important factor determining the number of active ribosomal RNA genes. UBF contains a dimerization domain, a C-terminal activation domain for interacting with SL1 and several DNA-binding HMG-boxes, and HHpred server gave out several HMG-box-containing structural homologs. However, none of those candidates is distinctively highly similar to UBF, like the similarity between CG10496 and UBF. In yeast, UBF is replaced by upstream activating factor complex (UAF) consisting of RRN5, RRN9, RRN10, UAF30, H3 and H4 [43]. UAF30 and RRN10 do not have any sequence homolog in *Drosophila*. RRN5 has a homolog with 20% similarity in *Drosophila ananassae*. RRN9 has a homolog with 20% similarity in *Drosophila pseudoobscura pseudoobscura*. RRN5 and RRN9 do not exhibit sequence homology in other *Drosophila* species.

Third, I also found that the factors regulating Pol I transcription termination including mammalian PTRF and TTF-1 do have sequence homologs in *Drosophila melanogaster*. The mouse PTRF has 392 aa, while its *Drosophila* homolog is a protein encoded by *CG43154* (isoform C only) which has more than 2000 aa. The human TTF-1 is about 100 kDa, while its *Drosophila* homolog is a protein encoded by *CG11180*, the isoforms of which are around 70 kDa and 80 kDa. Further studies are needed to see if these proteins play a role in Pol I transcription. It is possible that the length

differences in these proteins are related to their distinct interaction partners and associated DNA sequences in two different organisms.

In general, it is intriguing to look for novel Pol I regulators in different organisms, which not only helps with co-evolution studies but also helps understanding the regulatory mechanism of Pol I transcription. However, it will be more interesting and promising to look for tissue-specific or lineage-specific Pol I transcriptional regulators compared to the species-specific ones, which could serve as a potential target for treatment of cancers in specific tissues.

2. Does Udd directly associate with the rRNA gene promoter? Does Udd directly bind to Taf1B and CG10496?

For the first question: ChIP-qPCR demonstrated that Udd associated with the rRNA gene promoter. But Udd has 159 aa with no obvious DNA binding motifs, and further *in vitro* studies like EMSA gel shift assays are needed to see if Udd can directly contact the rDNA promoter. However, since Udd interacts with *Drosophila* Taf1B which has a zinc finger motif, Udd could associate with rDNA promoter through Taf1B-DNA interaction. In addition, Udd also interacts with CG10496, the structural homolog of which in human, Taf1C, can directly bind to rDNA promoter despite the lack of known DNA-binding motifs. It is possible that CG10496 can also directly contact the rDNA sequence. Additionally, if the Udd/Taf1B complex is similar to human SL1 complex, then Udd and Taf1B probably also interact with TBP, which also bind to rDNA sequence. However, different from TBP's function in TFIID recognizing TATA box in Pol II gene promoters, TBP in SL1 complex does not

bind to TATA box, and the association of TBP with the upstream factor UBF might be more important for recruiting SL1 to the promoter.

For the second question, although Udd and Taf1B are believed to interact with each other and are probably required for each other's stability, translocation and expression levels, there is no evidence demonstrating Udd and Taf1B can directly bind to each other. In vitro studies like GST pull-down assay and yeast two hybrid assay can be performed to examine direct interaction.

3. Why does knocking down Pol I transcriptional regulators usually exhibit a weaker phenotype than knocking down Pol I subunits?

I found that although complete deletion of Pol I regulators could be embryonic-lethal like udd^{null}, knockdown or weaker deletion of Udd, Taf1B, or other factors in the ovaries and other tissues exhibit a much weaker phenotype than knocking down Pol I subunits RPA1 and RpI135. Moreover, in those mutant cells with knockdown or mutation of *udd* or *Taf1B*, I observed that there were still a certain level of Pol I transcription going on, which was not reduced in the same ratio as the decrease of that Pol I regulator.

There are several explanations. First, many of these factors are involved in Pol I transcription initiation, and they mostly do not affect the elongating Pol I. Second, different from many other genes, in a single rRNA gene repeat (14.4 kb in human) there can be multiple Pol I machinery loaded and actively transcribing rRNAs: some are in the initiating step, some are in the elongation step, and others are in the termination step. In a cell, there are usually many copies of

rRNA genes and many Pol I complexes, and knocking down *udd* or *Taf1B* probably decrease the rRNA genes that are being actively transcribed. However, it could at the same time increase Pol I loading on the remaining active rRNA genes, which would only lead to a mild reduction of Pol I transcription. Human UBF is another example for this explanation [7, 215]. This explains the phenotype difference I observed. When knocking down Pol I complex in the germline, the germ cells could not survive and there was a strong germ cell loss marked with one or two germ cells remaining in the germarium. When knocking down *udd* or *Taf1B* in the germline, the rRNA levels as well as ribosome biogenesis levels in the egg chambers were not able to support the survival of endocycling nurse cells with repeated DNA replication and greatly increased protein synthesis. Moreover, in wild-type nurse cells I observed very high levels of rRNA transcription in the nurse cells, while in the mutants the levels are greatly reduced exhibiting egg chamber degeneration. However, the remaining rRNA transcription in the germarium after knocking down *udd* or *Taf1B* is still able to support the growth and proliferation of early germ cells to a certain level, although the germ cells in the germarium are quiescent and lost over time like a premature aging phenotype. Third, knocking down some of the factors like CG10496 in *Drosophila* may not affect other factors in the same complex too much, especially if there is some sort of redundancy for DNA-binding or protein interaction, Pol I transcription will still not get downregulated to the same degree.

4. Why does knockdown of *CG10496* not exhibit an obvious phenotype similar to *udd* deletion or *Taf1B* knockdown?

The RNAi line I made for *CG10496* driven by multiple Gal4 lines could result in an 85% or more reduction of this gene which is similar to the level of *Taf1B* knockdown, but it did not lead to a similar phenotype to that of *udd* deletion or *Taf1B* knockdown (basically no obvious defects). I found that knockdown of *CG10496,* although impaired the Udd nucleolar localization a little bit, did not affect the protein level of Udd and the transcript levels of *udd* and *Taf1B*. This is different from Taf1B and Udd, both of which seemed important for each other's stability and expression level. Therefore, knockdown of *CG10496* may not result in the same level of defects in this Udd/Taf1B/CG10496 complex. Moreover, if the interaction of CG10496 with other proteins or rDNA sequence has some redundancy with other factors in the same complex, the negative effects of *CG10496* knockdown will be further reduced.

CHAPTER V

Studying the regulation of rRNA transcription within GSCs and their differentiating daughters.

A. Introduction

The regulation of RNA Pol I transcription during development

During lineage and tissue development, cell growth, proliferation and differentiation must be tightly regulated both temporally and spatially. With in the same lineage, from the initial stem cells or precursor cells to differentiated progenitors, there are external cues from niches or other neighboring cells and intrinsic mechanisms controlling self-renewal or differentiation of those cells. For example, in *Drosophila* ovaries, a BMP family ligand Dpp produced in the cap cell niche binds to Punt and Tkv/Sax receptors on the membrane of germline stem cells and activates a series of downstream signaling cascades (see Chapter III Introduction for more information, **Figure 3.2**). One essential function of active Dpp signaling in GSCs is to directly repress the transcription of a key differentiation factor *bam*. Other signaling pathways like Notch and JAK-STAT pathways contribute Dpp ligand production in the niche, while EGFR pathway in the neighboring escort cells as well as Lsd1 and Type IV Collagens negatively regulates Dpp signaling. In the immediate germline differentiating daughters, Bam is expressed at high levels with reduced Dpp signaling, and it in turn represses Dpp signaling to a lower level and probably also inhibits the expression of other stem cell maintenance factors like Nanos and E-Cadherin through binding to their 3'UTRs [216, 217]. In those cells, the Smurf/Fused complex is also involved repressing Dpp downstream components. In later differentiating daughters, there are additional proteins transiently expressed at high levels and involved in regulating the RNA or protein levels of other factors to promote differentiation and proliferation (see Chapter III Introduction).

Despite of numerous studies focused on stem cell lineage differentiation and tissue development, it is not well known if and how rRNA transcription and ribosome biogenesis is differentially regulated in cells within the same lineage during differentiation or development. It is easily accepted that as the first and foremost step of ribosome biogenesis RNA Pol I transcription is essential for cell survival, and cancer cells usually exhibit upregulated rRNA levels. However, the rRNA transcription levels are not well examined or compared during development, although some Pol I regulators have been discovered to get activated or repressed upon changes of nutrients or energy status which modulates rRNA synthesis. Several groups have shown, from either primary or immortalized cell lines, that before and after induced *in vitro* differentiation there are changes (mostly a reduction) in rRNA transcription levels, which were related to changes of Pol I regulators UBF or SL1 quantity or activity [164-166]. No publications answer this question with direct *in vivo* studies. Moreover, it is also unknown if modulation of Pol I transcription could contribute to differentiation.

Here in this chapter, I show that in *Drosophila* ovaries, the level of rRNA transcription is correlated with the differentiation status of female germ cells. The pre-rRNA level was observed high in GSCs, and then got downregulated in early Bam-expressing differentiating cysts but upregulated again in the later more differentiated germ cells. This difference was demonstrated in both wild type ovaries and also undifferentiated ovaries (*bam* mutants) before and after introduced differentiation using a *bam* transgene under a heat shock promoter. In addition, increasing rRNA synthesis by Tif-IA overexpression leads to a mild expansion of GSCs, while downregulation but not depletion of Pol I transcription by reducing Taf1B or Udd in ovaries filled with undifferentiated GSC-like germ cells resulted in multicellular cyst formation. These results from *Drosophila* suggest that RNA Pol I

transcription is closely correlated with cell differentiation and tissue development, and the modulation of rRNA synthesis could be a part of the differentiation process.

B. Results

Bam expressing cells display lower levels of rRNA transcription.

In **Figure 4.17**, *in situ* run on assay combined with immunofluorescent staining of wild-type germaria for Udd and BrUTP demonstrated that germline stem cells displayed higher levels of Udd and pre-rRNAs while their early differentiating daughters exhibited reduced Udd and nascent rRNA levels, and then the levels became higher again in more differentiated cells. In Drosophila germline, Bam is a key differentiation factor both necessary and sufficient to promote stem cell differentiation [193, 197, 218]. Therefore, it was speculated that there might be an inverse correlation between *bam* expression and pre-rRNA levels. *In situ* run on assay combined with immunofluorescent staining of wild-type germaria for Bam and BrUTP revealed that as expected, Bam positive cells exhibited lower levels of rRNA transcription relative to stem cells and the later more differentiated cysts (**Figure 5.1**).

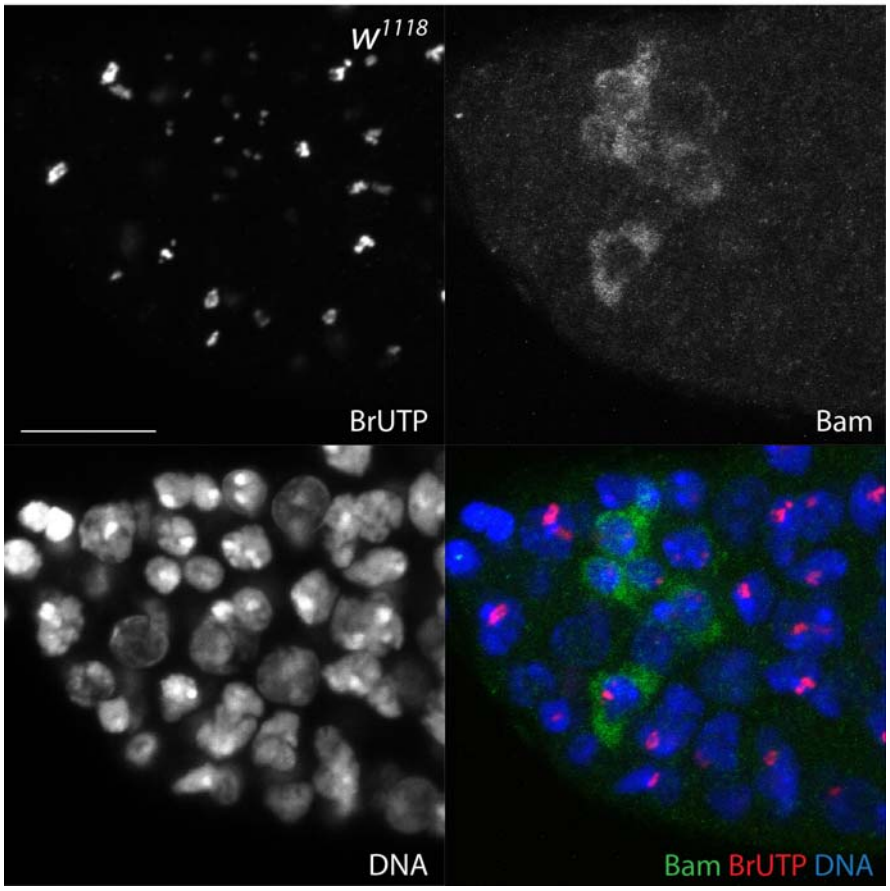

Figure 5.1 High level of Bam expression correlates with low level of pre-rRNA transcription. w^{1118} germarium is stained for Bam (green), BrUTP (red), DNA (blue). Scale bar represents 20 μm.

At the end of GSC mitotic division, the newly formed GSC daughter contains a greater amount of nucleolar Udd than the daughter displaced away from the cap cell niche.

In consideration of the differences between stem cells and their early differentiating daughters in the levels of Udd and rRNA transcription (**Figure 4.17 and Figure 5.1**), it was suspected that Udd, which is a RNA Pol I transcriptional regulator, might become asymmetrically enriched in the stem cell daughter during GSC mitosis. To test this, I first performed immunofluorescent staining in wild-type germaria looking for dividing GSCs. GSCs in anaphase or telophase is very hard to find due to the main reasons that: first, usually less than 10% GSCs are positive for the mitotic marker

Ser10-phosphorylated Histone H3 (PH3) which starts to appear in late S phase and gradually disappear at the end of mitosis; second, less than 5% out of those are in anaphase or telophase. In addition, the antibody against α-tublin which people usually use to label mitotic neuroblasts in *Drosophila* does not work well in the germaria, and the other marker PH3 does not exhibit high levels during telophase. Therefore, I was only able to find a few examples from a large amount of stained and mounted ovaries. These samples showed that the newly formed GSCs did contain more nucleolar Udd than the other stem cell daughter (**Figure 5.2**).

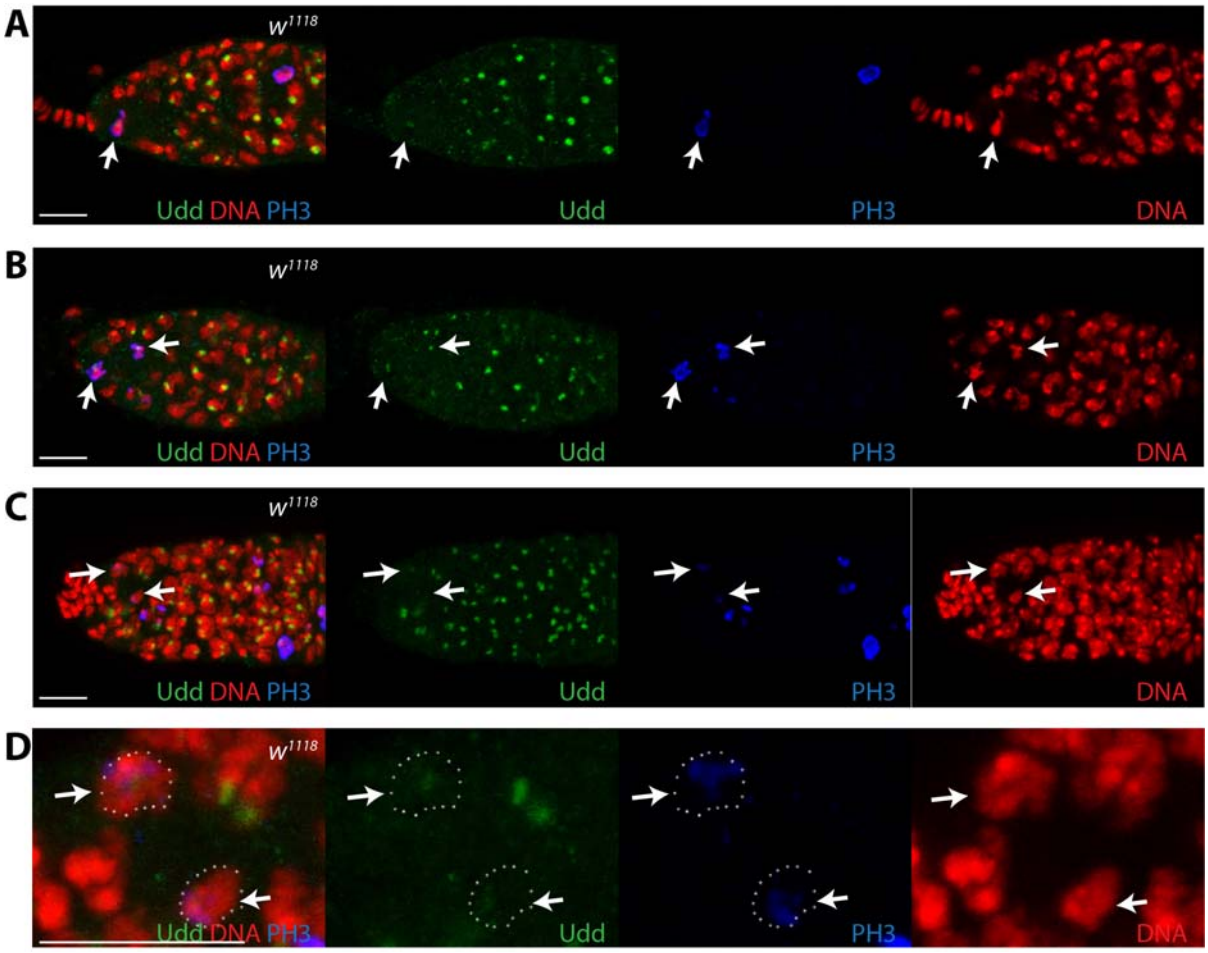

Figure 5.2 Immunofluorescent staining of fixed ovaries indicates Udd is more enriched in the anterior stem cell daughter immediately after GSC mitotic division. (A-D) Germaria stained for Udd (green), PH3 (blue) and DNA (red), with arrows pointing out the dividing GSC. (A) Metaphase GSC; (B) Anaphase GSC; (C) Telophase GSC; (D) Magnified image of telophase GSC in (C). Scale bars represent 10 μm.

In addition to using immunofluorescent staining to observe the changes of endogenous Udd, a C-terminal GFP-tagged Udd genomic transgene was created to test for time-lapse live cell microscopy. Before using this Udd-GFP line for live imaging, I first tested if it was able to rescue the lethality of udd^{null} and the sterility of udd^{1} mutants. It turned out that this Udd-GFP line was able to rescue both, no matter using one copy or two copies. One interesting phenotype I found from immunofluorescent staining was that the nucleolar Udd-GFP level in the germ cells is much lower in the wild-type background compared to that in the *udd* mutant background, as shown in **Figure 5.3**, although no matter in which background two copies of Udd-GFP always exhibited higher expression than one copy. In the following live imaging studies, an mRFP tagged His2Av transgene, as a nuclear marker, was recombined with Udd-GFP, and udd^{null}/udd^{null}*; udd-GFP, His2Av-mRFP/ udd-GFP, His2Av-mRFP* flies were used in order to achieve the strongest fluorescent signals from GFP and mRFP channels.

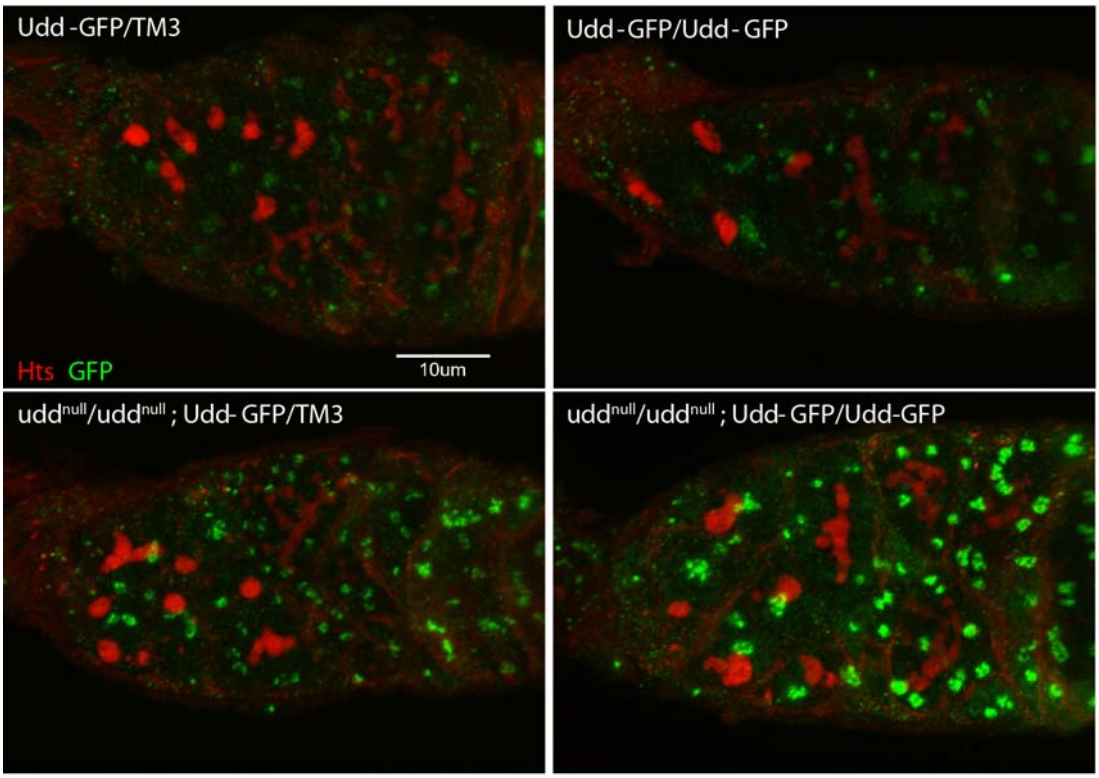

Figure 5.3 A rescuing C-terminal GFP-tagged Udd genomic transgene, designed for live imaging, exhibits higher nucleolar expression in *udd* mutant background than in wild-type background. In addition, two copies of Udd-GFP demonstrate higher nucleolar expression than one copy. Scale bars represent 10 μm.

Live imaging, which was performed mainly by a postdoctor in our lab, Dr. Nevine Shalaby using Leica microscope in Dr. Robin Hiesinger's lab, revealed discrete Udd localization from prometaphase to late anaphase in dividing germ cells. From fixed and stained samples, endogenous Udd remained associated with condensed chromosomes through most of mitosis, and it only disappeared from late metaphase to early anaphase and then quickly reappeared after that. However, live imaging results showed that Udd-GFP appeared to disperse for a longer period, from prometaphase to late anaphase (see Discussion).

Despite the difference in signal strength, at the end of telophase, both GFP-tagged and

endogenous Udd re-coalesce within the nucleoli of newly formed GSCs at higher levels relative to their siblings oriented away from the cap cells (**Figure 5.3 and 5.4**). In contrast, in multicellular cysts (from 2-cell cysts to 8-cell cysts), Udd appeared evenly distributed before and immediately after mitosis (**Figure 5.5**). These results indicate that newly formed GSCs contain a greater amount of nucleolar Udd than daughters displaced away from the cap cell niche.

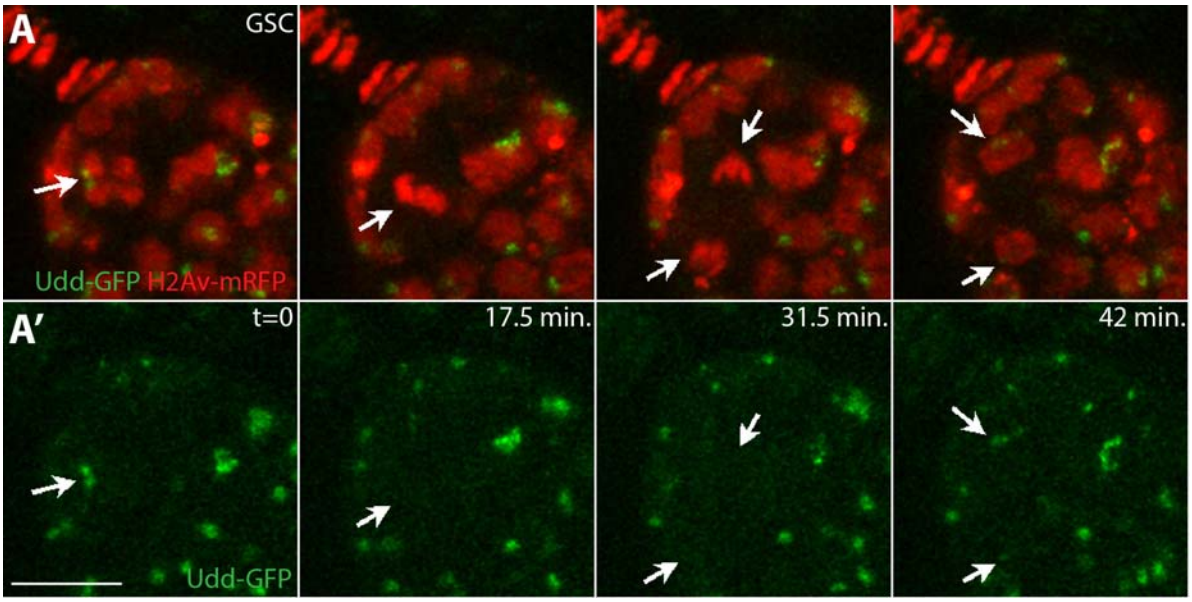

Figure 5.4 Immediately after mitosis, the anterior germline stem cell daughter contains higher levels of Udd than the daughter cell displaced away from the cap cells. (A) Still images from live imaging showing GFP-tagged Udd (green) and mRFP-tagged Histone H2Av (red). (A') Udd-GFP channel alone at the indicated times: t=0 (Prometaphase); t=17.5 minutes (Metaphase); t=31.5 minutes (Anaphase); t=42 minutes (Telophase). Scale bars represent 10 μm.

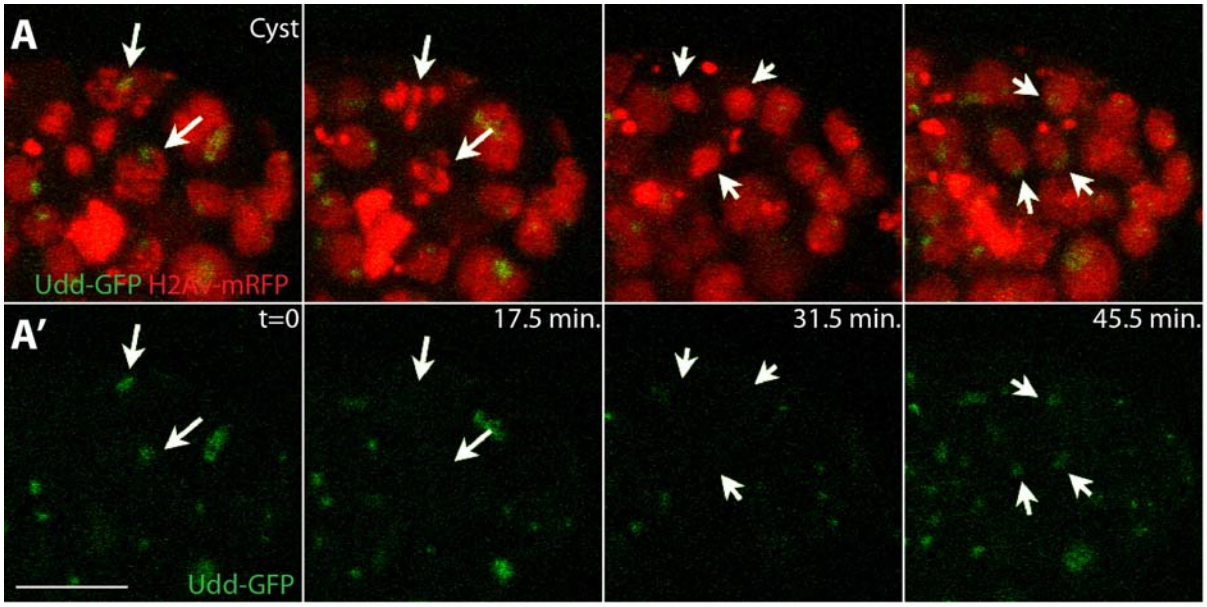

Figure 5.5 Udd appears equal in all the daughter cells divided from a single cyst. Here the example shows the division from a 2-cell cyst to a 4-cell cyst (A) Still images from live imaging showing GFP-tagged Udd (green) and mRFP-tagged Histone H2Av (red). (A') Udd-GFP channel alone at the indicated times: t=0 (Prophase); t=17.5 minutes (early Metaphase); t=31.5 minutes (late Anaphase); t=45.5 minutes (Telophase). Scale bars represent 10 μm.

Persistently low levels of Pol I transcription during early cyst differentiation correlate with the developmental state of these germ cells.

With the initial difference of Udd protein level which I found was set up at the end of GSC mitosis, it was important to examine if this was the major cause for the differences of nucleolar Udd and pre-rRNA levels between GSCs and early differentiating cysts. The first experiment I performed was to co-label nascent rRNAs and Udd protein in $bam^{\Delta 86}$ mutant ovaries. The $bam^{\Delta 86}$ allele carries a near complete deletion of the *bam* gene coding sequence and is mostly considered as a "null" allele [193, 197]. $bam^{\Delta 86}$ homozygous ovaries are filled with undifferentiated "stem cell-like" germ cells marked with round fusomes. In fact, in the $bam^{\Delta 86}$ mutant germaria there are still only two to three real GSCs adjacent to the cap cell niche with active Dpp signaling, and the rest germ cells are all

blocked to an intermediate state between GSCs and cystoblasts called “pre-cystoblasts” which have not started cyst differentiation yet. If the asymmetric segragation of Udd following mitosis is really the main or the only reason, in bam mutant ovaries the difference in Udd and nascent rRNA levels should still be observed between GSCs adjacent to cap cells and undifferentiated cell far away from niche. However, it was found that nucleolar Udd and BrUTP incorporation levels did not drop in *bam*$^{\Delta 86}$ mutant cells (**Figure 5.6**). Results form **Figure 5.1 and 5.6** suggest that persistently low levels of Pol I transcription during early cyst differentiation correlate with the developmental state of these germ cells and not with their position relative to the niche.

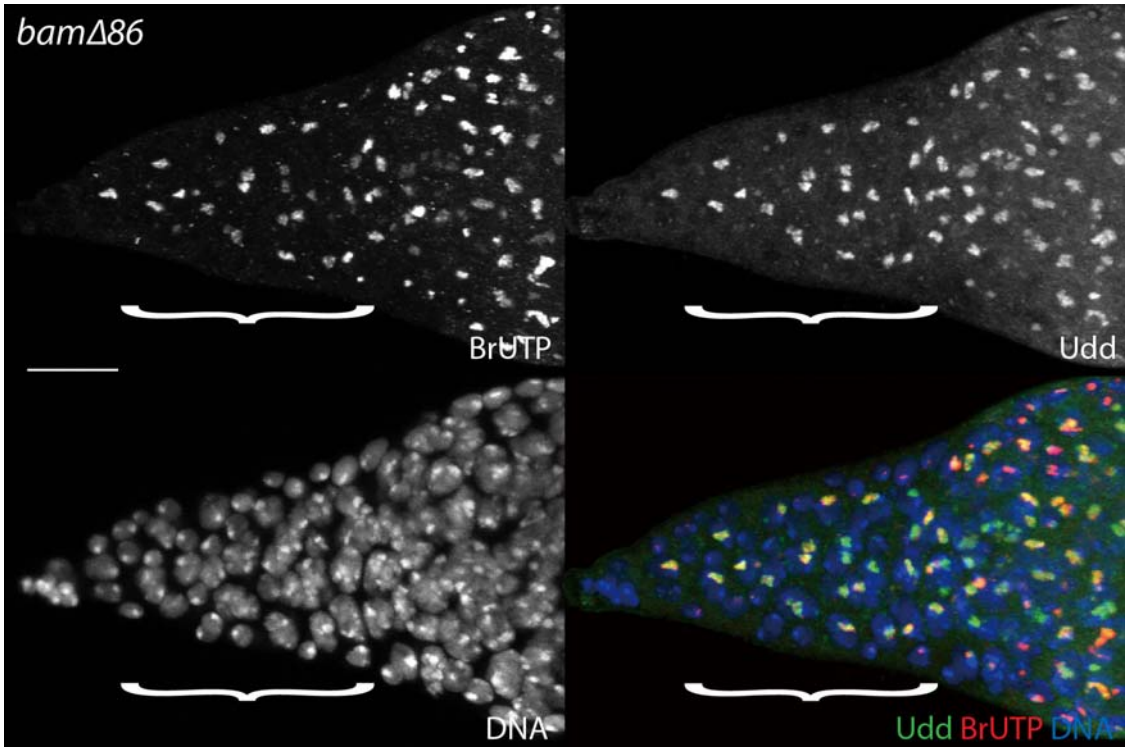

Figure 5.6 In *bam*$^{\Delta 86}$ mutant ovaries, no obvious difference in the levels of Udd and BrUTP incorporation is observed between GSCs adjacent to cap cells and undifferentiated cell far away from niche. Ovaries were pulse labeled with BrUTP (red), and stained for Udd (green) and DNA (blue). Scale bars represent 20 μm.

To further test this idea, an inducible *bam* transgene under the control of an hsp70 promoter

(gift from McKearin lab) [195] was introduced in a *bam*$^{\Delta 86}$ mutant background. Before induction by heat shock, all the germ cells were marked with round fusomes (**Figure 5.7A**), and Udd protein and BrUTP incorporation levels were high throughout the germline as expected (**Figure 5.8A**). After heat shock at 37℃, following *bam* expression all the germ cells started differentiation, which was observed by their branched fusomes (**Figure 5.7B**), and in these cells both nucleolar Udd and BrUTP incorporation levels decreased, reflecting the level of nascent rRNA production was reduced (**Figure 5.8B**).

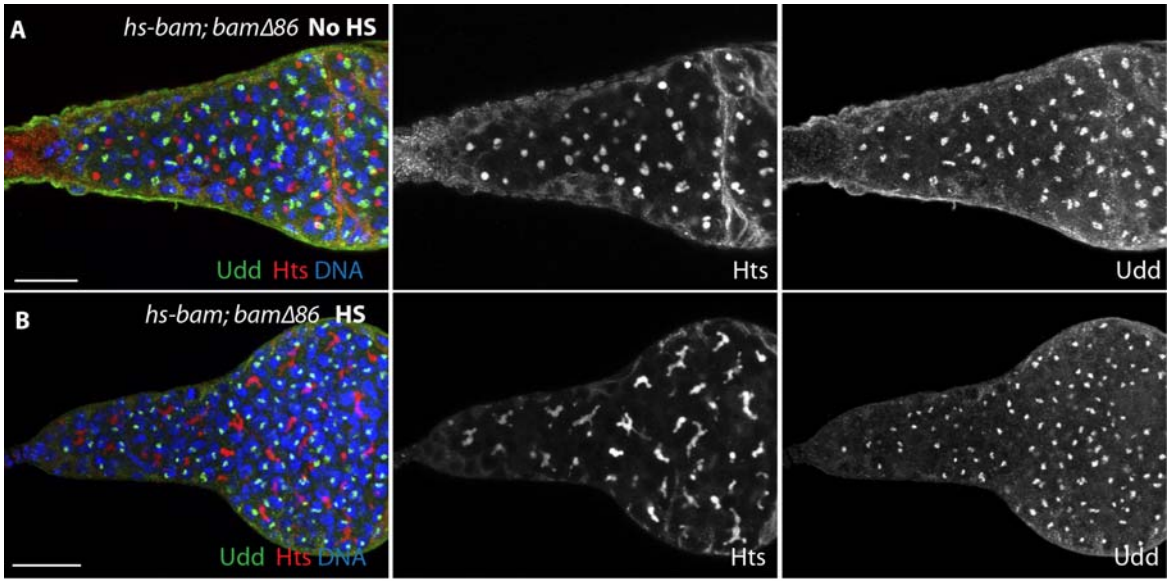

Figure 5.7 *bam* expression results in multicellular cyst formation. (A-B) Ovaries from *hs-bam*; *bam*$^{\Delta 86}$ females subjected to (A) no heat-shock or (B) two one-hour heat-shocks at 37°C on two consecutive days, were dissected 36 hours after the 1st heat shock and stained for Udd (green), Hts (red) and DNA (blue). Scale bars represent 20 μm.

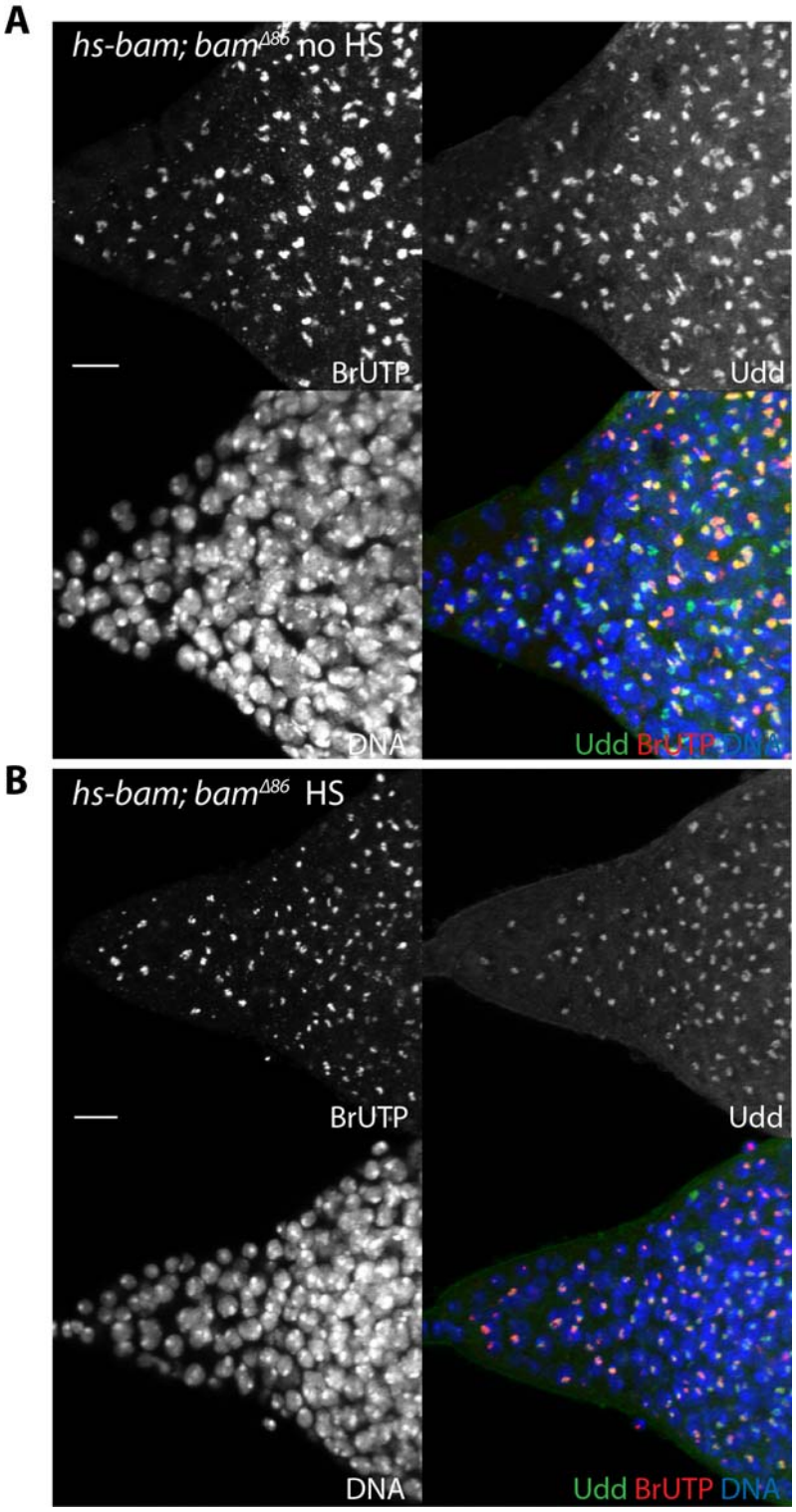

Figure 5.8 Bam-induced differentiation correlates with down-regulation of nucleolar Udd and newly synthesized rRNAs in early dividing cysts. Ovaries from *hs-bam*; $bam^{\Delta 86}$ females subjected to (A) no heat-shock or (B) two one-hour heat-shocks at 37°C on two consecutive days, were dissected 36 hours after the 1st heat shock, pulse labeled with BrUTP (red), and stained for Udd (green) and DNA (blue). Scale bars represent 10 μm.

In the experiments above, flies before and after heat shock were compared, however, since one feature of the heat shock response is a shutdown of normal protein synthesis for many housekeeping genes [219, 220], presumably heat shock might directly cause the reduction of Udd protein level as well as nascent rRNA levels. Therefore, another type of control, *bam*$^{\Delta 86}$ homozygotes without *hs-bam* transgene after heat shock, was used to eliminate the effects from heat shock stress. This time, comparing both flies post heat shock I found that germ cells form flies overexpressing Bam still had an obvious decrease in the levels of nucleolar Udd and BrUTP incorporation (**Figure 5.9**), while those cells in the control ovaries were still marked with round fusomes (**Figure 5.10**). These results together strongly suggest that down-regulation of rRNA transcription in the early dividing cysts correlates with the *bam*-dependent germline differentiation in female flies.

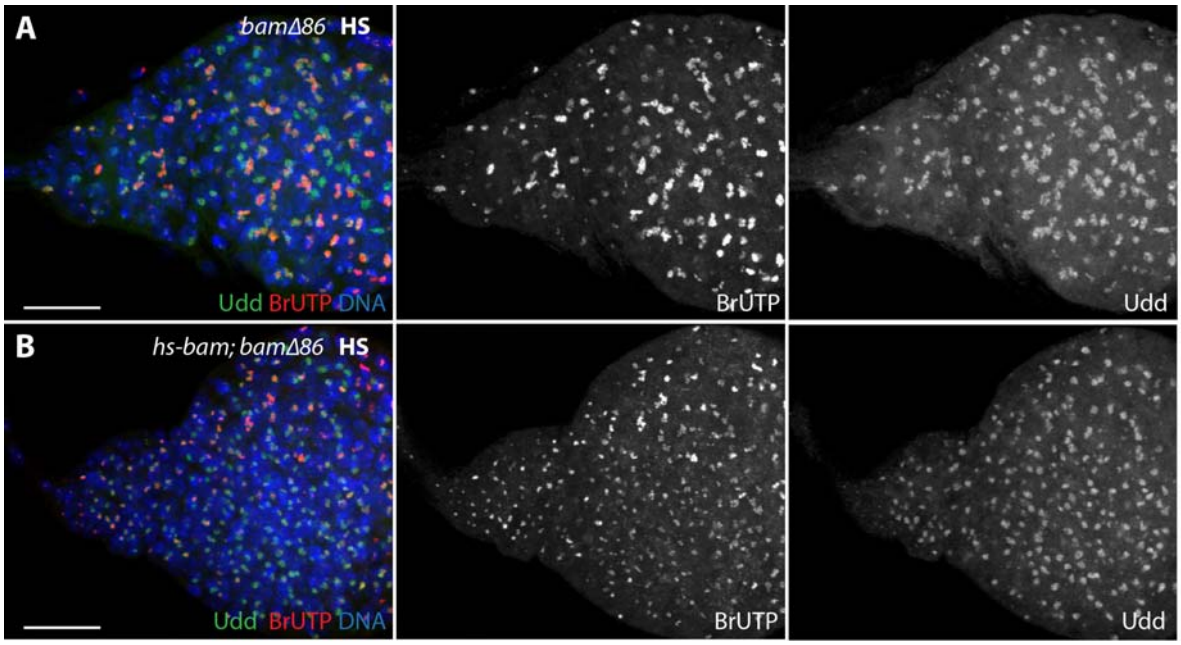

Figure 5.9 Bam-induced differentiation, not heat shock-induced stress response, correlates with down-regulation of nucleolar Udd and newly synthesized rRNAs in early dividing cysts. Ovaries from *bam*$^{\Delta 86}$ (2nd control, A) and *hs-bam*; *bam*$^{\Delta 86}$ (B) females subjected to two one-hour heat-shocks at 37°C on two consecutive days, dissected 36 hours post the 1st heat shock, pulse-labeled with BrUTP in the presence of α-amanitin, and stained for Udd (green), BrUTP (red) and DNA (blue). Scale bars represent 20 μm.

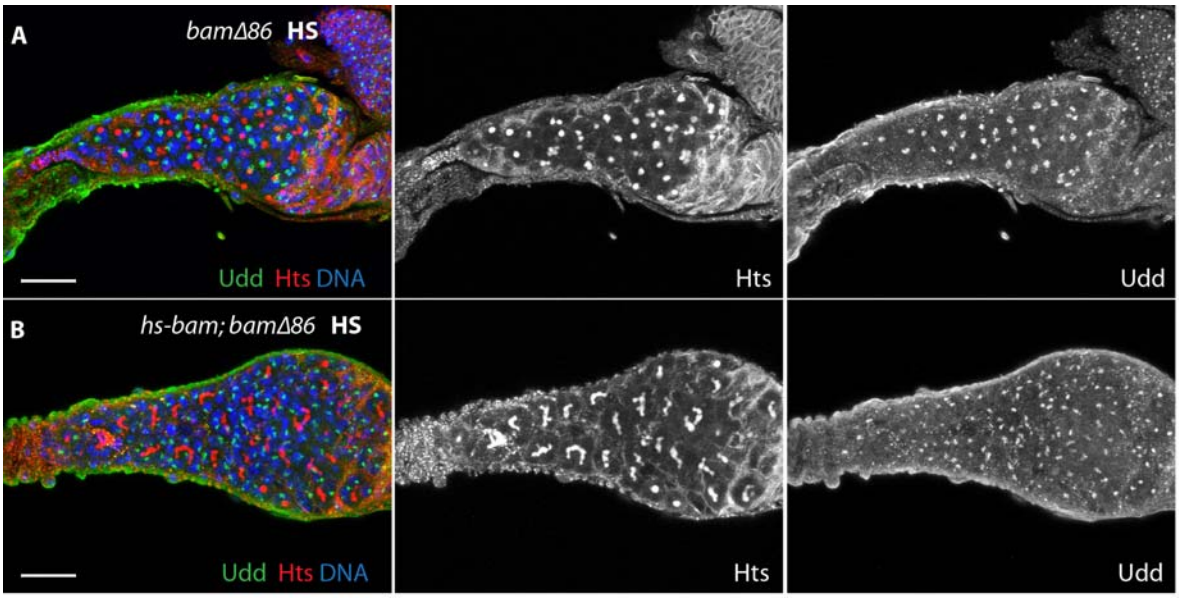

Figure 5.10 *bam* expression, not heat shock itself, results in multicellular cyst formation. (A-B) Ovaries from $bam^{\Delta 86}$ (2nd control, A) and *hs-bam*; $bam^{\Delta 86}$ (B) females subjected to (A) no heat-shock or (B) two one-hour heat-shocks at 37°C on two consecutive days, were dissected 36 hours after the 1st heat shock and stained for Udd (green), Hts (red) and DNA (blue). Scale bars represent 20 μm.

Downregulation of RNA Pol I transcription in a *bam* mutant background induces the formation of multicellular cysts.

Next, in order to test if reduced rRNA transcription is functionally significant to the differentiation state of the cells, I first crossed the udd^{1} mutation into a $bam^{\Delta 86}$ mutant background to examine the double mutant homozygous germ cells. As mentioned above, $bam^{\Delta 86}$ homozygous cells are arrested in an undifferentiated state called pre-cystoblasts (stem cell-like cells) and remained as single cells with round fusomes (**Figure 5.11**). *bam* mutant ovaries continued to grow over the course of 14 days (**Figure 5.11**). In contrast, udd^{1} $bam^{\Delta 86}$ double homozygous germaria often contained many multicellular cysts with elongated and branched fusomes (94.7%; n=94, 3-5 days old) and at day 14 udd^{1} $bam^{\Delta 86}$ double mutant germaria carried only a small number of germ cells, resembling *udd* single mutants at a similar time point (**Figure 5.11**). Then I used anti-phospho-Tyrosine antibody to label the

ring canal which is another marker for multicellular cysts in the germarium. Ring canals are first derived from arrested cleavage furrows at the interface of germ cells undergoing incomplete cytokinesis, and they are the gateway for nutrients, proteins, mRNAs and other information to flow in between cells [221, 222]. Ring canals have been previously used to evaluate the progress of germline cyst development, and they start to appear in multicellular cysts in the germaria and grow more and more obvious in egg chambers when the 16-cell cyst has become 15 nurse cells and one oocyte. There are several Tyrosine-phosphorylated proteins in the ring canal structure from female germline, including F-actin, Tyrosine kinases Tec29 and Src64, Kelch, etc., which is why this structure in the cysts can be detected using anti-phospho-Tyrosine antibody. Here, the results showed that there was not any obvious ring canal structure in the *bam* mutant ovaries as expected, while a lot of ring canals were clearly stained in *udd bam* double mutant cysts (**Figure 5.12**). In addition, it was found that most of the cysts consisted of four or eight cells (carrying three or seven ring canals in a single cyst), and fully formed 16-cell cysts were not observed.

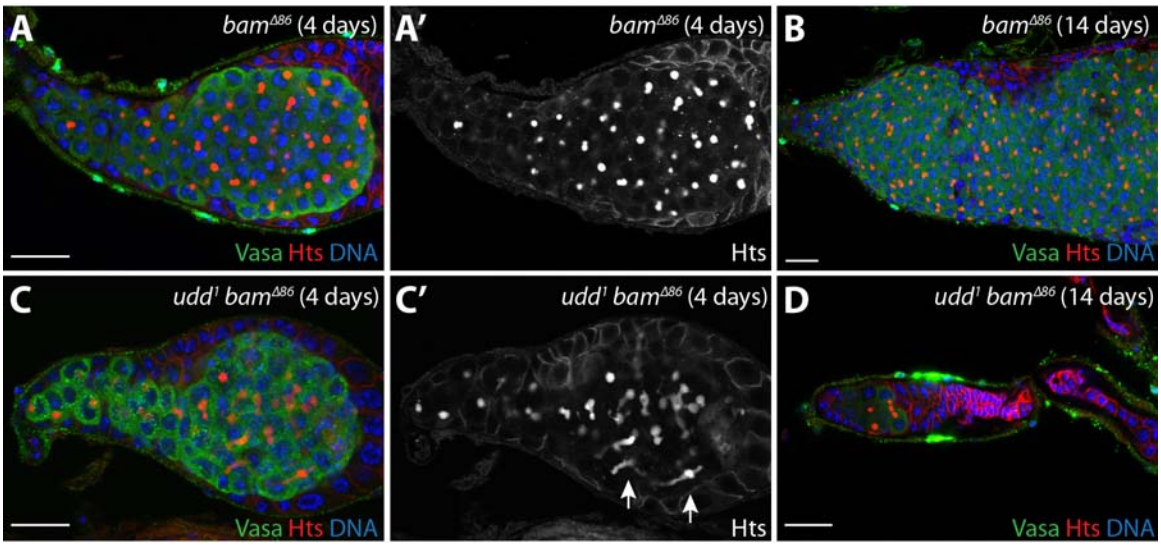

Figure 5.11 Down-regulation of rRNA synthesis by disrupting Udd in a *bam* mutant background results in multicellular cyst formation. (A,B) $bam^{\Delta 86}$ and (C,D) udd^{1} $bam^{\Delta 86}$ double mutant germaria stained for Vasa (green), Hts (red) and DNA (blue). (A', C') Hts alone. (A, C) 4-day-old germaria. (B, D) 14-day-old germaria showing that germ cells from *udd bam* double mutants get lost over time.

Scale bars represent 20 μm.

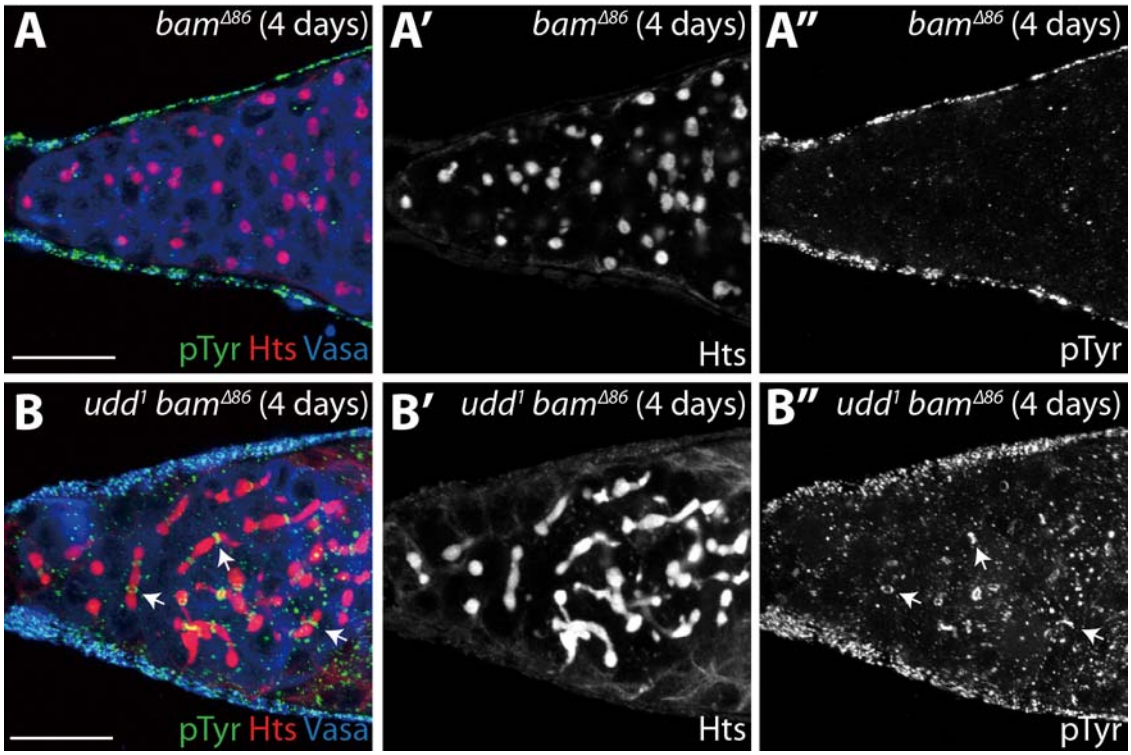

Figure 5.12 Down-regulation of rRNA synthesis in a *bam* mutant background promotes morphological changes during early cyst development. (A-A'') $bam^{\Delta 86}$ and (B-B'') udd^{1} $bam^{\Delta 86}$ double mutant germaria stained for Phosphotyrosine (pTyr) (green), Hts (red) and DNA (blue). (A', B') Hts staining alone. (A'', B'') pTyr staining alone. pTyr and Hts are two markers for multicellular cysts in the germline. Scale bars represent 20 μm.

In addition to *udd* mutation, $Taf1B^{RNAi}$ and $RpI135^{RNAi}$ were also examined in a bam^{RNAi} background to see if they have any similar phenotype. Knocking down *bam* in the germline using *nosGal4* at 29℃ gave rise to the same phenotype to $bam^{\Delta 86}$ homozygotes, marked by undifferentiated pre-cystoblastic tumor filled with round fusomes. It was observed that germline-specific RNAi knock-down of *Taf1B* driven by *nosGal4* in a bam^{RNAi} background resulted in the formation of multicellular cysts with branched fusomes similar to *udd bam* double mutants (**Figure 5.13**), while germline knockdown of *RpI135* exhibited a severe germ cell loss even in newly eclosed flies generating empty germaria with no or only one or two germ cells. This result was not surprising, since

RpI135 as a member of RNA Pol I complex plays an essential role in rRNA transcription and ribosome biogenesis, and without RpI135 there would not be even basal transcription and no germ cells would survive in that condition. The RNAi line for *CG10496* was not tested in this experiment, since CG10496 seemed less critical in this Udd complex and more importantly, germline knock-down of *CG10496* did not exhibit obvious germ cell loss even in aged flies.

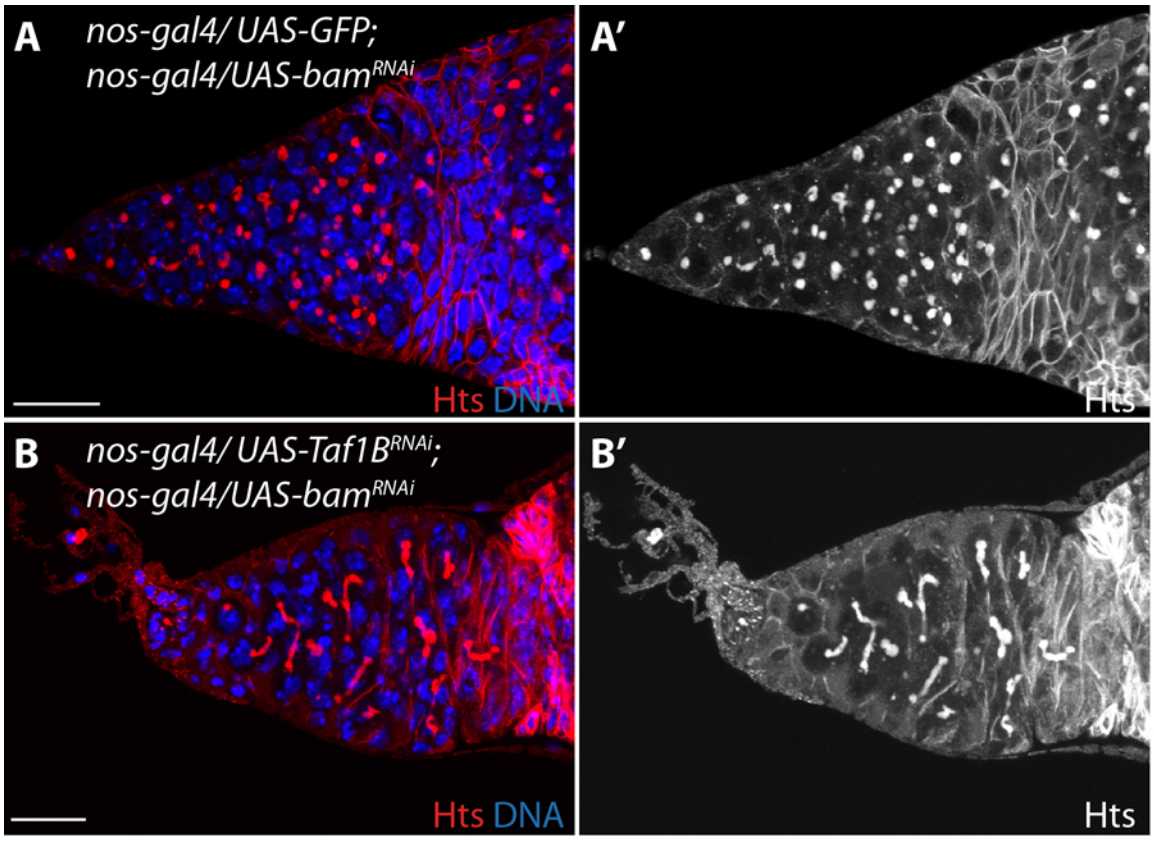

Figure 5.13 Down-regulation of rRNA synthesis by knocking down *Taf1B* in a *bam* loss of function background results in multicellular cyst formation similar to udd^{1} $bam^{\Delta 86}$. (A) Control *nos-gal4(II)/UAS-GFP;* *nos-gal4(III)/UAS-bam*^{RNAi} and (B) *nos-gal4(II)/UAS-Taf1B*^{RNAi}*;* *nos-gal4(III)/UAS-bam*^{RNAi} germaria (3-6 days old) stained for Hts (red) and DNA (blue). (A', B') Hts alone. Scale bars represent 20 μm.

The *udd bam* double mutant multicellular cysts are not molecularly differentiated.

To figure out the mechanism of cyst formation by knocking down RNA Pol I transcriptional regulators *udd* or *Taf1B* in a *bam* mutant background, I started to examine different aspects of the

cystic phenotype in more detail. First, I tested whether the multicellular cysts in *udd*^{1} *bam*$^{\Delta 86}$ double mutant germaria exhibited differentiation at molecular level. Usually the RNA binding protein Sex-Lethal (Sxl) is used to label stem cells and cystoblasts in the germaria and a second RNA binding protein Ataxin-2 binding protein 1 (A2bp1) is used to mark 4-cell, 8-cell and 16-cell cysts undergoing differentiation. It is known that in wild-type germaria these two markers are mutually exclusive (**Figure 5.14**) [223]. *bam*$^{\Delta 86}$ mutation leads to formation of undifferentiated precystoblastic tumor in homozygous germaria, resulting in the expansion of Sxl and the absence of A2bp1 throughout the germline (**Figure 5.14**). Interestingly it was found that similar to *bam*$^{\Delta 86}$ single mutants, *udd*^{1} *bam*$^{\Delta 86}$ double mutant germaria also displayed expanded Sxl expression and no observable A2bp1 (**Figure 5.14**). These results indicate that *udd bam* double mutant germline cells fail to undergo proper molecular differentiation despite cyst formation.

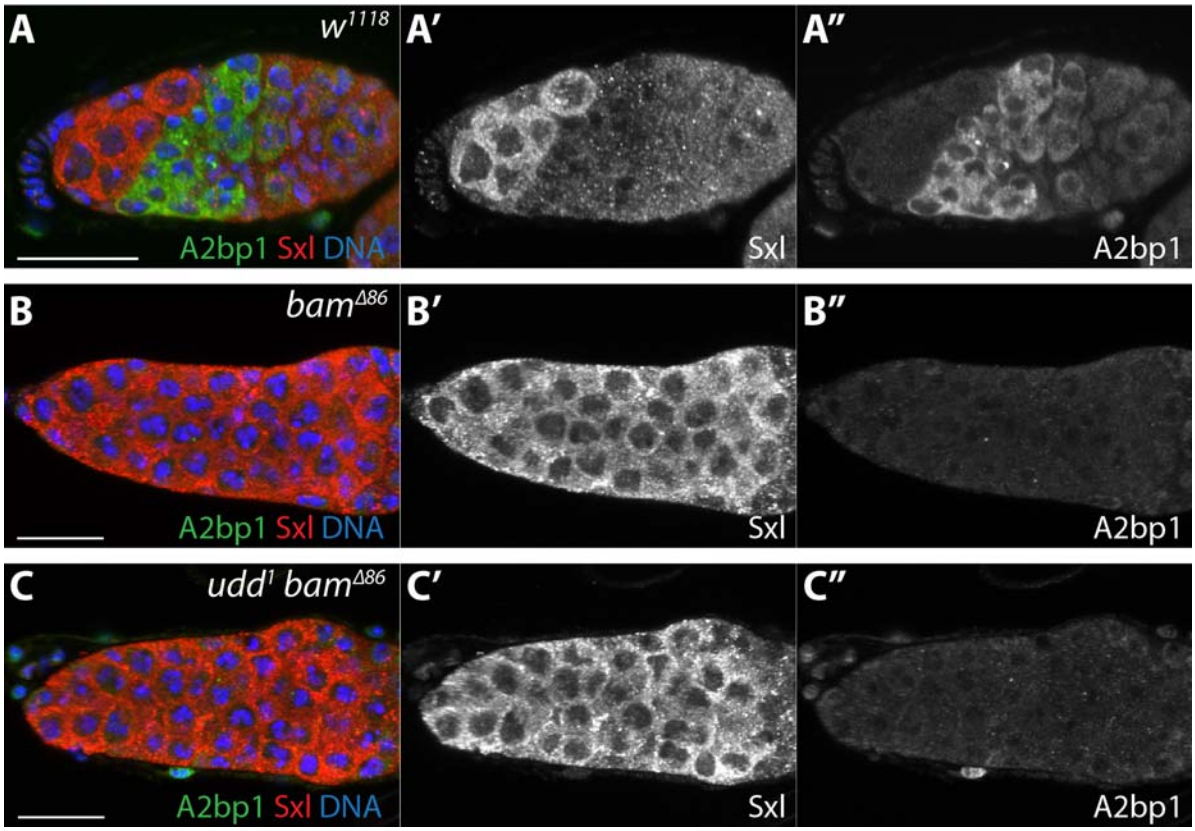

Figure 5.14 The *udd bam* double mutant multicellular cysts are not molecularly differentiated. (A) w^{1118} control, (B) $bam^{\Delta 86}$ and (C) udd^{1} $bam^{\Delta 86}$ germaria stained for A2bp1 (green), Sxl (red) and DNA (blue). (A', B', C') Sxl alone. (A", B", C") A2bp1 alone. Scale bars represent 20 μm.

Nucleolar region marked by Fibrillarin is not obviously changed when mutating *udd* or *Taf1B* in a *bam* mutant background.

Next, I examined the nucleolar size of young *udd bam* or *Taf1B bam* double mutant germ cells. Fibrillarin, a methyltransferase involved in pre-rRNA processing, is usually used to monitor the changes of nucleolar size in different tissue and cell lines. Here it was observed that the formation of cysts occurred without an obvious change in nucleolar size, based on Fibrillarin staining (**Figure 5.15**). Since these double mutant flies exhibit age-dependent germ cell loss and all germ cells will get lost eventually, only young flies (2-4 days old) were examined for this purpose.

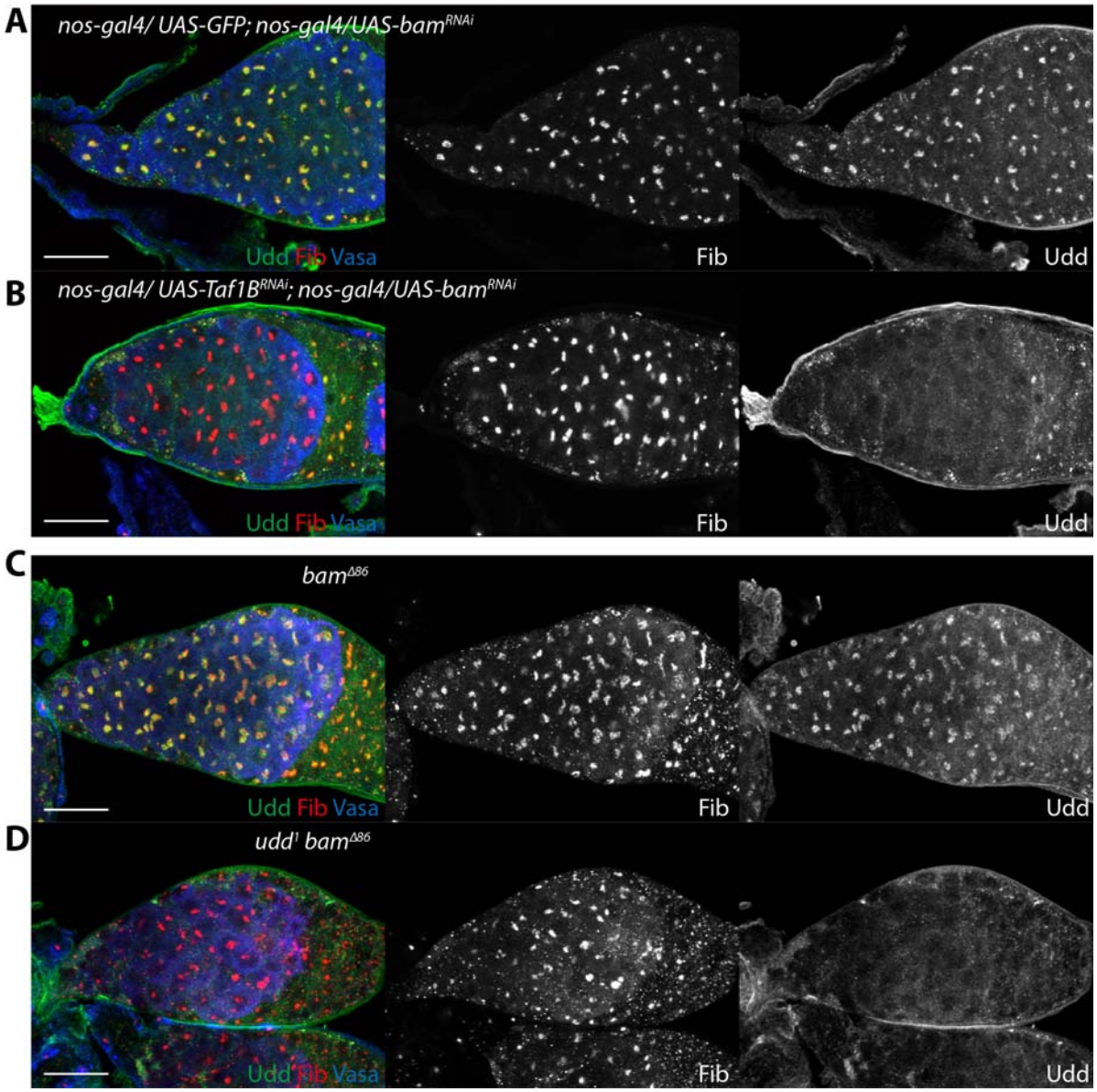

Figure 5.15 Nucleolar region marked by Fibrillarin is not obviously changed when mutating *udd* or *Taf1B* in a *bam* mutant background. (A-D) Germaria from 2 to 4 days old flies stained for Udd (green), Fibrillarin (red), Vasa (blue). (A) Control *nos-gal4(II)/UAS-GFP;nos-gal4(III)/UAS-bam*^{RNAi}; (B) *nos-gal4(II)/UAS-Taf1B*^{RNAi}*; nos-gal4(III)/UAS-bam*^{RNAi}; (C) control *bam*$^{\Delta 86}$; (D) *udd*^{1}; *bam*$^{\Delta 86}$. Fibrillarin still localizes to the nucleoli of germ cells that lack Udd and Taf1B and does not exhibit an obvious decrease in its level. Scale bars represent 20 μm.

However, in consideration of the fact that in those double mutants, the nucleolar portion where Udd and Taf1B stay and function is obviously disrupted, Fibrillarin is actually a poor surrogate to use as a global nucleolar marker, to monitor global nucleolar size change, or to represent changes of global ribosome biogenesis. In my opinion, Fibrillarin should be only used to mark the subnucleolar region where it functions and represent the steps of ribosome biogenesis it is involved in.

Downregulation of factors involved in other steps of ribosome biogenesis and protein translation also lead to multicellular cyst formation in a *bam* mutant background.

From the results above, the formation of multicellular cysts in the *udd bam* and *Taf1B bam* double mutants is induced by the reduction (but not depletion) of rRNA transcription caused by *udd* or *Taf1B* deletion, and then presumably it is related to the subsequent decrease of ribosome numbers and downregulation of protein translation. Consistent with this idea, I tested several TRIP RNAi lines for genes involved in different steps of ribosome biogenesis and protein translation in a *bam* mutant background to see if they also exhibited cyst formation. There were some RNAi lines, similar to RpI135^{RNAi}, when knocked down specifically in the germline giving rise to empty germaria without any germ cells even in newly eclosed flies no matter by itself or in a *bam* loss of function background, including the lines for translation initiation factors Eif4E and Eif4AIII and for ribosomal proteins RpS3 and RpL40. In that case, no fusome phenotype was able to be studied due to the strong germ cell loss. However, there were some other RNAi lines exhibiting similar but less severe germ cell loss, including germline-specific knock-down of the rRNA processing/ ribosome assembly factor Nopp140 [224], the ribosomal proteins RpL3 and RpS27a or the translation initiation factor Eif4AIII (one weak

line). In young flies it was observed that knocking down these factors in a *bam* loss-of-function background (either $bam^{\Delta 86}$ homozygotes or bam^{RNAi} germline knock-down) also resulted in the formation of multicellular cysts with branched fusome (**Figure 5.16; 5.17**). Therefore, attenuation of factors involved in different steps of ribosome biogenesis and protein translation may help foster incomplete cytokinesis which then leads to cyst formation in a *bam* mutant background (see Discussion).

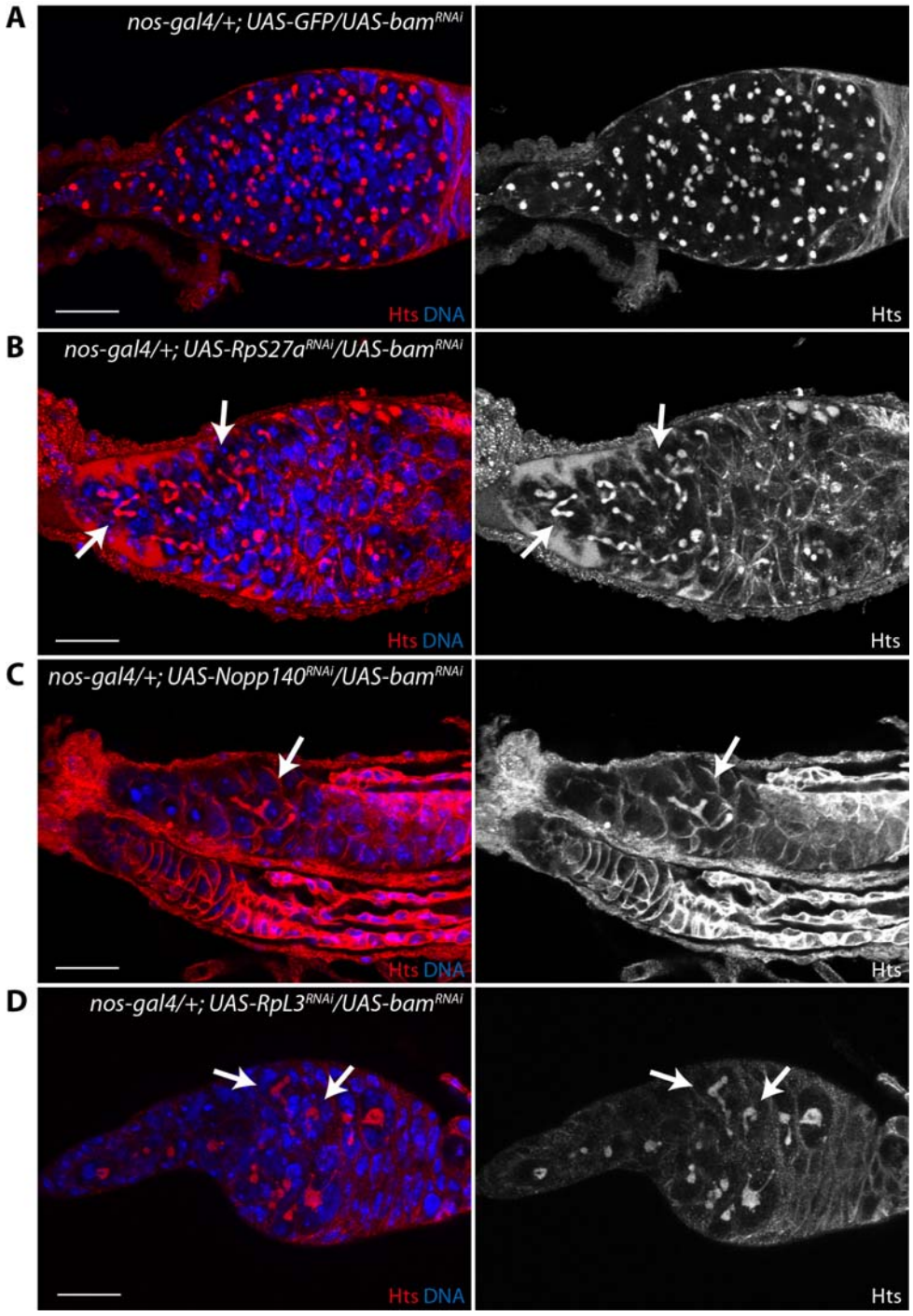

Figure 5.16 Down-regulation of ribosome biogenesis promotes morphological changes during early cyst development in *bam* loss-of-function background. *nos-gal4* was used to drive (A) control: *UAS-GFP* and *UAS-bam*^{RNAi}; (B) *UAS-RpS27a*^{RNAi} and *UAS-bam*^{RNAi}; (C) *UAS-Nopp140*^{RNAi} and *UAS-bam*^{RNAi}; (D) *UAS-RpL3*^{RNAi} and *UAS-bam*^{RNAi} at 29℃. RpS27A is a component of the small ribosomal subunit; RpL3 is a component of the large ribosomal subunit; and Nopp140 is involved in rRNA processing and ribosome assembly. (A-D) Germaria from 3-6 days old flies stained for Hts (red) and DNA (blue). Scale bars represent 20 μm.

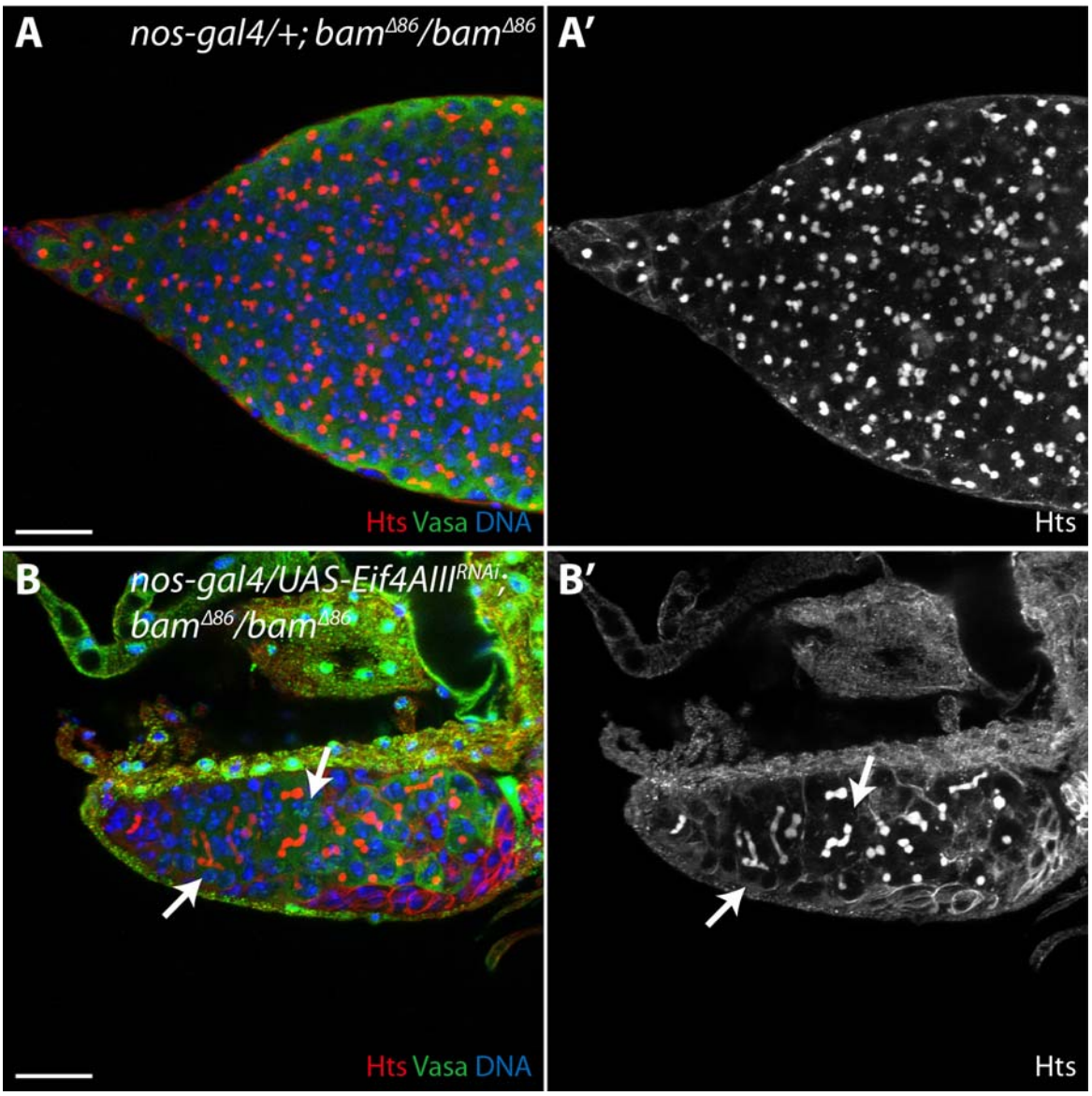

Figure 5.17 Down-regulation of protein translation promotes morphological changes during early cyst development in a *bam* mutant background. (A) control *nos-gal4/+; bam*$^{\Delta 86}$/ *bam*$^{\Delta 86}$ and (B) *nos-gal4/UAS-Eif4AIII*^{RNAi}(II); *bam*$^{\Delta 86}$/ *bam*$^{\Delta 86}$ Germaria from 2-5 days old flies at room temperature stained for Vasa (green), Hts (red) and DNA (blue). (A', B') Hts alone. Note: in order to reduce protein translation, Eif4E^{RNAi} and two other lines for Eif4AIII^{RNAi} on the 3rd chromosome were also tested in a *bam*^{RNAi} background and the progeny exhibited empty germaria as soon as they eclose, therefore no fusome phenotype was able to be examined. Scale bars represent 20 μm.

Up-regulation of RNA Pol I transcription in the germaria leads to a modest increase of GSC-like cells marked by round fusomes.

According to the experimental results above, *bam*-induced early cyst differentiation exhibited relatively low levels of nascent rRNAs, and attenuation of Pol I transcription by mutating *udd* or *Taf1B* in undifferentiated cells led to cyst formation marked by branched fusome, indicating that there is a correlation between downregulation of Pol I transcription and early differentiating cyst formation and modulation of Pol I transcription might be part of the stem cell differentiation program. If this is indeed the case, increasing Pol I activity in stem cell daughters exiting the niche might delay their ability to form cysts and increase the number of undifferentiated cells with round fusome.

For the purpose of increasing rRNA transcription, I first tested Udd overexpression with Gal4/UAS system driven by different germline Gal4 lines. No obvious increase of round fusome numbers was observed at the tip of germaria. It was not surprising, since Udd, Taf1B and CG10496 work together in a complex associating with rDNA promoter, and all factors in this complex might need to be overexpressed together to exhibit an obvious change. Moreover, the conservation of Taf1B and CG10496 with mammalian SL1 complex members indicates this Udd complex may be functionally similar to SL1 complex in consideration of promoting Pol I transcription, and it has not been shown that overexpressing SL1 complex in vivo is able to upregulate Pol I transcription.

Previous work showed that over-expression of Tif-IA itself, a conserved factor that forms a preinitiation complex with RNA Pol I and bridges rDNA promoter-associated Pol I regulatory factors with the Pol I complex, resulted in upregulation of pre-rRNA transcription in *Drosophila* [225].

Although it was hard to drive high levels of Tif-IA expression in the germline (**Figure 5.18 A-B**) with the *UAS-HA-Tif-IA* construct I created, low levels of Tif-IA over-expression resulted in a modest but highly significant increase (p-value<0.0001; unpaired two tailed t test) in both the number of single cells with round fusomes within germaria and the percentage of germaria that contained over five single undifferentiated cells (**Figure 5.18 C-E**). These observations further indicate that modulation of Pol I activity influences the morphological changes that accompany early germline differentiation.

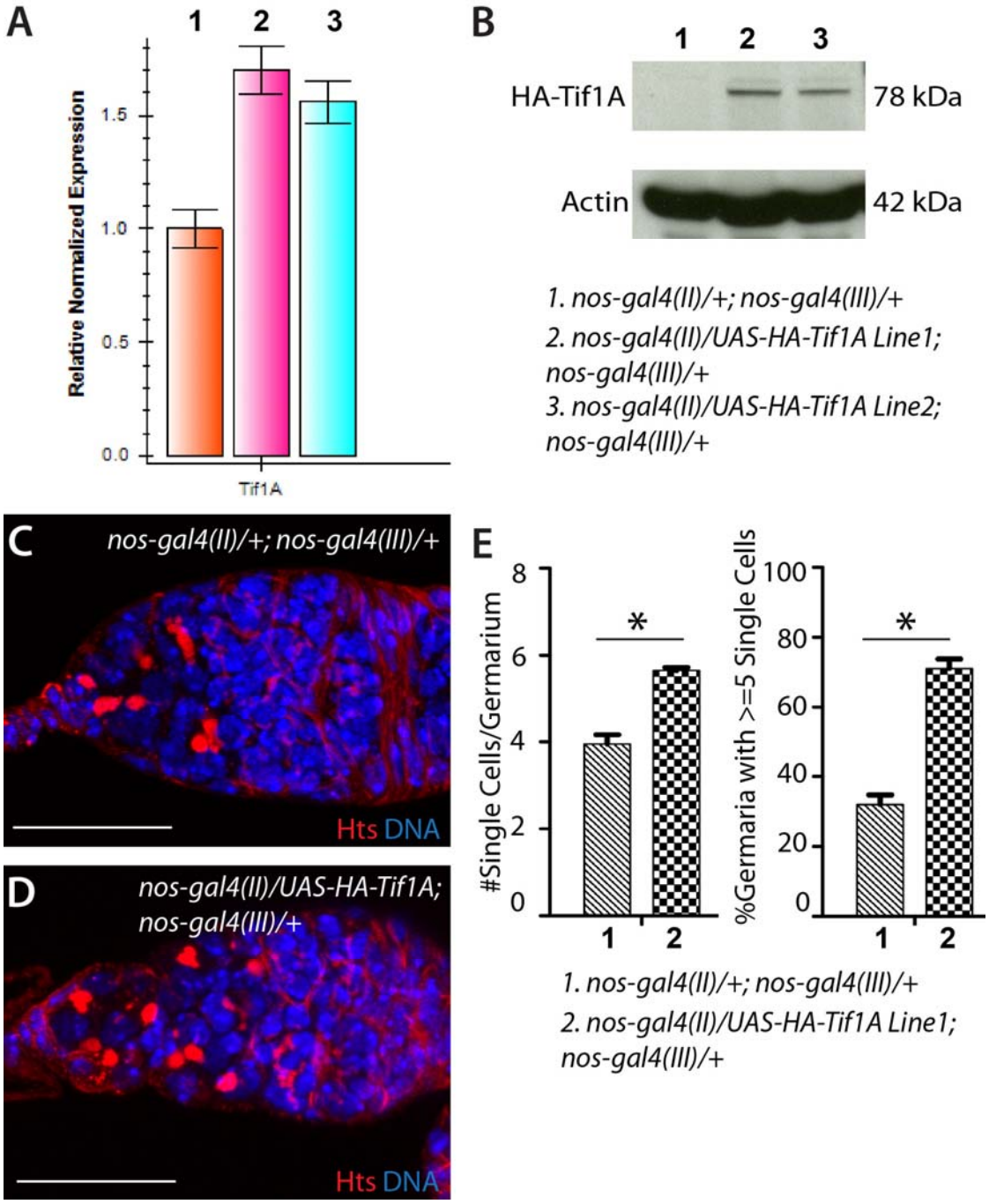

Figure 5.18 Tif-IA overexpression leads to a modest increase of GSC-like undifferentiated cells marked by round fusomes. Overexpressing *Tif-IA* itself is able to upregulate RNA Pol I transcription. (A) RT-qPCR and (B) western blots demonstrate that *Tif-IA* expression level is mildly increased in flies carrying *UASp-HA-Tif-IA* transgene compared to flies with only *nos-gal4*. (C-D) Germaria from *nos-gal4* control flies (C) and *nos-gal4* with *UASp-HA-Tif-IA* flies (D) stained for Hts (red) and DNA (blue). (E) Quantification of the fusome phenotype observed in (C) and (D). Two ways of quantification were performed: 1. average number of round fusome at the tip of each germarium; 2. percentage of germaria with equal or more than five round fusomes. Two nos-gal4 lines on the 2nd and 3rd chromosomes respectively were used together; two individual lines for *UASp-HA-Tif-IA* with the same landing site were tested, and in C-E only results using line 1 were shown.

C. Discussion

1. The dynamics of nucleolar breakdown and reassembly during mitosis, including changes of Pol I transcription machinery, rRNA processing machinery and other factors involved in ribosome assembly.

Live cell imaging studies in mammalian cell lines have demonstrated the dynamic changes of nucleolar factors involved in different steps of ribosome biogenesis during the process of premitotic nucleolar breakdown and postmitotic reassembly [226-228].

Nucleolar disassembly does not start until metaphase, the first step of which is marked by disappearance of Pol I subunits from the FC region. Following the onset of nucleolar disassembly, the nuclear envelope (NE) starts to lose its function and then breaks down. Within the window of NE breakdown, the rRNA processing factors in the DFC region, e.g. Fibrillarin and other processing and assembly factors enriched in the GC region, e.g. B23, Nucleolin and Nop52, together with the partially processed rRNAs quickly dissociate from the nucleolus and are preserved in perichromosomal regions (PRs) and in different cytoplasmic particles called nucleolus-derived foci (NDF).

The postmitotic reassembly starts from nuclear accumulation of nucleolar proteins during anaphase. First, the rRNA processing factors, like Fibrillarin, are transported from PRs and multiple cytoplasmic particles to the nucleus and form different prenucleolar bodies (PNBs). Then the NE function is restored, which is followed by transportation of Pol I subunits to the rDNA-containing NORs. Different from the rRNA processing/assembly factors, during mitosis the Pol I subunits do not form cytoplasmic or nuclear particles. After reassembly at NORs, RNA Pol I initiates rRNA

transcription before the processing/assembly factors are gradually delivered from PNBs to Pol I-containing NORs. Finally, a functional nucleolus is reformed, marked by the fusion of multiple NORs with FC, DFC and GC regions.

Besides mammalian UBF which surprisingly remains associated with the rDNA-containing NORs throughout mitosis, there are not much live cell studies about the dynamic changes of transcription initiation factor SL1 complex and other Pol I regulators during mitosis. Here we show in live *Drosophila* ovaries that Udd, a novel Pol I transcriptional regulator binding to the *Drosophila* homologs of SL1 components, exhibits a similar dynamic change to mammalian Pol I subunits that it disappears from the nucleolus during metaphase and early anaphase and reassembles in the NORs starting from late anaphase. No matter if these Pol I regulators dissociate from NORs or not during M phase, several mammalian factors including SL1 components, the termination factor TTF-1 as well as UBF are phosphorylated and deactivated by cdc2/cyclinB kinase or other kinases. The mitotic phosphorylation events impair their interactions between each other or with rDNA sequence. It is intriguing to see if *Drosophila* Udd, Taf1B and CG10496 exhibit similar repressive modifications during M phase.

In *Drosophila* there is no homolog of UBF, however, it is possible that there is some unknown factor with similar functions to UBF and remaining associated with NORs during mitosis. This unknown factor would probably be more critical for recruiting Pol I and Pol I-associated factors like Udd/Taf1B and setting up the initial quantitative difference of rRNA transcription machinery within the two stem cell daughters at the end of mitosis.

2. Live imaging with Udd-GFP and immunostaining of fixed ovaries against endogenous Udd reveals dynamic regulation of Udd localization.

The asymmetric inheritance of Udd between two GSC daughter cells at the end of mitotic division was observed in both time-lapse live ovary imaging using GFP-tagged Udd and also immunofluorescent staining of fixed ovaries detecting endogenous Udd. The resolution of these two methods was not high enough to detect multiple tiny NOR spots during nucleolar reassembly as previously observed in mammalian cell lines. For all the cells examined in the ovaries, I found that either there was not any nucleolar Udd (in the middle of mitosis), or only one Udd dot was observed in each cell (or associate with each set of chromosomes during late mitosis). Probably the anti-Udd antiserum is not able to give a sharp enough staining and the Udd-GFP signal is too weak. Another possibility is that the cells in the whole ovary might be different from immortalized cells.

Despite the similarity observed in two methods at the end of mitosis, I found there was some difference in the middle of mitosis. From immunostained fixed ovaries, I observed the disappearance of endogenous Udd from chromosome in the middle of metaphase and at the onset of anaphase, similar to the mitotic changes of Pol I subunits in mammalian cells. However, Udd-GFP in living imaging disappeared for a longer period during mitosis, from prometaphase to early telophase.

This difference is probably due to the weak signal strength of Udd-GFP, although the flies used for this purpose carry two copies of Udd-GFP and no enough Udd. There are several reasons contributing to this: first, it has no signal amplification from primary and secondary antibodies like fixed samples; second, the live imaging was performed under 20× objective with resonant scanning method in order to take images faster and to reduce bleaching, both of which decreases resolution

compared to using 63× objective with regular laser scanning method; third, live tissues are easily photo-bleached under the scope, especially after long period of scanning; fourth, although Udd-GFP rescued the lethality and sterility of *udd* mutants, the large GFP tag might affect the potential posttranslational modifications of Udd, impair the normal folding of Udd, or interfere with Udd's interaction with other proteins, all of which might reduce the nucleolar localization of Udd-GFP and further weaken the nucleolar GFP signals.

3. Comparing to the *udd* trangenes expressed in a wild-type background, why do they exhibit higher nucleolar levels in the *udd* mutant background?

I made two rescuing transgenic lines for Udd, one is a cDNA construct HA-Udd controlled by Gal4-UAS system, and the other is a genomic construct Udd-GFP under the endogenous Udd promoter. For both lines, I found that the transgene expression in the nucleoli was higher in the *udd* mutant background.

I first examined the expression levels of transgenes in the whole ovarian lysates. The HA-Udd expression was similar in both backgrounds as examined by anti-HA and anti-Udd western blots. However, both anti-GFP and anti-Udd antibodies failed to detect Udd-GFP in the ovaries by western blot despite that Udd-GFP fluorescence was clearly observed. Results with HA-Udd transgene suggest that there might be some factors controlling the nucleolar transport of Udd, restricting the size of nucleolus and limiting the total amount of Udd in the nucleolus. These factors might regulate Udd localization directly, or regulate the PTMs and/or activities of Udd or Udd-associated factors which subsequently impair their nucleolar localization.

Additionally, for the difference of Udd-GFP observed under four different conditions in Figure 5.4, there is one simple explanation if the total amount of nucleolar Udd is really limited by some factor. Assuming the control over Udd-GFP expression and endogenous Udd expression is equal and assuming the upper nucleolar localization limit is 1.5 fold compared to wild-type flies at regular condition (1 fold), when there is one copy of Udd-GFP and two copies of endogenous Udd, the total level of functional nucleolar Udd is 1.5 and the level of nucleolar Udd-GFP is 0.5; when there are two copies of each, the total level of functional Udd is still 1.5, while the level of Udd-GFP is 0.75; when there is only one copy of Udd-GFP and no endogenous Udd, the level of nucleolar GFP signal is 1 or more; finally when there are only two copies of Udd-GFP, the level of nucleolar GFP signal is 1.5. The above statement is based on an assumption, and it is unknown whether the protein level of Udd-GFP is comparable to that of endogenous Udd or not.

4. Are the multicellular cysts formed in double mutants caused by a decrease in global translation or in the translation of specific mRNAs?

It is still unknown whether reduction of global translation or the translation of specific mRNAs leads to cyst formation in the *udd bam* and *Taf1B bam* double mutants. I observed that at least Nanos and Sxl protein levels were not obviously reduced in *udd bam* double mutants compared to *bam* mutants, which suggests that it is possible that the translation of a subset of mRNA transcripts is actually reduced more than the others. Among these strongly affected genes, only a few could be more critical for the phenotypic changes in a certain cell type or a specific tissue.

But how could only a subset of mRNAs be seriously affected? First, when ribosome

biogenesis and protein translation are reduced instead of being completely deleted, the cells might prefer to translate the proteins with housekeeping functions as compensation, like factors regulating cell survival, cell cycle progression and the positive regulators of those proteins. Subsequently some of the less translated proteins, which control the maintenance of a specific cell feature, might induce cell fate changes at least partially such as transformation or differentiation. For example, here I observed phenotypic changes when knocking down *udd*, *Taf1B* and other factors in both undifferentiated germ cells and undifferentiated eye primordial cells (see Discussion Question 6 and Figure 5.20 below): in the ovaries, the undifferentiated GSC-like cells marked with round fusomes were replaced by multicellular cysts with branched fusomes; in the eye region, an eye-to antennal transformation phenotype appeared when knocking down those factors in the embryonic and larval undifferentiated eye cells (Figure 5.20). In general, I tend to believe that the transcripts that are affected most and that induce divergent phenotypic changes in different tissues or cell types are probably varied.

In addition, in one cell there might be different types of ribosomes functioning in translation of various mRNA transcripts. When there are not enough materials for all kinds of protein synthesis due to the lack of rRNAs, ribosomes, translation factors, etc., in this condition some types of ribosomes may be more active and efficient than the others and the translation of a certain transcripts are maintained while the others are reduced.

5. Can *Drosophila* Udd, Taf1B, CG10496 and Tif-IA be regulated through posttranslational modifications?

There are no direct studies about PTMs of *Drosophila* Pol I regulators. In western blots detecting HA-Taf1B and Flag-Taf1B in S2 cells, I constantly observed two bands next to each other and Udd seemed to interact more with the lower band. This suggests that Taf1B might be posttranslationally modified and its activity could be modulated.

The PTMs of mammalian basal Pol I regulators have been extensively studied (see Chapter I the posttranslational modification part). According to the sequence or secondary structure conservation between *Drosophila* Tif-IA, Taf1B, CG10496 and human Tif-IA, Taf1B and Taf1C, the factors in *Drosophila* probably also carry multiple PTM sites.

Human Tif-IA is phosphorylated at multiple serine and threonine residues by different kinases including MAPKs, CKII, PI3K, S6K, AMPK, CDK2, JNK2, etc. upon stimulation by growth factors, nutrients, changes of nutrient or energy status and changes of Pol I machinery status on a transcribing rDNA (initiation or elongation). Phosphorylated Tif-IA is subsequently activated or repressed through promoting or disrupting its interaction with Pol I subunits or SL1 components.

Human and mouse SL1 components also carry phosphorylation sites. Taf1B and Taf1C are phosphorylated at both M phase and interphase, while TBP is phosphorylated only during M phase. Although it is unknown how SL1 phosphorylations occur during interphase and how they affect Pol I transcription, the mitotic phosphorylations of Taf1C and TBP by cdc2/cylinB or other M phase kinases probably repress SL1 activity. In addition to phosphorylations, Taf1B is also acetylated and activated by histone acetyltransferase PCAF which increases SL1 binding to rDNA promoter.

It is intriguing to examine if there are any specific PTMs in *Drosophila* Pol I regulators and if the PTMs affect the activities and localizations of these factors and their partners. The difference in

PTMs of Pol I factors and/or the changes in their expression levels could be the major causes for different rRNA gene transcription levels during differentiation and development in multiple tissues and lineages. Moreover, it is possible that forced constitutive activation of *Drosophila* Pol I regulators in the germarium could cause a stronger GSC expansion phenotype.

6. In addition to the developmental changes observed in undifferentiated germ cells, an eye-to-antennal transformation phenotype was also observed when knocking down factors involved in RNA Pol I transcription specifically in the early undifferentiated eye region.

Besides the germline tissue, I also observed that knocking down Pol I associated factors in the eye, specifically in the undifferentiated regions including embryonic eye primordia and the undifferentiated part of larval eye discs, resulted in not only smaller eyes but also additional antennal segments appearing at that region in adult flies (Figure 5.19). This phenotype was not observed when the knockdown occurred during adult stage when the eye cells are terminally differentiated. Previously the DiMario group reported a similar eye-to-antennal phenotype with a ubiquitous knockdown of *Drosophila* nucleostemin 1 (NS1), a factor affecting rRNA processing and the large ribosomal subunit biogenesis [167]. Both studies suggest that different rRNA levels are required during development of eye and antenna, which might affect the expression levels of specific genes needed for either antenna or eye development. These intriguing *in vivo* findings from Drosophila tissues indicate that RNA Pol I transcription, as the first step of ribosome biogenesis, is not only important for cell growth and proliferation but also necessarily correlated with cell fate changes which are linked to cell differentiation and tissue development.

Here are some additional notes for the eye phenotypes I observed: according to my knockdown experience with *udd* RNAi lines, the transformation phenotype was more obvious when the RNAis were expressed at high levels in the embryos and 1st instar larvae. However, when the knockdown was too strong and the cells could not survive, nothing was able to grow out in the eye region and the transformation phenotype was not observed. Lastly, very high percentage of lethality (95%-100%) were also observed with RNAi lines for Pol I subunits RPA1 and RpI135, which could be due to the RNAi expression in the central nervous system besides eye primordia.

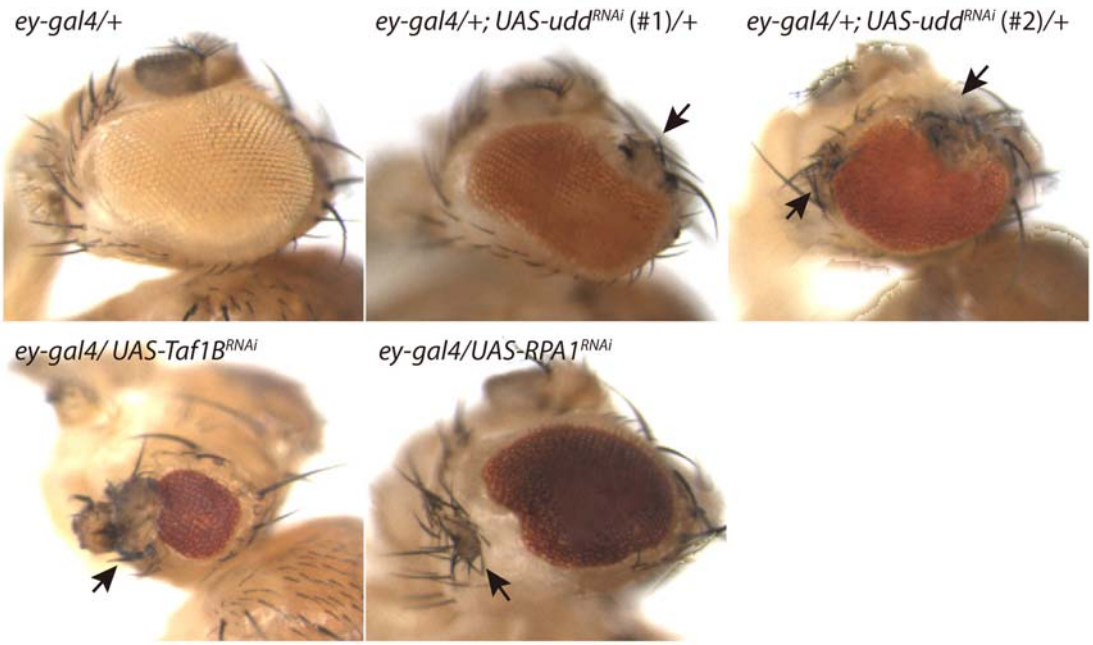

Figure 5.19. Knockdown of factors involved in RNA Pol I transcription in the undifferentiated eye region results in an eye-to-antennal transformation phenotype. Arrows point out the additional antenna segments growing in the eye region. *ey-gal4* was used to drive the expression of somatic RNAi lines for *udd*, *Taf1B* and *RPA1* (a.k.a. *RPA190*) in the eye, more specifically, in the embryonic eye primodia and the undifferentiated part of the larval eye discs. The crosses for udd^{RNAi} and $Taf1B^{RNAi}$ lines were set up at 29℃, while the progeny of $RPA1^{RNAi}$ lines were achieved at 18℃, since they were 100% lethal at 29 degree. Note: $RpI135^{RNAi}$ and another $RPA1^{RNAi}$, the RNAi lines for the first and second largest subunits of RNA Pol I complex, were also examined and the progeny were 100% lethal.

7. The relationship between Brat, Bam and Udd / rRNA transcription is worth studying.

In Drosophila female germline differentiating cysts, a TRIM-NHL protein Brat plays an important role in repressing the Dpp downstream component Mad translation[229]. Brat is not expressed in GSCs due to its translational repression by Nanos/Pumilio. Interestingly, in other Drosophila tissues Brat has been reported as a negative regulator of cell growth and proliferation, and *brat* mutants exhibited increased levels of mature rRNAs [230]. It is not known yet if Brat directly represses the translation of Pol I subunits' or Pol I regulators' mRNAs, including the transcripts of Udd, Taf1B, Tif-IA, etc.

Several experiments can be performed next to see if Brat is the bridge or link between Bam and Udd/Taf1B as well as Pol I transcription. First, examine if overexpressing Brat protein in the *bam* mutant background exhibits multicellular cysts similar to *udd bam* double mutants. For this overexpression purpose the Brat transgene should have only ORF but not any UTRs, which is to avoid the Nanos/Pumilio-mediated repression of Brat translation. Second, examine if in the background of Brat mutants or mutant clones, heat shock-mediated overexpression of Bam within the bam mutant background could still induce changes of fusome morphology (or other markers distinguishing GSCs and cysts) and modulations of the Udd, Taf1B, and BrUTP labeled pre-rRNA levels. Third, Brat could be a main reason why I was not able to get a very strong overexpression of several Pol I regulators in the germaria. For example, *Tif-IA* was not able to be strongly expressed in the germ cells; *HA-Udd*, although clearly expressed in the nucleoli, seemed to exhibit a cytoplasmic accumulation which was more obvious in the early cysts; in addition, both HA-Udd and Udd-GFP exhibited more obvious nucleolar localization in the *udd* mutant background. In order to see if Brat restricts their nucleolar

expression, one should look into if overexpressing those factors in *brat* mutant clones can increase their nucleolar expression levels.

Bibliography

1. Grummt, I., *Life on a planet of its own: regulation of RNA polymerase I transcription in the nucleolus.* Genes Dev, 2003. **17**(14): p. 1691-702.
2. Moss, T. and V.Y. Stefanovsky, *At the center of eukaryotic life.* Cell, 2002. **109**(5): p. 545-8.
3. Russell, J. and J.C. Zomerdijk, *RNA-polymerase-I-directed rDNA transcription, life and works.* Trends Biochem Sci, 2005. **30**(2): p. 87-96.
4. Bouteille, M. and D. Hernandez-Verdun, *Localization of a gene: the nucleolar organizer.* Biomedicine, 1979. **30**(6): p. 282-7.
5. Dammann, R., et al., *Chromatin structures and transcription of rDNA in yeast Saccharomyces cerevisiae.* Nucleic Acids Res, 1993. **21**(10): p. 2331-8.
6. McStay, B. and I. Grummt, *The epigenetics of rRNA genes: from molecular to chromosome biology.* Annu Rev Cell Dev Biol, 2008. **24**: p. 131-57.
7. Sanij, E. and R.D. Hannan, *The role of UBF in regulating the structure and dynamics of transcriptionally active rDNA chromatin.* Epigenetics, 2009. **4**(6): p. 374-82.
8. Camier, S., A.M. Dechampesme, and A. Sentenac, *The only essential function of TFIIIA in yeast is the transcription of 5S rRNA genes.* Proc Natl Acad Sci U S A, 1995. **92**(20): p. 9338-42.
9. Sorensen, P.D., et al., *Fine mapping of human 5S rRNA genes to chromosome 1q42.11----q42.13.* Cytogenet Cell Genet, 1991. **57**(1): p. 26-9.
10. Cech, T.R., *Structural biology. The ribosome is a ribozyme.* Science, 2000. **289**(5481): p. 878-9.
11. Moore, P.B. and T.A. Steitz, *The involvement of RNA in ribosome function.* Nature, 2002. **418**(6894): p. 229-35.
12. Munro, J.B., et al., *Navigating the ribosome's metastable energy landscape.* Trends Biochem Sci, 2009. **34**(8): p. 390-400.
13. Appels, R. and J. Dvorak, *Relative Rates of Divergence of Spacer and Gene-Sequences within the Rdna Region of Species in the Triticeae - Implications for the Maintenance of Homogeneity of a Repeated Gene Family.* Theoretical and Applied Genetics, 1982. **63**(4): p. 361-365.
14. Heix, J. and I. Grummt, *Species-Specificity of Transcription by Rna-Polymerase-I.* Current Opinion in Genetics & Development, 1995. **5**(5): p. 652-656.
15. Moss, T. and V.Y. Stefanovsky, *Promotion and regulation of ribosomal transcription in eukaryotes by RNA polymerase I.* Prog Nucleic Acid Res Mol Biol, 1995. **50**: p. 25-66.
16. Bywater, M.J., et al., *Dysregulation of the basal RNA polymerase transcription apparatus in cancer.* Nat Rev Cancer, 2013. **13**(5): p. 299-314.
17. Memet, S., et al., *RPA190, the gene coding for the largest subunit of yeast RNA polymerase A.* J Biol Chem, 1988. **263**(6): p. 2830-9.
18. Naryshkina, T., et al., *Role of second-largest RNA polymerase I subunit Zn-binding domain in enzyme assembly.* Eukaryot Cell, 2003. **2**(5): p. 1046-52.
19. Miller, G., et al., *hRRN3 is essential in the SL1-mediated recruitment of RNA polymerase I to rRNA gene promoters.* Embo Journal, 2001. **20**(6): p. 1373-1382.
20. Beckmann, H., et al., *Coactivator and promoter-selective properties of RNA polymerase I TAFs.* Science, 1995. **270**(5241): p. 1506-9.
21. Knutson, B.A. and S. Hahn, *Yeast Rrn7 and human TAF1B are TFIIB-related RNA polymerase I general transcription factors.* Science, 2011. **333**(6049): p. 1637-40.

22. Naidu, S., et al., *TAF1B is a TFIIB-like component of the basal transcription machinery for RNA polymerase I.* Science, 2011. **333**(6049): p. 1640-2.
23. McStay, B., M.W. Frazier, and R.H. Reeder, *xUBF contains a novel dimerization domain essential for RNA polymerase I transcription.* Genes Dev, 1991. **5**(11): p. 1957-68.
24. Tuan, J.C., W. Zhai, and L. Comai, *Recruitment of TATA-binding protein-TAFI complex SL1 to the human ribosomal DNA promoter is mediated by the carboxy-terminal activation domain of upstream binding factor (UBF) and is regulated by UBF phosphorylation.* Mol Cell Biol, 1999. **19**(4): p. 2872-9.
25. Huang, R., et al., *Upstream binding factor up-regulated in hepatocellular carcinoma is related to the survival and cisplatin-sensitivity of cancer cells.* FASEB J, 2002. **16**(3): p. 293-301.
26. Panov, K.I., et al., *UBF activates RNA polymerase I transcription by stimulating promoter escape.* Embo Journal, 2006. **25**(14): p. 3310-22.
27. Stepanchick, A., et al., *DNA binding by the ribosomal DNA transcription factor rrn3 is essential for ribosomal DNA transcription.* J Biol Chem, 2013. **288**(13): p. 9135-44.
28. Hirschler-Laszkiewicz, I., et al., *Rrn3 becomes inactivated in the process of ribosomal DNA transcription.* J Biol Chem, 2003. **278**(21): p. 18953-9.
29. Panov, K.I., J.K. Friedrich, and J.C. Zomerdijk, *A step subsequent to preinitiation complex assembly at the ribosomal RNA gene promoter is rate limiting for human RNA polymerase I-dependent transcription.* Mol Cell Biol, 2001. **21**(8): p. 2641-9.
30. Zhang, Y., et al., *The RNA polymerase-associated factor 1 complex (Paf1C) directly increases the elongation rate of RNA polymerase I and is required for efficient regulation of rRNA synthesis.* J Biol Chem, 2010. **285**(19): p. 14152-9.
31. Assfalg, R., et al., *TFIIH is an elongation factor of RNA polymerase I.* Nucleic Acids Res, 2012. **40**(2): p. 650-9.
32. Iben, S., et al., *TFIIH plays an essential role in RNA polymerase I transcription.* Cell, 2002. **109**(3): p. 297-306.
33. Jansa, P., et al., *The transcript release factor PTRF augments ribosomal gene transcription by facilitating reinitiation of RNA polymerase I.* Nucleic Acids Res, 2001. **29**(2): p. 423-9.
34. Jansa, P. and I. Grummt, *Mechanism of transcription termination: PTRF interacts with the largest subunit of RNA polymerase I and dissociates paused transcription complexes from yeast and mouse.* Mol Gen Genet, 1999. **262**(3): p. 508-14.
35. Mason, S.W., M. Wallisch, and I. Grummt, *RNA polymerase I transcription termination: similar mechanisms are employed by yeast and mammals.* J Mol Biol, 1997. **268**(2): p. 229-34.
36. Grummt, I., et al., *A transcription terminator located upstream of the mouse rDNA initiation site affects rRNA synthesis.* Cell, 1986. **47**(6): p. 901-11.
37. Guetg, C., et al., *The NoRC complex mediates the heterochromatin formation and stability of silent rRNA genes and centromeric repeats.* Embo Journal, 2010. **29**(13): p. 2135-46.
38. Henderson, S. and B. Sollner-Webb, *A transcriptional terminator is a novel element of the promoter of the mouse ribosomal RNA gene.* Cell, 1986. **47**(6): p. 891-900.
39. Langst, G., P.B. Becker, and I. Grummt, *TTF-I determines the chromatin architecture of the active rDNA promoter.* Embo Journal, 1998. **17**(11): p. 3135-45.
40. Nemeth, A., et al., *Epigenetic regulation of TTF-I-mediated promoter-terminator interactions of rRNA genes.* Embo Journal, 2008. **27**(8): p. 1255-65.
41. Xie, W., et al., *The chromatin remodeling complex NuRD establishes the poised state of rRNA genes*

characterized by bivalent histone modifications and altered nucleosome positions. Proc Natl Acad Sci U S A, 2012. **109**(21): p. 8161-6.

42. Yuan, X., et al., *Activation of RNA polymerase I transcription by cockayne syndrome group B protein and histone methyltransferase G9a.* Mol Cell, 2007. **27**(4): p. 585-95.
43. Schneider, D.A., *RNA polymerase I activity is regulated at multiple steps in the transcription cycle: recent insights into factors that influence transcription elongation.* Gene, 2012. **493**(2): p. 176-84.
44. Evers, R. and I. Grummt, *Molecular coevolution of mammalian ribosomal gene terminator sequences and the transcription termination factor TTF-I.* Proc Natl Acad Sci U S A, 1995. **92**(13): p. 5827-31.
45. Conconi, A., et al., *Two different chromatin structures coexist in ribosomal RNA genes throughout the cell cycle.* Cell, 1989. **57**(5): p. 753-61.
46. Santoro, R. and I. Grummt, *Molecular mechanisms mediating methylation-dependent silencing of ribosomal gene transcription.* Mol Cell, 2001. **8**(3): p. 719-25.
47. Frescas, D., et al., *JHDM1B/FBXL10 is a nucleolar protein that represses transcription of ribosomal RNA genes.* Nature, 2007. **450**(7167): p. 309-13.
48. Feng, W., et al., *PHF8 activates transcription of rRNA genes through H3K4me3 binding and H3K9me1/2 demethylation.* Nat Struct Mol Biol, 2010. **17**(4): p. 445-50.
49. Santoro, R., J. Li, and I. Grummt, *The nucleolar remodeling complex NoRC mediates heterochromatin formation and silencing of ribosomal gene transcription.* Nat Genet, 2002. **32**(3): p. 393-6.
50. Dekker, J., et al., *Capturing chromosome conformation.* Science, 2002. **295**(5558): p. 1306-11.
51. Denissov, S., et al., *A model for the topology of active ribosomal RNA genes.* EMBO Rep, 2011. **12**(3): p. 231-7.
52. Sander, E.E. and I. Grummt, *Oligomerization of the transcription termination factor TTF-I: implications for the structural organization of ribosomal transcription units.* Nucleic Acids Res, 1997. **25**(6): p. 1142-7.
53. Strohner, R., et al., *NoRC--a novel member of mammalian ISWI-containing chromatin remodeling machines.* Embo Journal, 2001. **20**(17): p. 4892-900.
54. Santoro, R. and I. Grummt, *Epigenetic mechanism of rRNA gene silencing: temporal order of NoRC-mediated histone modification, chromatin remodeling, and DNA methylation.* Mol Cell Biol, 2005. **25**(7): p. 2539-46.
55. Zhou, Y. and I. Grummt, *The PHD finger/bromodomain of NoRC interacts with acetylated histone H4K16 and is sufficient for rDNA silencing.* Curr Biol, 2005. **15**(15): p. 1434-8.
56. Zhou, Y., R. Santoro, and I. Grummt, *The chromatin remodeling complex NoRC targets HDAC1 to the ribosomal gene promoter and represses RNA polymerase I transcription.* Embo Journal, 2002. **21**(17): p. 4632-40.
57. Mayer, C., et al., *Intergenic transcripts regulate the epigenetic state of rRNA genes.* Mol Cell, 2006. **22**(3): p. 351-61.
58. Santoro, R., et al., *Intergenic transcripts originating from a subclass of ribosomal DNA repeats silence ribosomal RNA genes in trans.* EMBO Rep, 2010. **11**(1): p. 52-8.
59. Schmitz, K.M., et al., *Interaction of noncoding RNA with the rDNA promoter mediates recruitment of DNMT3b and silencing of rRNA genes.* Genes Dev, 2010. **24**(20): p. 2264-9.
60. Calkins, A.S., J.D. Iglehart, and J.B. Lazaro, *DNA damage-induced inhibition of rRNA synthesis by DNA-PK and PARP-1.* Nucleic Acids Res, 2013.
61. Boamah, E.K., et al., *Poly(ADP-Ribose) polymerase 1 (PARP-1) regulates ribosomal biogenesis in*

Drosophila nucleoli. PLoS Genet, 2012. **8**(1): p. e1002442.

62. Guerrero, P.A. and K.A. Maggert, *The CCCTC-binding factor (CTCF) of Drosophila contributes to the regulation of the ribosomal DNA and nucleolar stability.* PLoS One, 2011. **6**(1): p. e16401.
63. Torrano, V., et al., *Targeting of CTCF to the nucleolus inhibits nucleolar transcription through a poly(ADP-ribosyl)ation-dependent mechanism.* J Cell Sci, 2006. **119**(Pt 9): p. 1746-59.
64. van de Nobelen, S., et al., *CTCF regulates the local epigenetic state of ribosomal DNA repeats.* Epigenetics Chromatin, 2010. **3**(1): p. 19.
65. Yu, W., et al., *Poly(ADP-ribosyl)ation regulates CTCF-dependent chromatin insulation.* Nat Genet, 2004. **36**(10): p. 1105-10.
66. Bradsher, J., et al., *CSB is a component of RNA pol I transcription.* Mol Cell, 2002. **10**(4): p. 819-29.
67. Caputo, M., et al., *The CSB repair factor is overexpressed in cancer cells, increases apoptotic resistance, and promotes tumor growth.* DNA Repair (Amst), 2013. **12**(4): p. 293-9.
68. Shen, M., et al., *The chromatin remodeling factor CSB recruits histone acetyltransferase PCAF to rRNA gene promoters in active state for transcription initiation.* PLoS One, 2013. **8**(5): p. e62668.
69. Bierhoff, H., et al., *Noncoding transcripts in sense and antisense orientation regulate the epigenetic state of ribosomal RNA genes.* Cold Spring Harb Symp Quant Biol, 2010. **75**: p. 357-64.
70. Murayama, A., et al., *Epigenetic control of rDNA loci in response to intracellular energy status.* Cell, 2008. **133**(4): p. 627-39.
71. Song, T., et al., *The NAD+ synthesis enzyme NMNAT1 regulates rRNA transcription.* J Biol Chem, 2013.
72. Percipalle, P., et al., *The chromatin remodelling complex WSTF-SNF2h interacts with nuclear myosin 1 and has a role in RNA polymerase I transcription.* EMBO Rep, 2006. **7**(5): p. 525-30.
73. Sarshad, A., et al., *Nuclear myosin 1c facilitates the chromatin modifications required to activate rRNA gene transcription and cell cycle progression.* PLoS Genet, 2013. **9**(3): p. e1003397.
74. Vintermist, A., et al., *The chromatin remodelling complex B-WICH changes the chromatin structure and recruits histone acetyl-transferases to active rRNA genes.* PLoS One, 2011. **6**(4): p. e19184.
75. Tanaka, Y., et al., *JmjC enzyme KDM2A is a regulator of rRNA transcription in response to starvation.* Embo Journal, 2010. **29**(9): p. 1510-22.
76. Bjorkman, M., et al., *Systematic knockdown of epigenetic enzymes identifies a novel histone demethylase PHF8 overexpressed in prostate cancer with an impact on cell proliferation, migration and invasion.* Oncogene, 2012. **31**(29): p. 3444-56.
77. Nakamura, S., et al., *JmjC-domain containing histone demethylase 1B-mediated p15(Ink4b) suppression promotes the proliferation of leukemic progenitor cells through modulation of cell cycle progression in acute myeloid leukemia.* Mol Carcinog, 2013. **52**(1): p. 57-69.
78. Grierson, P.M., et al., *BLM helicase facilitates RNA polymerase I-mediated ribosomal RNA transcription.* Hum Mol Genet, 2012. **21**(5): p. 1172-83.
79. Shiratori, M., et al., *WRN helicase accelerates the transcription of ribosomal RNA as a component of an RNA polymerase I-associated complex.* Oncogene, 2002. **21**(16): p. 2447-54.
80. Zhang, H., J.C. Wang, and L.F. Liu, *Involvement of DNA topoisomerase I in transcription of human ribosomal RNA genes.* Proc Natl Acad Sci U S A, 1988. **85**(4): p. 1060-4.
81. Ray, S., et al., *Topoisomerase IIalpha promotes activation of RNA polymerase I transcription by facilitating pre-initiation complex formation.* Nat Commun, 2013. **4**: p. 1598.
82. Nitiss, J.L., *Targeting DNA topoisomerase II in cancer chemotherapy.* Nat Rev Cancer, 2009. **9**(5): p.

338-50.

83. Russell, B., et al., *Chromosome breakage is regulated by the interaction of the BLM helicase and topoisomerase IIalpha.* Cancer Res, 2011. **71**(2): p. 561-71.
84. Grierson, P.M., S. Acharya, and J. Groden, *Collaborating functions of BLM and DNA topoisomerase I in regulating human rDNA transcription.* Mutat Res, 2013. **743-744**: p. 89-96.
85. Gupta, R. and R.M. Brosh, Jr., *DNA repair helicases as targets for anti-cancer therapy.* Curr Med Chem, 2007. **14**(5): p. 503-17.
86. Wang, J., et al., *PHF6 regulates cell cycle progression by suppressing ribosomal RNA synthesis.* J Biol Chem, 2013. **288**(5): p. 3174-83.
87. Deng, W., et al., *Cytoskeletal protein filamin A is a nucleolar protein that suppresses ribosomal RNA gene transcription.* Proc Natl Acad Sci U S A, 2012. **109**(5): p. 1524-9.
88. Qiu, H., et al., *Identification of novel nuclear protein interactions with the N-terminal part of filamin A.* Biosci Biotechnol Biochem, 2011. **75**(1): p. 145-7.
89. Yue, J., et al., *Filamin-A as a marker and target for DNA damage based cancer therapy.* DNA Repair (Amst), 2012. **11**(2): p. 192-200.
90. Yue, J., et al., *The cytoskeleton protein filamin-A is required for an efficient recombinational DNA double strand break repair.* Cancer Res, 2009. **69**(20): p. 7978-85.
91. Zhang, Y., et al., *Identification of DHX33 as a mediator of rRNA synthesis and cell growth.* Mol Cell Biol, 2011. **31**(23): p. 4676-91.
92. Fukawa, T., et al., *DDX31 regulates the p53-HDM2 pathway and rRNA gene transcription through its interaction with NPM1 in renal cell carcinomas.* Cancer Res, 2012. **72**(22): p. 5867-77.
93. Kihm, A.J., et al., *Phosphorylation of the rRNA transcription factor upstream binding factor promotes its association with TATA binding protein.* Proc Natl Acad Sci U S A, 1998. **95**(25): p. 14816-20.
94. Voit, R., M. Hoffmann, and I. Grummt, *Phosphorylation by G1-specific cdk-cyclin complexes activates the nucleolar transcription factor UBF.* EMBO J, 1999. **18**(7): p. 1891-9.
95. Voit, R. and I. Grummt, *Phosphorylation of UBF at serine 388 is required for interaction with RNA polymerase I and activation of rDNA transcription.* Proc Natl Acad Sci U S A, 2001. **98**(24): p. 13631-6.
96. Mariappan, M.M., et al., *Ribosomal biogenesis induction by high glucose requires activation of upstream binding factor in kidney glomerular epithelial cells.* Am J Physiol Renal Physiol, 2011. **300**(1): p. F219-30.
97. Malumbres, M. and M. Barbacid, *Cell cycle, CDKs and cancer: a changing paradigm.* Nat Rev Cancer, 2009. **9**(3): p. 153-66.
98. Klein, J. and I. Grummt, *Cell cycle-dependent regulation of RNA polymerase I transcription: the nucleolar transcription factor UBF is inactive in mitosis and early G1.* Proc Natl Acad Sci U S A, 1999. **96**(11): p. 6096-101.
99. Lin, C.Y., et al., *CK2-mediated stimulation of Pol I transcription by stabilization of UBF-SL1 interaction.* Nucleic Acids Res, 2006. **34**(17): p. 4752-66.
100. Voit, R., et al., *The nucleolar transcription factor mUBF is phosphorylated by casein kinase II in the C-terminal hyperacidic tail which is essential for transactivation.* EMBO J, 1992. **11**(6): p. 2211-8.
101. Hanif, I.M., et al., *Casein Kinase II: an attractive target for anti-cancer drug design.* Int J Biochem Cell Biol, 2010. **42**(10): p. 1602-5.
102. Voit, R., et al., *Activation of mammalian ribosomal gene transcription requires phosphorylation of the*

nucleolar transcription factor UBF. Nucleic Acids Res, 1995. **23**(14): p. 2593-9.

103. Hannan, K.M., et al., *mTOR-dependent regulation of ribosomal gene transcription requires S6K1 and is mediated by phosphorylation of the carboxy-terminal activation domain of the nucleolar transcription factor UBF.* Mol Cell Biol, 2003. **23**(23): p. 8862-77.
104. Wu, A., et al., *Regulation of upstream binding factor 1 activity by insulin-like growth factor I receptor signaling.* J Biol Chem, 2005. **280**(4): p. 2863-72.
105. Drakas, R., X. Tu, and R. Baserga, *Control of cell size through phosphorylation of upstream binding factor 1 by nuclear phosphatidylinositol 3-kinase.* Proc Natl Acad Sci U S A, 2004. **101**(25): p. 9272-6.
106. Wu, S., et al., *IRS-2, but not IRS-1, can sustain proliferation and rescue UBF stabilization in InR or InR defective signaling of 32D myeloid cells.* Cell Cycle, 2009. **8**(19): p. 3218-26.
107. Hannan, K.M., L.I. Rothblum, and L.S. Jefferson, *Regulation of ribosomal DNA transcription by insulin.* Am J Physiol, 1998. **275**(1 Pt 1): p. C130-8.
108. Sun, H., X. Tu, and R. Baserga, *A mechanism for cell size regulation by the insulin and insulin-like growth factor-I receptors.* Cancer Res, 2006. **66**(23): p. 11106-9.
109. Stefanovsky, V., et al., *Growth factor signaling regulates elongation of RNA polymerase I transcription in mammals via UBF phosphorylation and r-chromatin remodeling.* Mol Cell, 2006. **21**(5): p. 629-39.
110. Stefanovsky, V.Y., et al., *An immediate response of ribosomal transcription to growth factor stimulation in mammals is mediated by ERK phosphorylation of UBF.* Mol Cell, 2001. **8**(5): p. 1063-73.
111. Meraner, J., et al., *Acetylation of UBF changes during the cell cycle and regulates the interaction of UBF with RNA polymerase I.* Nucleic Acids Res, 2006. **34**(6): p. 1798-806.
112. Pelletier, G., et al., *Competitive recruitment of CBP and Rb-HDAC regulates UBF acetylation and ribosomal transcription.* Mol Cell, 2000. **6**(5): p. 1059-66.
113. Ali, S.A., et al., *A RUNX2-HDAC1 co-repressor complex regulates rRNA gene expression by modulating UBF acetylation.* J Cell Sci, 2012. **125**(Pt 11): p. 2732-9.
114. Hirschler-Laszkiewicz, I., et al., *The role of acetylation in rDNA transcription.* Nucleic Acids Res, 2001. **29**(20): p. 4114-24.
115. Lee, J., et al., *Dysregulation of upstream binding factor-1 acetylation at K352 is linked to impaired ribosomal DNA transcription in Huntington's disease.* Cell Death Differ, 2011. **18**(11): p. 1726-35.
116. Zhao, J., et al., *ERK-dependent phosphorylation of the transcription initiation factor TIF-IA is required for RNA polymerase I transcription and cell growth.* Mol Cell, 2003. **11**(2): p. 405-13.
117. Philimonenko, V.V., et al., *Nuclear actin and myosin I are required for RNA polymerase I transcription.* Nat Cell Biol, 2004. **6**(12): p. 1165-72.
118. Mayer, C., et al., *mTOR-dependent activation of the transcription factor TIF-IA links rRNA synthesis to nutrient availability.* Genes Dev, 2004. **18**(4): p. 423-34.
119. Bierhoff, H., et al., *Phosphorylation by casein kinase 2 facilitates rRNA gene transcription by promoting dissociation of TIF-IA from elongating RNA polymerase I.* Mol Cell Biol, 2008. **28**(16): p. 4988-98.
120. Hoppe, S., et al., *AMP-activated protein kinase adapts rRNA synthesis to cellular energy supply.* Proc Natl Acad Sci U S A, 2009. **106**(42): p. 17781-6.
121. Mayer, C., H. Bierhoff, and I. Grummt, *The nucleolus as a stress sensor: JNK2 inactivates the transcription factor TIF-IA and down-regulates rRNA synthesis.* Genes Dev, 2005. **19**(8): p. 933-41.
122. Heix, J., et al., *Mitotic silencing of human rRNA synthesis: inactivation of the promoter selectivity*

factor SL1 by cdc2/cyclin B-mediated phosphorylation. EMBO J, 1998. **17**(24): p. 7373-81.

123. Kuhn, A., et al., *Mitotic phosphorylation of the TBP-containing factor SL1 represses ribosomal gene transcription.* J Mol Biol, 1998. **284**(1): p. 1-5.
124. Muth, V., et al., *Acetylation of TAF(I)68, a subunit of TIF-IB/SL1, activates RNA polymerase I transcription.* EMBO J, 2001. **20**(6): p. 1353-62.
125. Sirri, V., P. Roussel, and D. Hernandez-Verdun, *The mitotically phosphorylated form of the transcription termination factor TTF-1 is associated with the repressed rDNA transcription machinery.* J Cell Sci, 1999. **112 (Pt 19)**: p. 3259-68.
126. Fath, S., et al., *Differential roles of phosphorylation in the formation of transcriptional active RNA polymerase I.* Proc Natl Acad Sci U S A, 2001. **98**(25): p. 14334-9.
127. Gerber, J., et al., *Site specific phosphorylation of yeast RNA polymerase I.* Nucleic Acids Res, 2008. **36**(3): p. 793-802.
128. Patel, J.H., et al., *Analysis of genomic targets reveals complex functions of MYC.* Nat Rev Cancer, 2004. **4**(7): p. 562-8.
129. van Riggelen, J., A. Yetil, and D.W. Felsher, *MYC as a regulator of ribosome biogenesis and protein synthesis.* Nat Rev Cancer, 2010. **10**(4): p. 301-9.
130. Grandori, C., et al., *c-Myc binds to human ribosomal DNA and stimulates transcription of rRNA genes by RNA polymerase I.* Nat Cell Biol, 2005. **7**(3): p. 311-8.
131. Arabi, A., et al., *c-Myc associates with ribosomal DNA and activates RNA polymerase I transcription.* Nat Cell Biol, 2005. **7**(3): p. 303-10.
132. Hannan, K.M., et al., *Dysregulation of RNA polymerase I transcription during disease.* Biochim Biophys Acta, 2013. **1829**(3-4): p. 342-60.
133. Grewal, S.S., et al., *Myc-dependent regulation of ribosomal RNA synthesis during Drosophila development.* Nat Cell Biol, 2005. **7**(3): p. 295-302.
134. Finlay, C.A., P.W. Hinds, and A.J. Levine, *The p53 proto-oncogene can act as a suppressor of transformation.* Cell, 1989. **57**(7): p. 1083-93.
135. Feng, Z., et al., *The tumor suppressor p53: cancer and aging.* Cell Cycle, 2008. **7**(7): p. 842-7.
136. Zhang, Y., Y. Xiong, and W.G. Yarbrough, *ARF promotes MDM2 degradation and stabilizes p53: ARF-INK4a locus deletion impairs both the Rb and p53 tumor suppression pathways.* Cell, 1998. **92**(6): p. 725-34.
137. Budde, A. and I. Grummt, *p53 represses ribosomal gene transcription.* Oncogene, 1999. **18**(4): p. 1119-24.
138. Zhai, W. and L. Comai, *Repression of RNA polymerase I transcription by the tumor suppressor p53.* Mol Cell Biol, 2000. **20**(16): p. 5930-8.
139. Karni-Schmidt, O., et al., *p53 is localized to a sub-nucleolar compartment after proteasomal inhibition in an energy-dependent manner.* J Cell Sci, 2008. **121**(Pt 24): p. 4098-105.
140. Karni-Schmidt, O., et al., *Energy-dependent nucleolar localization of p53 in vitro requires two discrete regions within the p53 carboxyl terminus.* Oncogene, 2007. **26**(26): p. 3878-91.
141. Kruger, T. and U. Scheer, *p53 localizes to intranucleolar regions distinct from the ribosome production compartments.* J Cell Sci, 2010. **123**(Pt 8): p. 1203-8.
142. Manning, A.L. and N.J. Dyson, *pRB, a tumor suppressor with a stabilizing presence.* Trends Cell Biol, 2011. **21**(8): p. 433-41.
143. Cavanaugh, A.H., et al., *Activity of RNA polymerase I transcription factor UBF blocked by Rb gene*

product. Nature, 1995. **374**(6518): p. 177-80.

144. Voit, R., K. Schafer, and I. Grummt, *Mechanism of repression of RNA polymerase I transcription by the retinoblastoma protein.* Mol Cell Biol, 1997. **17**(8): p. 4230-7.
145. Hannan, K.M., et al., *Rb and p130 regulate RNA polymerase I transcription: Rb disrupts the interaction between UBF and SL-1.* Oncogene, 2000. **19**(43): p. 4988-99.
146. Lim, M.J. and X.W. Wang, *Nucleophosmin and human cancer.* Cancer Detect Prev, 2006. **30**(6): p. 481-90.
147. Di Fiore, P.P., *Playing both sides: nucleophosmin between tumor suppression and oncogenesis.* J Cell Biol, 2008. **182**(1): p. 7-9.
148. Murano, K., et al., *Transcription regulation of the rRNA gene by a multifunctional nucleolar protein, B23/nucleophosmin, through its histone chaperone activity.* Mol Cell Biol, 2008. **28**(10): p. 3114-26.
149. Li, Z. and S.R. Hann, *Nucleophosmin is essential for c-Myc nucleolar localization and c-Myc-mediated rDNA transcription.* Oncogene, 2013. **32**(15): p. 1988-94.
150. Bonetti, P., et al., *Nucleophosmin and its AML-associated mutant regulate c-Myc turnover through Fbw7 gamma.* J Cell Biol, 2008. **182**(1): p. 19-26.
151. Korgaonkar, C., et al., *Nucleophosmin (B23) targets ARF to nucleoli and inhibits its function.* Mol Cell Biol, 2005. **25**(4): p. 1258-71.
152. Kurki, S., et al., *Nucleolar protein NPM interacts with HDM2 and protects tumor suppressor protein p53 from HDM2-mediated degradation.* Cancer Cell, 2004. **5**(5): p. 465-75.
153. Zhang, C., L. Comai, and D.L. Johnson, *PTEN represses RNA Polymerase I transcription by disrupting the SL1 complex.* Mol Cell Biol, 2005. **25**(16): p. 6899-911.
154. Chan, J.C., et al., *AKT promotes rRNA synthesis and cooperates with c-MYC to stimulate ribosome biogenesis in cancer.* Sci Signal, 2011. **4**(188): p. ra56.
155. Hannan, K.M., et al., *Signaling to the ribosome in cancer--It is more than just mTORC1.* IUBMB Life, 2011. **63**(2): p. 79-85.
156. Sears, R., et al., *Ras enhances Myc protein stability.* Mol Cell, 1999. **3**(2): p. 169-79.
157. Sears, R., et al., *Multiple Ras-dependent phosphorylation pathways regulate Myc protein stability.* Genes Dev, 2000. **14**(19): p. 2501-14.
158. Young, D.W., et al., *Mitotic occupancy and lineage-specific transcriptional control of rRNA genes by Runx2.* Nature, 2007. **445**(7126): p. 442-6.
159. Cameron, E.R. and J.C. Neil, *The Runx genes: lineage-specific oncogenes and tumor suppressors.* Oncogene, 2004. **23**(24): p. 4308-14.
160. Martin, J.W., et al., *The Role of RUNX2 in Osteosarcoma Oncogenesis.* Sarcoma, 2011. **2011**: p. 282745.
161. Bakshi, R., et al., *The leukemogenic t(8;21) fusion protein AML1-ETO controls rRNA genes and associates with nucleolar-organizing regions at mitotic chromosomes.* J Cell Sci, 2008. **121**(Pt 23): p. 3981-90.
162. Tseng, H., et al., *Mouse ribosomal RNA genes contain multiple differentially regulated variants.* PLoS One, 2008. **3**(3): p. e1843.
163. Ihara, M., H. Tseng, and R.M. Schultz, *Expression of variant ribosomal RNA genes in mouse oocytes and preimplantation embryos.* Biol Reprod, 2011. **84**(5): p. 944-6.
164. Bowman, L.H., *rDNA transcription and pre-rRNA processing during the differentiation of a mouse myoblast cell line.* Dev Biol, 1987. **119**(1): p. 152-63.

165. Comai, L., et al., *Inhibition of RNA polymerase I transcription in differentiated myeloid leukemia cells by inactivation of selectivity factor 1.* Cell Growth Differ, 2000. **11**(1): p. 63-70.
166. Poortinga, G., et al., *MAD1 and c-MYC regulate UBF and rDNA transcription during granulocyte differentiation.* EMBO J, 2004. **23**(16): p. 3325-35.
167. Rosby, R., et al., *Knockdown of the Drosophila GTPase nucleostemin 1 impairs large ribosomal subunit biogenesis, cell growth, and midgut precursor cell maintenance.* Mol Biol Cell, 2009. **20**(20): p. 4424-34.
168. Drygin, D., W.G. Rice, and I. Grummt, *The RNA polymerase I transcription machinery: an emerging target for the treatment of cancer.* Annu Rev Pharmacol Toxicol, 2010. **50**: p. 131-56.
169. Drygin, D., et al., *Anticancer activity of CX-3543: a direct inhibitor of rRNA biogenesis.* Cancer Res, 2009. **69**(19): p. 7653-61.
170. Drygin, D., et al., *Targeting RNA polymerase I with an oral small molecule CX-5461 inhibits ribosomal RNA synthesis and solid tumor growth.* Cancer Res, 2011. **71**(4): p. 1418-30.
171. Bywater, M.J., et al., *Inhibition of RNA polymerase I as a therapeutic strategy to promote cancer-specific activation of p53.* Cancer Cell, 2012. **22**(1): p. 51-65.
172. Andrews, W.J., et al., *Old drug, new target: ellipticines selectively inhibit RNA polymerase I transcription.* J Biol Chem, 2013. **288**(7): p. 4567-82.
173. Thibault, S.T., et al., *A complementary transposon tool kit for Drosophila melanogaster using P and piggyBac.* Nat Genet, 2004. **36**(3): p. 283-7.
174. Parks, A.L., et al., *Systematic generation of high-resolution deletion coverage of the Drosophila melanogaster genome.* Nat Genet, 2004. **36**(3): p. 288-92.
175. Bischof, J., et al., *An optimized transgenesis system for Drosophila using germ-line-specific φC31 integrases.* Proceedings of the National Academy of Sciences, 2007. **104**(9): p. 3312-3317.
176. Venken, K.J., et al., *P[acman]: a BAC transgenic platform for targeted insertion of large DNA fragments in D. melanogaster.* Science, 2006. **314**(5806): p. 1747-51.
177. Brand, A.H. and N. Perrimon, *Targeted gene expression as a means of altering cell fates and generating dominant phenotypes.* Development, 1993. **118**(2): p. 401-15.
178. Rorth, P., *Gal4 in the Drosophila female germline.* Mech Dev, 1998. **78**(1-2): p. 113-8.
179. Xu, T. and G.M. Rubin, *Analysis of genetic mosaics in developing and adult Drosophila tissues.* Development, 1993. **117**(4): p. 1223-37.
180. Blair, S.S., *Genetic mosaic techniques for studying Drosophila development.* Development, 2003. **130**(21): p. 5065-72.
181. Garzino, V., C. Moretti, and J. Pradel, *Nuclear antigens differentially expressed during early development of Drosophila melanogaster.* Biol Cell, 1987. **61**(1-2): p. 5-13.
182. Giordano, E., et al., *minifly, a Drosophila gene required for ribosome biogenesis.* The Journal of cell biology, 1999. **144**(6): p. 1123-33.
183. Dansereau, D.A. and P. Lasko, *The development of germline stem cells in Drosophila.* Methods Mol Biol, 2008. **450**: p. 3-26.
184. de Cuevas, M. and A.C. Spradling, *Morphogenesis of the Drosophila fusome and its implications for oocyte specification.* Development, 1998. **125**(15): p. 2781-9.
185. Cooley, L., *Drosophila ring canal growth requires Src and Tec kinases.* Cell, 1998. **93**(6): p. 913-5.
186. Yue, L. and A.C. Spradling, *hu-li tai shao, a gene required for ring canal formation during Drosophila oogenesis, encodes a homolog of adducin.* Genes Dev, 1992. **6**(12B): p. 2443-54.

187. Bastock, R. and D. St Johnston, *Drosophila oogenesis.* Curr Biol, 2008. **18**(23): p. R1082-7.
188. de Cuevas, M. and E.L. Matunis, *The stem cell niche: lessons from the Drosophila testis.* Development, 2011. **138**(14): p. 2861-9.
189. Xie, T. and A.C. Spradling, *decapentaplegic is essential for the maintenance and division of germline stem cells in the Drosophila ovary.* Cell, 1998. **94**(2): p. 251-260.
190. Xie, T. and A.C. Spradling, *A niche maintaining germ line stem cells in the Drosophila ovary.* Science, 2000. **290**(5490): p. 328-30.
191. Chen, D. and D. McKearin, *Dpp signaling silences bam transcription directly to establish asymmetric divisions of germline stem cells.* Current biology : CB, 2003. **13**(20): p. 1786-91.
192. Chen, D. and D.M. McKearin, *A discrete transcriptional silencer in the bam gene determines asymmetric division of the Drosophila germline stem cell.* Development, 2003. **130**(6): p. 1159-70.
193. McKearin, D. and B. Ohlstein, *A role for the Drosophila bag-of-marbles protein in the differentiation of cystoblasts from germline stem cells.* Development, 1995. **121**(9): p. 2937-47.
194. McKearin, D.M. and A.C. Spradling, *bag-of-marbles: a Drosophila gene required to initiate both male and female gametogenesis.* Genes Dev, 1990. **4**(12B): p. 2242-51.
195. Chen, D. and D. McKearin, *Dpp signaling silences bam transcription directly to establish asymmetric divisions of germline stem cells.* Curr Biol, 2003. **13**(20): p. 1786-91.
196. Song, X., et al., *Bmp signals from niche cells directly repress transcription of a differentiation-promoting gene, bag of marbles, in germline stem cells in the Drosophila ovary.* Development, 2004. **131**(6): p. 1353-64.
197. Ohlstein, B. and D. McKearin, *Ectopic expression of the Drosophila Bam protein eliminates oogenic germline stem cells.* Development, 1997. **124**(18): p. 3651-62.
198. Chen, S.Y., S. Wang, and T. Xie, *Restricting self-renewal signals within the stem cell niche: multiple levels of control.* Current Opinion in Genetics & Development, 2011. **21**(6): p. 684-689.
199. Song, X., et al., *Notch signaling controls germline stem cell niche formation in the Drosophila ovary.* Development, 2007. **134**(6): p. 1071-80.
200. Wang, L., Z. Li, and Y. Cai, *The JAK/STAT pathway positively regulates DPP signaling in the Drosophila germline stem cell niche.* J Cell Biol, 2008. **180**(4): p. 721-8.
201. Lopez-Onieva, L., A. Fernandez-Minan, and A. Gonzalez-Reyes, *Jak/Stat signalling in niche support cells regulates dpp transcription to control germline stem cell maintenance in the Drosophila ovary.* Development, 2008. **135**(3): p. 533-40.
202. Eliazer, S., N.A. Shalaby, and M. Buszczak, *Loss of lysine-specific demethylase 1 nonautonomously causes stem cell tumors in the Drosophila ovary.* Proc Natl Acad Sci U S A, 2011. **108**(17): p. 7064-9.
203. Liu, M., T.M. Lim, and Y. Cai, *The Drosophila female germline stem cell lineage acts to spatially restrict DPP function within the niche.* Sci Signal, 2010. **3**(132): p. ra57.
204. Wang, X., et al., *Type IV collagens regulate BMP signalling in Drosophila.* Nature, 2008. **455**(7209): p. 72-7.
205. Venken, K.J., et al., *Versatile P[acman] BAC libraries for transgenesis studies in Drosophila melanogaster.* Nat Methods, 2009. **6**(6): p. 431-4.
206. Boisvert, F.M., et al., *The multifunctional nucleolus.* Nat Rev Mol Cell Biol, 2007. **8**(7): p. 574-85.
207. Tschochner, H. and E. Hurt, *Pre-ribosomes on the road from the nucleolus to the cytoplasm.* Trends Cell Biol, 2003. **13**(5): p. 255-63.
208. Mougey, E.B., et al., *The terminal balls characteristic of eukaryotic rRNA transcription units in*

chromatin spreads are rRNA processing complexes. Genes Dev, 1993. **7**(8): p. 1609-19.

209. Krejci, E., et al., *Modulo, a new maternally expressed Drosophila gene encodes a DNA-binding protein with distinct acidic and basic regions.* Nucleic acids research, 1989. **17**(20): p. 8101-15.
210. Perrin, L., et al., *Dynamics of the sub-nuclear distribution of Modulo and the regulation of position-effect variegation by nucleolus in Drosophila.* J Cell Sci, 1998. **111 (Pt 18)**: p. 2753-61.
211. Guruharsha, K.G., et al., *A protein complex network of Drosophila melanogaster.* Cell, 2011. **147**(3): p. 690-703.
212. Seifarth, W., et al., *Identification of the genes coding for the second-largest subunits of RNA polymerases I and III of Drosophila melanogaster.* Mol Gen Genet, 1991. **228**(3): p. 424-32.
213. Granneman, S. and S.J. Baserga, *Crosstalk in gene expression: coupling and co-regulation of rDNA transcription, pre-ribosome assembly and pre-rRNA processing.* Curr Opin Cell Biol, 2005. **17**(3): p. 281-6.
214. Giordano, E., et al., *minifly, a Drosophila gene required for ribosome biogenesis.* J Cell Biol, 1999. **144**(6): p. 1123-33.
215. Sanij, E., et al., *UBF levels determine the number of active ribosomal RNA genes in mammals.* J Cell Biol, 2008. **183**(7): p. 1259-74.
216. Shen, R., et al., *eIF4A controls germline stem cell self-renewal by directly inhibiting BAM function in the Drosophila ovary.* Proc Natl Acad Sci U S A, 2009. **106**(28): p. 11623-8.
217. Li, Y., et al., *Bam and Bgcn antagonize Nanos-dependent germ-line stem cell maintenance.* Proc Natl Acad Sci U S A, 2009. **106**(23): p. 9304-9.
218. Lavoie, C.A., B. Ohlstein, and D.M. McKearin, *Localization and function of Bam protein require the benign gonial cell neoplasm gene product.* Dev Biol, 1999. **212**(2): p. 405-13.
219. Velichko, A.K., et al., *Mechanisms of heat shock response in mammals.* Cell Mol Life Sci, 2013.
220. Matts, R.L. and R. Hurst, *The Relationship between Protein-Synthesis and Heat-Shock Proteins Levels in Rabbit Reticulocyte Lysates.* Journal of Biological Chemistry, 1992. **267**(25): p. 18168-18174.
221. Tilney, L.G., M.S. Tilney, and G.M. Guild, *Formation of actin filament bundles in the ring canals of developing Drosophila follicles.* J Cell Biol, 1996. **133**(1): p. 61-74.
222. Kelso, R.J., A.M. Hudson, and L. Cooley, *Drosophila Kelch regulates actin organization via Src64-dependent tyrosine phosphorylation.* Journal of Cell Biology, 2002. **156**(4): p. 703-713.
223. Tastan, O.Y., et al., *Drosophila ataxin 2-binding protein 1 marks an intermediate step in the molecular differentiation of female germline cysts.* Development, 2010. **137**(19): p. 3167-76.
224. Cui, Z. and P.J. DiMario, *RNAi knockdown of Nopp140 induces Minute-like phenotypes in Drosophila.* Molecular biology of the cell, 2007. **18**(6): p. 2179-91.
225. Grewal, S.S., J.R. Evans, and B.A. Edgar, *Drosophila TIF-IA is required for ribosome synthesis and cell growth and is regulated by the TOR pathway.* The Journal of cell biology, 2007. **179**(6): p. 1105-13.
226. Dundr, M., T. Misteli, and M.O. Olson, *The dynamics of postmitotic reassembly of the nucleolus.* J Cell Biol, 2000. **150**(3): p. 433-46.
227. Leung, A.K., et al., *Quantitative kinetic analysis of nucleolar breakdown and reassembly during mitosis in live human cells.* J Cell Biol, 2004. **166**(6): p. 787-800.
228. Savino, T.M., et al., *Nucleolar assembly of the rRNA processing machinery in living cells.* J Cell Biol, 2001. **153**(5): p. 1097-110.
229. Harris, R.E., et al., *Brat promotes stem cell differentiation via control of a bistable switch that restricts*

BMP signaling. Dev Cell, 2011. **20**(1): p. 72-83.

230. Frank, D.J., B.A. Edgar, and M.B. Roth, *The Drosophila melanogaster gene brain tumor negatively regulates cell growth and ribosomal RNA synthesis.* Development, 2002. **129**(2): p. 399-407.